약학박사학위논문

Part Ⅰ: Selective *O*-alkylation based practical and efficient synthesis of Gefitinib, an EGFR kinase inhibitor

Part Ⅱ: Practical synthesis of Levocabastine, a H_1 receptor antagonist

Part Ⅰ. Selective *O*-alkylation을 이용하는 실용적이고 효율적인 Gefitinib의 합성법에 관한 연구

Part Ⅱ. H_1 receptor antagonist인 Levocabastine의 실용적인 합성법 개발

2018년 2월

서울대학교 대학원

약학과 약품제조화학전공

강 성 권

Part Ⅰ: Selective *O*-alkylation based practical and efficient synthesis of Gefitinib, an EGFR kinase inhibitor

Part Ⅰ. Selective *O*-alkylation을 이용하는 실용적이고 효율적인 Gefitinib의 합성법에 관한 연구

국문초록

Gefitinib은 AstraZeneca에 의해 개발된 표피 성장 인자 수용체 (Epidermal growth factor receptor; EGFR)의 첫번째 선택적 억제제로써, 2003년에 비소세포폐암 (Non Small Cell Lung Cancer) 적응증에 대해 이레사(Iressa)라는 제품명으로 허가 받았다. Gefitinib은 EGFR intracellular kinase domain의 ATP binding을 경쟁적으로 억제하여 tyrosine kinase에 의한 downstream signaling을 차단함으로써 암세포의 성장을 억제하는 효과를 나타내게 된다.

Gefitinib은 quinazoline moiety를 기본 골격으로, 4번 탄소 위치에 aniline group, 6번 탄소 위치에 morpholinopropoxy group이 치환되어 있는 구조를 가지고 있다. 이러한 구조적인 특징으로 인해 morpholino group의 도입을 위한 *O*-alkylation이 수행되어야만 한다. 이때 aniline group의 반응성에 의한 *N*-alkylated 부산물이 과량 발생하게 되고, 이의 해결을 위해 다수의 연구진에 의해 합성법들이 연구되었다.

본 연구진은 상기의 문제를 해결하기 위해 TMS를 transient protection group으로 이용하는 새로운 시도를 하였다. 마지막 합성 단계인 *O*-alkylation 반응 진행 시, 반응성이 강한 aniline group에 TMS를 일시적으로 결합시켜 반응성을 억제한 후, 선택적으로 *O*-alkylation을 완료하고, 수분 첨가를 통해 간단하게 TMS를 제거하여 부산물의 생성을 최대한 억제하면서 목적화합물을 높은 순도와 수율로 얻을 수 있었다. 또한 다양한 anilinoquinazoline 구조 및 간단한 aminophenol 구조를 이용하여 선택성 및 재현성을 확인하였다. 이러한 선택적인 *O*-alkylation에 대한 새로운 route는 amino-alcohol group을 동시에 가지는 약물들의 합성에 유용하게 이용될 수 있을 것이다.

본 연구진은 transient protection이라는 새로운 concept을 도입하여 기존에 알려진 gefitinib의 합성법을 modification 함으로써, 효율적이고 실용적인 제법의 개발을 완료하였다.

주요어: Gefitinib, Quinazoline, EGFR, Transient protection group

학번: 2009-31060

Table of Contents

List of Tables

List of Figures

List of Schemes

Abbreviations

ABL: Abelson leukaemia protein

Ac: acetyl

ATP : Adenosine tri phosphate

BCR: Breakpoint cluster region protein

Bn: Benzyl

CYS-773 : Cysteine-773

DIPEA : Diisopropylethylamine

DMAP: *N*,*N*-dimethylaminopyridine

DMF: *N*,*N*-dimethylformamide

DMSO: Dimethylsulfoxide

EGF: Epidermal growth factor

EGFR : Epidermal growth factor receptor

ErbB : Avian erythroblastosis oncogene B

FDA : Food and Drug Administration

HER: Human EGF receptor

HPLC : High-performance liquid chromatography

hr : hour

HRMS : High-resolution mass spectrometry

IC_{50} : The half maximal inhibitory concentration

IPA : Isopropyl alcohol

MCF-7 : Michigan Cancer Foundation-7

MS: Mass spectrometry

NSCLC : Non small cell lung cancer

NMR : Nuclear magnetic resonance spectroscopy

RTK : Receptor tyrosine kinase

TBAB: Tetrabutylammonium bromide

TEA : Triethylamine

TKs : Tyrosine kinase

TMS : Trimethylsilyl

TMSI : Trimethylsilyl Iodide

TLC : Thin layer chromatography

I. Introduction

1. Targeted cancer therapy

Targeted cancer therapies[1] are drugs or other substances that block the growth and spread of cancer by interfering with specific molecules ("molecular targets") that are involved in the growth, progression, and spread of cancer. Targeted cancer therapies are sometimes called "molecularly targeted drugs," "molecularly targeted therapies," "precision medicines," or similar names. Targeted therapies are currently the focus of much anticancer drug development. They are a cornerstone of precision medicine, a form of medicine that uses information about a person's genes and proteins to prevent, diagnose, and treat disease.

Many targeted cancer therapies have been approved by the Food and Drug Administration (FDA) to treat specific types of cancer (Table 1).[2]

Table 1. FDA approved small molecule kinase inhibitors and monoclonal antibody for use of cancer therapy

Name	Targets	Oncology uses
Small molecule inhibitors for cancer		
Dasatinib	BCR-ABL, SRC family, c-KIT, PDGFR	Chronic myeloid leukemia (CML), acute lymphocytic leukemia
Erlotinib	EGFR	Non-small cell lung cancer(NSCLC), pancreatic cancer
Gefitinib	EGFR	NSCLC
Imatinib	BCR-ABL, c-KIT, PDGFR	Acute lymphocytic leukemia, CML, Gastrointestinal stromal tumor
Lapatinib	HER2/neu, EGFR	Breast cancer
Sorafenib[a]	BRAF, VEGFR, EGFR, PDGFR	Renal cell carcinoma(RCC), Hepatocellular carcinoma
Sunitinib[a]	VEGFR, PDGFR, c-KIT, FLT3	RCC, gastrointestinal stromal tumor
Temsirolimus[a]	mTOR, VEGF	RCC
Pazopanib[a]	VEGFR-1, VEGFR-2, VEGFR-3, PDGFR-a/β, and c-kit	RCC
Nilotinib	BCR-ABL	CML
Crizotinib	ALK, HGFR	NSCLC
Vemurafenib	BRAF	Late-stage melanoma
Monoclonal antibodies for cancer		
Alemtuzumab	CD52	Chronic lymphocytic leukemia
Bevacizumab[a]	VEGF	Colorectal cancer, NSCLC, RCC
Cetuximab	EGFR	Colorectal cancer, head and neck cancer
Gemtuzumab Ozogamicin	CD33	Relapsed acute myeloid leukemia
Ibritumomab Tiuxetan	CD20	Non-Hodgkin's lymphoma (NHL) (with yttrium-90 or indium-111)
Panitumumab	EGFR	Colorectal cancer
Rituximab	CD20	NHL
Tositumomab	CD20	NHL (with Iodine-131)
Trastuzumab	HER2/neu	Breast cancer with HER2/neu overexpression
Ipilimumab	CTLA-4	Late-stage melanoma

[a] Agents with antiangiogenic mechanism

Others are being studied in clinical trials (research studies with people), and many more are in preclinical testing (research studies with animals).

The development of targeted therapies requires the identification of good targets - that is, targets that play a key role in cancer cell growth and survival. One approach to identify potential targets is to compare the amounts of individual proteins in cancer cells with those in normal cells. Proteins that are present in cancer cells but not normal cells or that are more abundant in cancer cells would be potential targets, especially if they are known to be involved in cell growth or survival. Another approach to identify potential targets is to determine whether cancer cells produce mutant proteins that drive cancer progression.

Researchers also look for abnormalities in chromosomes that are present in cancer cells but not in normal cells. Sometimes these chromosome abnormalities result in the creation of a fusion gene (a gene that incorporates parts of two different genes) whose product, called a fusion protein, may drive cancer development. Such fusion proteins are potential targets for targeted cancer therapies. For example, imatinib mesylate (Gleevec®) targets the BCR-ABL fusion protein, which is made from pieces of two genes that get joined together in some leukemia cells and promotes the growth of leukemic cells.

Once a candidate target has been identified, the next step is to develop a therapy that affects the target in a way that interferes with its ability to promote cancer cell growth or survival. Most targeted therapies are either small molecules or monoclonal antibodies. Small-molecule compounds are typically developed for targets that are located inside the cell because such agents are able to enter cells relatively easily. Monoclonal antibodies are relatively large and generally cannot enter cells, so they are used only for targets that are outside cells or on the cell surface. Candidate small molecules are usually identified in what are known as "high-throughput screens," in which the effects of thousands of test compounds on a specific target protein are examined. Compounds that affect the target (sometimes called "lead compounds") are then chemically modified to produce numerous closely related versions of the lead

compound. These related compounds are then tested to determine which are most effective and have the fewest effects on non target molecules.

Targeted therapies do have some limitations. One is that cancer cells can become resistant to them. Resistance can occur in two ways: the target itself changes through mutation so that the targeted therapy no longer interacts well with it, and/or the tumor finds a new pathway to achieve tumor growth that does not depend on the target. For these reasons, targeted therapies may work best in combination.[3] Another approach is to use a targeted therapy in combination with one or more traditional chemotherapy drugs. Another limitation of targeted therapy at present is that drugs for some identified targets are difficult to develop because of the target's structure and/or the way its function is regulated in the cell.

2. Epidermal growth factor receptor

Epidermal growth factor receptor (EGFR) is located at the cell surface area and plays a central role in regulating cell proliferation and differentiation.[4] This receptor consists of an extracellular ligand-binding domain, a transmembrane lipophilic domain, and an intracellular tyrosine kinase domain (**Figure 1**). The binding of a ligand to an extracellular EGFR domain induces either homodimerization or heterodimerization,[5-7] thus leading to autophosphorylation of the tyrosine residue in the dimer.[8,9] The activation of the intracellular signaling cascades induced by the autophosphorylation of the receptor affects gene transcription. This gives rise to cancer cell proliferation, reduced apoptosis, invasion and metastasis and stimulates tumor-induced angiogenesis. Thus, overexpression of the EGFR, which is intimately relevant to the EGFR signaling pathway (**Figure 2**), increases cancer cell proliferation and reduces cell apoptosis.[10] The overexpression of EGFR is observed in many human tumors such as non-small cell lung cancer (NSCLC) and prostate, breast, colorectal, head and neck, ovarian, gastric, and pancreatic cancers.[11]

Figure 1. The structure of epidermal growth factor receptor

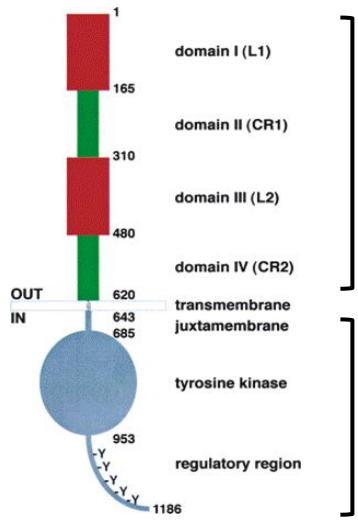

Figure 2. EGFR signaling pathway

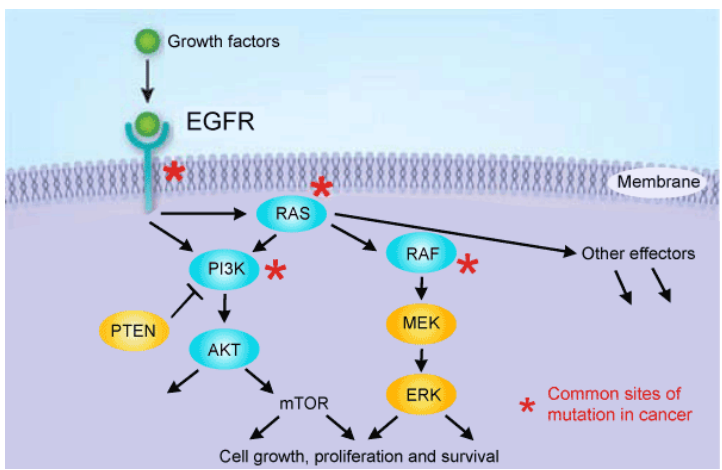

Epidermal growth factor receptor (EGFR, also known as ErbB-1 or HER-1) inhibitors[12] (**Table 2**) are either tyrosine kinase inhibitors or monoclonal antibodies that slow down or stop cell growth (*Drugs. Com*). Mutations of EGFRs can lead to continual or abnormal activation of the receptors causing unregulated cell division, which can account for some types of cancers.

Table 2. List of EGFR inhibitors

Drug name	Generic name	Indication	Company	Remark
Iressa	Gefitinib	NSCLC	AstraZeneca	Small molecule
Tarceva	Erlotinib	Lung or Pancreatic	Genentech	Small molecule
Tykerb	Lapatinib	Breast	GSK	Small molecule
Erbitux	Cetuximab	Colorectal	BMS	Monoclonal antibody
Vectibix	Panitumumab	Colorectal	Amgen	Monoclonal antibody
Caprelsa	Vandetanib	medullary thyroid	AstraZeneca	Small molecule
Portrazza	Necitumumab	NSCLC	Lilly	Monoclonal antibody
Tagrisso	Osimertinib	NSCLC	AstraZeneca	Small molecule

Tyrosine kinase inhibitors bind to the tyrosine kinase domain in the epidermal growth factor receptor and stop the activity of the EGFR. Monoclonal antibodies bind to the extracellular component of the epidermal growth factor receptors, prevent the actual substrates from binding to the receptors therefore prevent activation of the epidermal growth factor receptor. EGFR inhibitors are used to treat non-small-cell lung cancer, pancreatic cancer, breast cancer, colon cancer and some other cancers that are caused by epidermal growth factor receptor up-regulation.

3. 4-Anilinoquinazoline

Since 1994, when Fry et al. first discovered that 4-anilinoquinazoline (PD153035) acts as a EGFR tyrosine kinase specific inhibitor, quinazoline derivatives have become one of the hotspots of anti-cancer drugs research.[13-20] Among the quinazoline derivatives, especially 4-substituted aniline quinazoline, 4-anilinoquinazolines, have been prevalent motifs for pharmaceutical molecules in recent years, notably as EGFR inhibitors. As shown in **Figure 3**, the chemical structure of the representative drugs consisting of 4-anilinoquinazoline as a core part.

Figure 3. The chemical structure of drugs consisting of 4-anilinoquinazoline

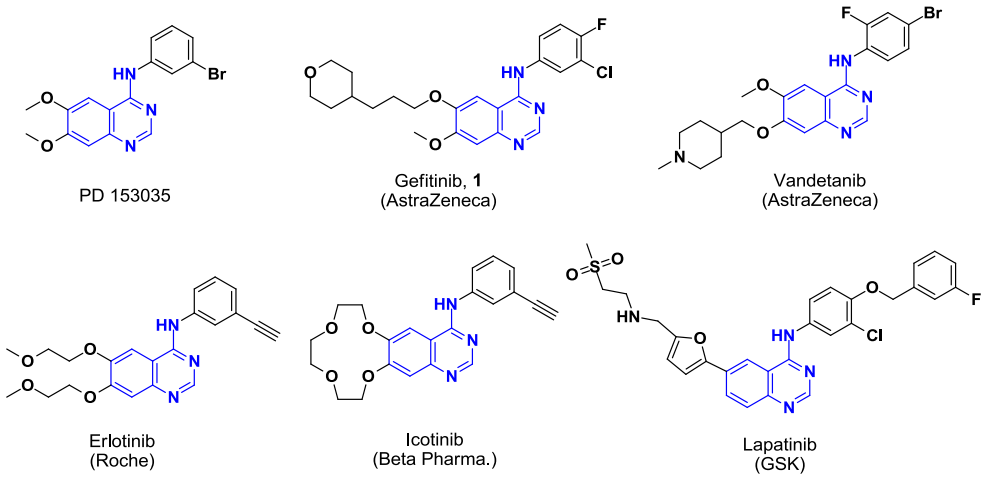

It was revealed that the quinazoline moiety interacts to the hinge domain of the kinase and the aniline moiety inserts into the hydrophobic pocket, which are crucial for EGFR inhibitory activity. The side chains at the C-6 and C-7 positions are out of pharmacophore which exerts good compatibility for long ether chains or other moieties. Therefore, many novel EGFR inhibitors have been designed and synthesized through incorporating an alkoxy moiety *via* *O*-alkylation of hydroxyl group at the C-6 or C-7 position of the 4-anilinoquinazoline scaffold.[21-28] However, in most case of alkylation of anilinoquinazolines with alkyl halide, a mixture of *O*- and *N*-alkylated, and *N*,*O*-dialkylated derivatives were generated without decent selectivity. It is a tedious work to separate and purify them. Thus, the development of new synthetic strategies which allow access to selective *O*-alkylation of 4-anilinoquinazolines is of interest to both laboratory and industry preparation of EGFR inhibitors.

3-1. 6,7-Dialkoxy-4-Anilinoquinazoline

Preclinical docking models have shown that EGFR inhibitors derived from quinazoline, including gefitinib, PD153035, erlotinib, and lapatinib, occupy the ATP-binding site of EGFR and effectively exert anti-cancer activity. To investigate the structural determinants

that modulate the interaction with EGFR and design novel EGFR inhibitors, a series of 6,7-dialkoxy-4-anilinoquinazoline with excellent anti-cancer activity was synthesized.[29-35]

Zhao *et al.*[29] designed and synthesized novel azaspirocycle or azetidine substituted 4-anilinoquinazoline derivatives. Their *in vitro* anti-tumor activities and EGFR inhibitory potencies were evaluated in two lung cancer cell lines, HCC827 and A549. Most of the target compounds possessed good anti-cancer activity against HCC827 and A549 cells. In particular, compounds **2** and **3,** containing 2-oxa-6-azaspiro[3.4]octane substituents (**Figure 4**), were found to possess higher EGFR inhibitory activities compared to the lead compound, gefitinib.

Figure 4. The chemical structure of compound 2, 3

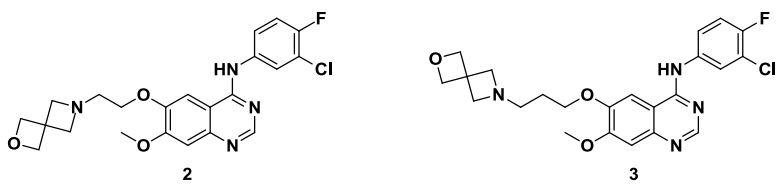

Conconi *et al.*[30] synthesized many 4-anilinoquinazoline compounds by modifying the quinazoline scaffold or the aniline moiety. Further studies revealed that these compounds possessed antiproliferation activity in many human tumor cell lines through inhibiting receptor and non-receptor TKs. For instance, compounds **4** and **5** (**Figure 5**) were found to possess high EGFR inhibitory activities with IC_{50} values of 0.002 μM and 0.027 μM, respectively.

Figure 5. The chemical structures of compound 4, 5

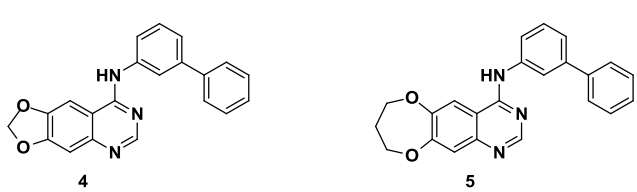

Cai *et al.*[35] reported many potential EGFR inhibitors. In most tested tumor cell lines including lung, liver, pancreatic, colon, breast, head and neck cancer, compound **6** (7-{4-(3-ethynylphenylamino)-7-methoxyquinazolin-6-yloxy}-*N*-hydroxyheptanamide; **Figure 6**) displayed efficient antiproliferative activity, which was greater than that of the positive control drugs. Particularly, compound **6** displayed excellent EGFR inhibitor activity which was better than that of Erlotinib and Lapatinib.

Figure 6. The chemical structure of compound 6

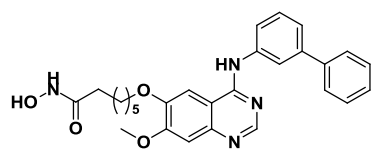

6

3-2. 6-amino-4-anilinoquinazoline

The structure and activity relationship of quinazoline EGFR inhibitors suggests that the selectivity of EGFR could be promoted through varying the aniline substitution pattern of the C-4 arylamino group. Also, structure analysis demonstrated the tolerance of bulky substituents at the C-6 position of quinazoline. Modifications at the C-6 position of quinazoline can provide enough space to allow covalent bonding or hydrogen bonding interactions with the Cys-773 of EGFR. Based on this knowledge, a series of 6-amino-4-anilinoquinazoline derivatives were reported for EGFR inhibition.[36-42]

Rao *et al.*[37] synthesized some 4-anilinoquinazoline compounds. Among them, compounds **7** and **8** (**Figure 7**) exhibited excellent *in vitro* anti-tumor bioactivity in A549 and MCF-7 cells. Docking EGFR evaluations were performed on compounds **7** and **8**; the results suggested that the quinazoline ring binds the hydrophobic pocket of the EGFR *N*-terminal domain.

Figure 7. The chemical structures of compound 7, 8

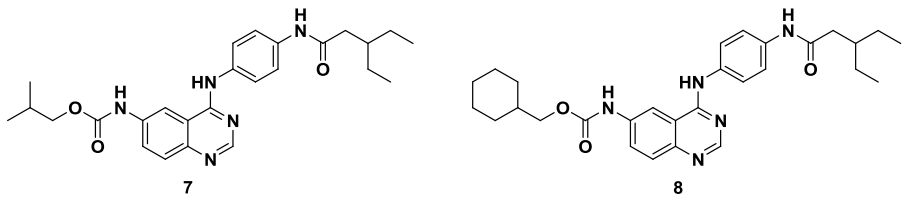

Li *et al.*[41] designed some 4,6-substituted-(diphenylamino)quinazolines. Bioassays indicated that the derivatives possessed antiproliferative and EGFR inhibitory bioactivities. Particularly, compound **9** (**Figure 8**) possessed the highest inhibition potency in the tested cells.

Figure 8. The chemical structure of compound 9

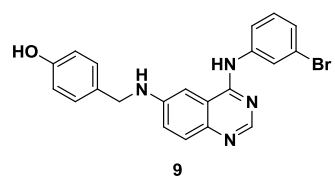

Previous studies have suggested that EGFR inhibitors could be synthesized by fusing a quinazoline scaffold with dioxygenated rings. Li *et al.*[42] synthesized some oxygenated alkane quinazolines for EGFR inhibition. Bioassays showed that most of these compounds exhibited EGFR inhibitory activities through inhibiting EGFR phosphorylation. Structure-activity relationships indicated that the activity was associated with the size of the fused dioxygenated ring. Among the tested compounds, **10** containing a heptatomic ring (**Figure 9**), displayed excellent inhibition activity in enzyme and cell assays.

Figure 9. The chemical structure of compound 10

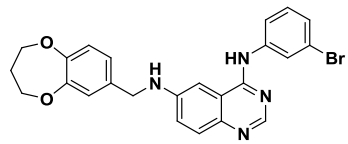

10

3-3. 6-alkoxy-4-anilinoquinazoline

RTK (receptor tyrosine kinases) play a key role in cell signaling pathways. EGFR belongs to the ErbB RTK family. EGFR overexpression can lead to out-of-control EGFR-mediated signaling, which occurs in many cancer cells. Thus EGFR is a potential target for anti-cancer drug development. Many previous studies have demonstrated the EGFR inhibition activity of 6-alkoxy-4-anilinoquinazoline.[43,44]

Ban *et al.*[43] designed and synthesized boron-conjugated 4-anilinoquinazolines. Biological assays indicated that compounds **11** and **12** (**Figure 10**) inhibited EGF-induced EGFR phosphorylation in A431 cells.

Figure 10. The chemical structures of compound 11, 12

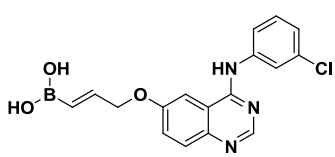

11

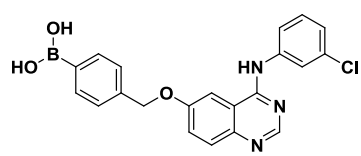

12

4. Transient protection *via* TMS

A trimethylsilyl group is a functional group in organic chemistry. This group consists of three methyl groups bonded to a silicon atom [$-Si(CH_3)_3$], which is in turn bonded to the rest of a molecule. A trimethylsilyl group bonded to a methyl group forms tetramethylsilane, which is abbreviated as TMS as well. Compounds with trimethylsilyl groups are not normally found in nature. Chemists sometimes use a trimethylsilylating reagent to derivatize non-volatile compounds such as alcohols, phenols, or carboxylic acids by substituting a trimethylsilyl group for a hydrogen in the hydroxyl groups on the compounds. Trimethylsilyl groups on a molecule have a tendency to make it more volatile, often making the compounds more amenable to analysis by gas chromatography or mass spectrometry. When attached to certain functional groups such as alcohol or amine group, trimethylsilyl groups may also be used as transient groups during chemical synthesis or some other chemical reactions. Moreover, trimethylsilyl groups were quite attractive to chemists in terms of facile removable character by a simple work-up.

5. Previous syntheses

Gefitinib (marketed by AstraZeneca), the first selective inhibitor of EGFR kinase domain, was approved in May 2003 for treatment of recurrent NSCLC (Non Small Cell Lung Cancer).[45] Since then, it has been widely used worldwide and synthetic methods for gefitinib consisting of 4-anilinoquinazoline moiety have been continuously reported.[46-49]

According to the procedure described in a **Scheme 1**,[46] gefitinib is synthesized using 6,7-dimethoxy quinazolin-4-one as a starting material in a sequence of selective demethylation, condensation with chlorofluoroaniline and, finally the introduction of a 3-morpholinopropoxy side chain. This procedure affords an excess of an *N*-alkylated impurity (**19**) of *N*-(3-chloro-4-fluorophenyl)-7-methoxy-6-(3-morpholinopropoxy)-*N*-(3-morpholinopropyl)quinazoline-4-amine in the final step. Accordingly, the *N*-alkylated impurity should be removed by column chromatography, however this lowers the yield and limits the utility of this synthesis in a commercial process.

Scheme 1. Gibson's route

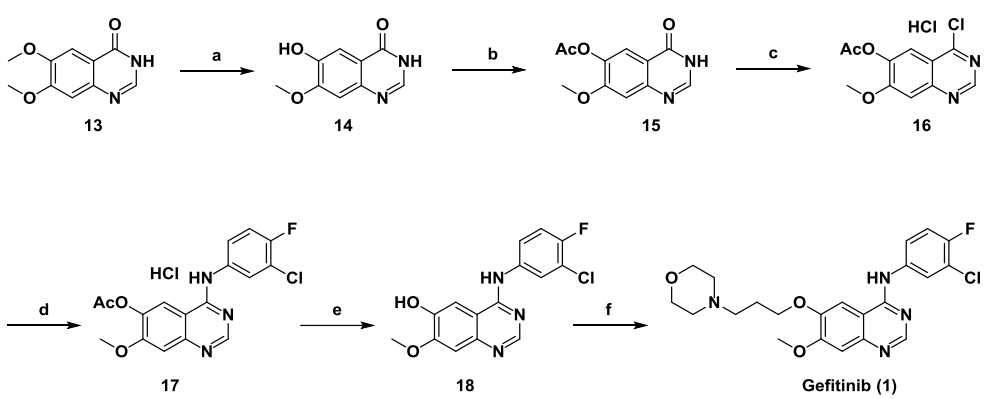

Reagents and conditions: (a) L-methionine, MsOH, reflux, 46.6%; (b) acetic anhydride, 100 °C, 75.0%; (c) thionyl chloride, DMF, 90 °C; (d) 3-chloro-4-fluoroaniline, isopropanol, 90 °C, 56.0% (for 2 steps); (e) ammonium hydroxide, MeOH, r.t. to reflux, 95.0%, (f) 3-morpholinopropyl chloride, DMF, 80 °C, 50.0%

To overcome this problem, an improved process for the synthesis of gefitinib using 3-hydroxy-4-methoxy benzonitrile as a starting material has been reported (**Scheme 2**).[47] This procedure includes an introduction a morpholinopropyl group prior to quinazoline ring formation to suppress the generation of the *N*-alkylated impurity. However, the extra steps required for the synthesis of quinazoline moiety makes this process inefficient and not economically viable in commercial production.

In 2004, Gilday et al. reported a new process involving a rearrangement of 3-(3-chloro-4-fluorophenyl)-7-methoxy-6-(3-morpholinopropoxy)-3,4-dihydroquinazoline-4-imine as a key reaction (**Scheme 3**).[48] This process is also considered not industrially suitable because it requires an excessive amount of chlorofluoroaniline. Furthermore, isomerization of an imine intermediate used for ring cyclization reaction requires a high temperature (110 °C) and a long reaction time (96 hr); this is a drawback of this process.

Scheme 2. Gilday's route for synthesis of gefitinib

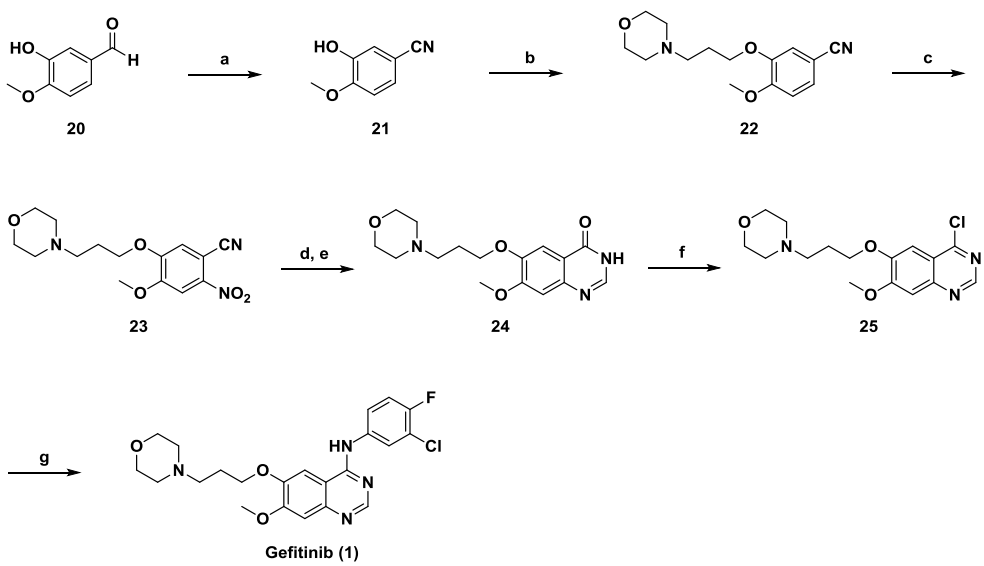

Reagents and conditions: (a) sodium formate, formic acid, 85 °C, 94.0%; (b) 3-morpholinopropyl chloride, K_2CO_3, DMF, 85 °C; (c) H_2SO_4, HNO_3, 35 °C, 76.3% (for 2 steps); (d) sodium dithionite, H_2O, 70 °C; (e) potassium hydroxide, formic acid, formamide, 95 °C, 77.7% (for 2 steps); (f) phosphorous oxychloride, TEA, toluene, 50 °C (g) 3-chloro-4-fluoroaniline, IPA, 66 °C, 72.8% (for 2 steps)

Scheme 3. Gilday's another route *via* dimroth rearrangement

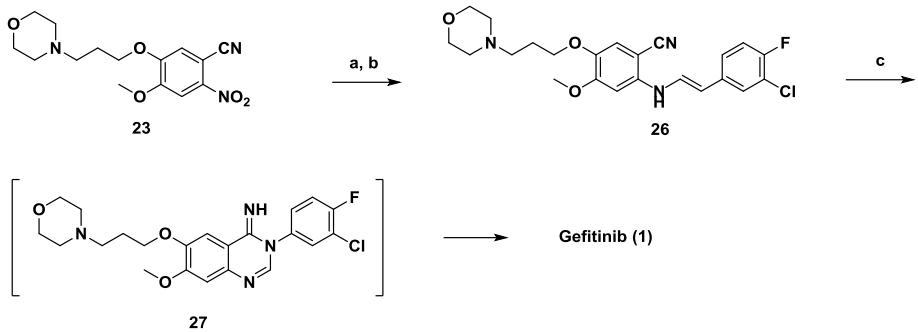

Reagents and conditions: (a) sodium dithionite, H_2O, 70 °C, 99.0%; (b) toluene, 110 °C, 96 hr, 70.7%; (c) toluene, 110 °C, 24 hr, 68.0%;

Kumar reported an improvement in the *O*-alkylation reaction of intermediate **18** with 81% yield and high purity (> 99%) to afford gefitinib (**Scheme 4**).[49] However, this process is not suitable for commercial production due to its long reaction steps (total 10 steps).

Scheme 4. Kumar's route

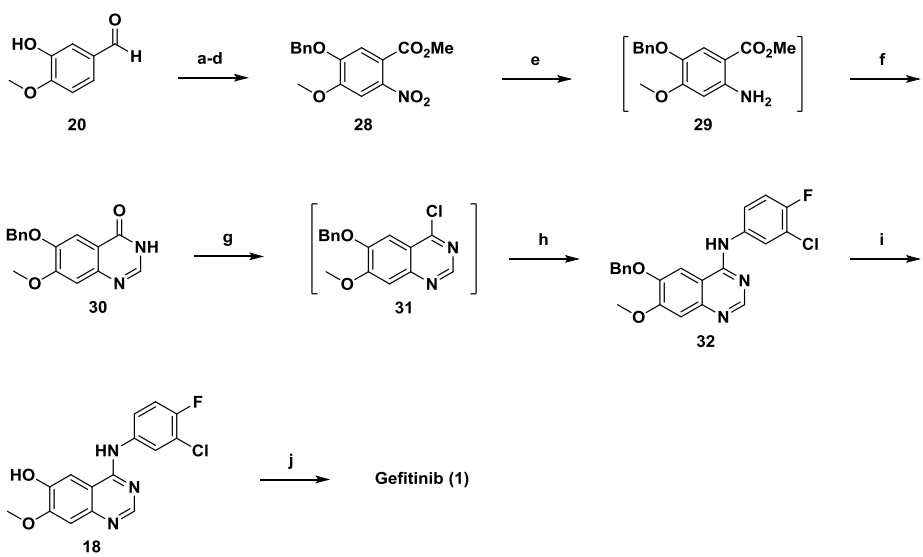

Reagents and conditions: (a) sulfamic acid, sodium chlorite, 5-10 °C, 83%; (b) methanolic HCl, 50-55 °C, 4 hr, 88.2%; (c) acetone, KI, K_2CO_3, benzyl chloride, reflux, 91.3%; (d) acetic acid, conc. HNO_3, 25-40 °C, 93.5%; (e) Fe/acetic acid, 50-60 °C; (f) formamidine acetate, reflux, 12 hr, 91.0% (for 2 steps); (g) oxalyl chloride, DIPEA, chloroform, 60-65 °C; (h) 3-chloro-4-fluoroaniline, IPA, 60-65 °C, 93.0% (for 2 steps); (i) methane sulfonic acid, chloroform, reflux, 91%; (j) KI, K_2CO_3, TBAB, 3-morpholinopropyl chloride, reflux, 81%

As can be seen from the previously reported literatures, introduction of morpholinopropyl group at C-6 position of the quinazoline ring is a necessary part of improvement in order to improve the overall yield and reduce process steps. Herein we describe our recent studies on the selective *O*-alkylation of 4-anilinoquinazolines and its application to a highly practical and efficient synthesis of gefitinib.

II. Results and Discussion

1. Synthetic strategy for gefitinib synthesis

Synthetic strategy for the successful synthesis of gefitinib are as follows, outlined in **Figure 11**. The key part of our strategy involves selective *O*-alkylation of 4-anilinoquinazolines, which suppressed the generation of *N*-alkylation product, by using a transient TMS protection group. We anticipated the dramatic improvements over the conventional synthetic procedures reported previously through the use of this process. By employing our process, we also planned to produce gefitinib from commercially available starting material, on a multigram scale.

Figure 11. Synthetic strategy for the synthesis of 6-alkoxy quinazoline derivatives

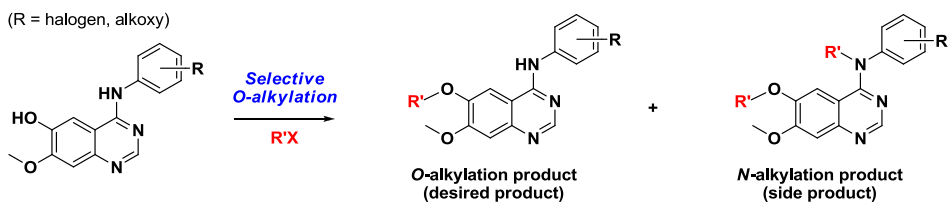

2. Screening results for *O*-alkylation of various compounds

2-1. *O*-alkylation of 18 with an assistance of TMSI as a transient protection group

We initially investigated selective *O*-alkylation of intermediate **18** to suppress the undesired *N*-alkylation. We explored the effect of acid-amine salt, catalysts, and protection to develop a sustainable and economical process (**Table 3**).

Upon use of acid-amine salt as a masking group for aniline, the *N*-alkylation product of 13.5% (entry 1) was observed after completion of the reaction. The use of DMAP or KI as a

Table 3. *O*-alkylation of 18 with an assistance of TMSI as a transient protection group

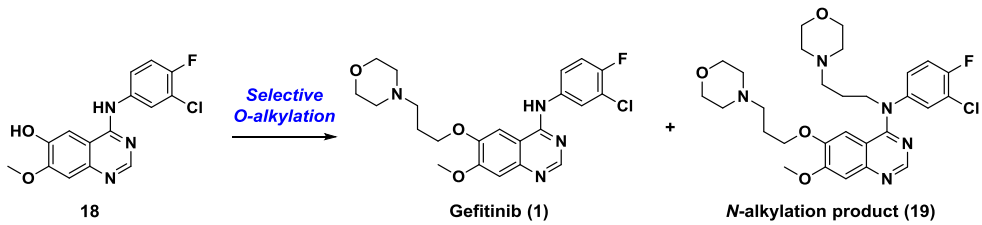

Entry	*N*-protecting agent	Catalyst	*N*-alkylation product before purification[a] (%)	*N*-alkylation product after purification[a] (%)	Yield[b] (%)
1	HCl	-	13.5	1.2	64.5
2	-	DMAP	10.0	1.0	61.6
3	-	KI	20.0	1.3	63.9
4	TMSI	-	2.2	0.2	78.5
5	TMSI	DMAP	0.3	N.D.	90.1

[a] Determined by HPLC. [b] Isolated yield.

catalyst also gave poor results (entries 2 and 3). Interestingly, transient protection with TMSI in the presence of DMAP as a catalyst afforded only 0.3% of the *N*-alkylation product (entry 5), compared to approximately 30% for the previously known method.[50] In addition, the *N*-alkylated impurity was completely removed by a simple purification process. The postulated mechanism for the selective *O*-alkylation is depicted in **Figure 12**.

Figure 12. Postulated mechanism for selective *O*-alkylation of 18 using a transient protection group

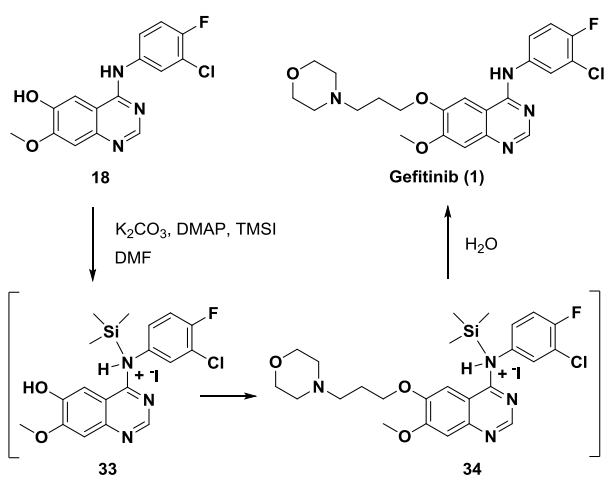

Upon treatment of hydroxyquinazoline (**18**) with alkylating agent, base, catalyst, and TMSI, initial binding of TMS to the aniline amine appears to afford the amine salt intermediate (**33**), which is substantially a TMS-protected form of substrate **18**. Subsequently, the *O*-alkylated intermediate **34** is formed through a selective *O*-alkylation with morpholinopropyl chloride. The TMS group was easily removed with water during the simple work-up procedure and gefitinib was obtained with high purity. Obviously, the amino group could not undergo *N*-alkylation because of transient TMS-protection of the amino group. We confirmed the postulated mechanism by analysis of NMR spectra of the proposed intermediates.[51]

2-2. *O*-alkylation of 4-anilinoquinazoline moieties with an assistance of TMSI

Table 4. Selective *O*-alkylation of 4-anilinoquinazoline moieties with an assistance of TMSI

Entry	R^1	R^2	*N*-protection agent	*N*-alkylated product[a] (%)	Yield[b] (%) (product)
1	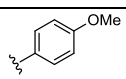	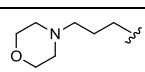	-	23.2	64.5
2	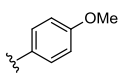	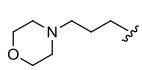	TMSI	0.2	88.6 (**35**)
3	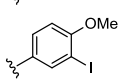	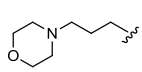	-	39.7	53.9
4	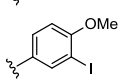	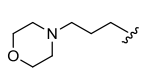	TMSI	1.3	83.5 (**36**)
5	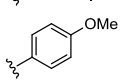		-	30.6	54.4
6	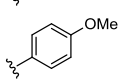		TMSI	9.5	75.0 (**37**)
7	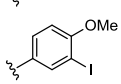		-	21.5	62.0
8	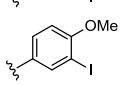		TMSI	4.4	80.2 (**38**)

[a] Determined by HPLC after completion of reaction. [b] Isolated yield after purification.

Next, we explored the applicability of the selective *O*-alkylation to other anilinoquinazoline moieties. As in the case of gefitinib, the selective *O*-alkylation with transient protection was possible in a variety of anilinoquinazolines regardless of substituents on aniline and alkylation reagent. (**Table 4**).

2-3. Alkylation of amino alcohols

Table 5. Alkylation of amino alcohols

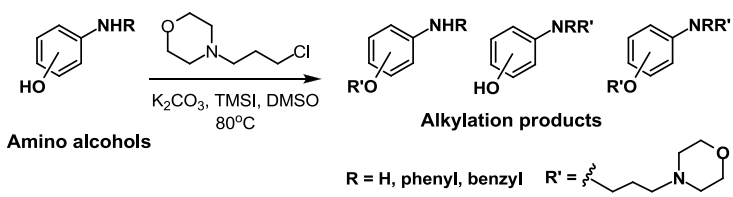

Amino Alcohol		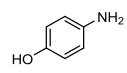	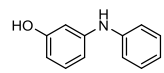	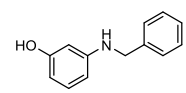
Major Product	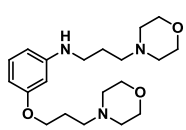	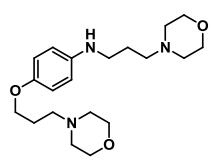	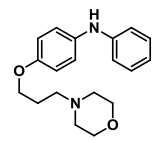	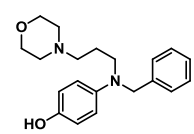
	di-alkylation product (**39**)	*di*-alkylation product (**40**)	*O*-alkylation product (**41**)	*N*-alkylation product (**42**)

We further examined the selective *O*-alkylation of the synthetically important aminophenol moieties under the optimized conditions as shown in **Table 5**. The primary amines produced preferentially a *di*-alkylation product (**39**, **40**) by both *O* and *N*-alkylation. As anticipated, 3-(phenylamino)phenol showed a good selectivity for the *O*-alkylation product **41**. However, alkylation of 3-(benzylamino)phenol produced only the *N*-alkylated product **42**, which is likely due to the good nucleophilicity of arylalkyl amine.

3. Examination of deacetylation conditions for the preparation of intermediate 18

Deacetylation of **17** according to the reported procedure[46] (r.t., 17 hr and then reflux, 1.5 hr) produced 4-(3-chloro-4-fluorophenylamino)-7-methoxyquinazolin-6-ol (**18**) along with unreacted **17** (approximately 2%), which ultimately affected the purity of the final gefitinib. Thus, an additional purification process to remove the remained **17** was necessary and limited its utilization for the commercial production. We have also examined other reported deacetylation conditions[52] as shown in **Table 6**. Deacetylation of **17** (entry 4) by lithium hydroxide treatment was completed in 0.5 hr and less than 0.1% of unreacted **17** was observed. Deacetylation of **17** with sodium hydroxide (entry 2) or potassium hydroxide (entry 3) was completed in 1 hr, which is shorter than that with NH_4OH (18.5 hr), with only approximately 0.1% of **17** remained. However, additional procedure to remove the Na or K adduct was still necessary because the byproducts were less soluble in a solution of MeOH and water used for the deacetylation. Fortunately, the Li adduct was more soluble in a solution of MeOH and water, and the byproduct was easily removed by filtration of the reaction mixture.

Table 6. Examination of deacetylation conditions for the preparation of intermediate 18

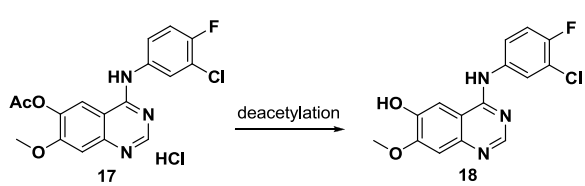

Entry	Reagent	Temperature	Reaction time (hr)	Remained **17** (%)[a]
1	NH_4OH	r.t. to reflux	18.5	2.0
2	NaOH	r.t.	1	0.1
3	KOH	r.t.	1	0.1
4	LiOH	r.t.	0.5	0.1

[a] Determined by HPLC after completion of reaction.

4. Optimal process for Gefitinib

Our synthesis of gefitinib includes four reaction steps starting from 7-methoxy-4-oxo-3,4-dihydroquinazolin-6-yl acetate (**15**) as shown in **Scheme 1**. Chlorination of quinazolone **15** followed by condensation with 3-chloro-4-fluoroaniline at 65 °C afforded **17** in a quantitative yield. Acetoxyquinazoline **17** was conveniently converted into hydroxyquinazoline **18** in a 90% yield after lithium hydroxide treatment in a mixture of MeOH and water (1:1). Finally, facile alkylation of hydroxyquinazoline **18** with 4-(3-chloropropyl)morpholine in the presence of TMSI followed by purification utilizing recystallization afforded pure gefitinib (**1**) with more than 99 % purity by HPLC.

Scheme 5. Optimal process for Gefitinib

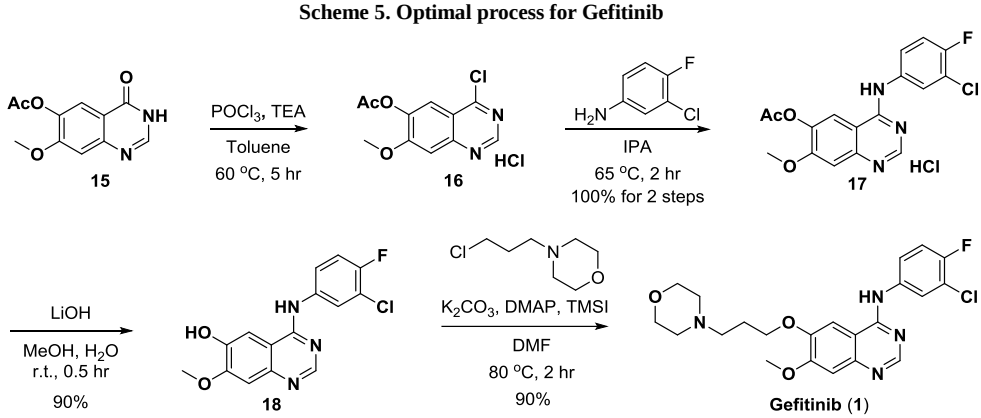

III. Conclusion

We have developed an efficient and practical large-scale process for the preparation of gefitinib with high purity (> 99% by HPLC). The key step of the synthesis includes selective *O*-alkylation, which significantly suppressed the generation of *N*-alkylation product, by using a transient TMS protection group. Our process ultimately provided significant improvement in both the yield and purity of the final gefitinib. By employing our process, we produced Gefitinib with a 81.1% overall yield from a commercially available starting material, 7-methoxy-4-oxo-3,4-dihydroquinazolin-6-yl acetate (**15**), on a multigram scale. We further confirmed that our procedure is applicable for a variety of anilinoquinazolines and can be widely utilized by synthetic and medicinal chemists.

IV. Experimental

General experimental

^{1}H spectra and ^{13}C spectra were recorded using a Bruker DPX 400 Spectrometer. All purity values were obtained by HPLC analysis using HPLC 1200 Series from Agilent Technologies. All NMR spectra were measured using 400 UltraShield NMR. Chemical shifts are expressed in parts per million (ppm, δ) downfield from tetramethylsilane, and were referenced to the deuterated solvent (DMSO-d_6). ^{1}H-NMR data are reported in the order of chemical shift, multiplicity (s, singlet; d, doublet; t, triplet; q, quartet; m, multiplet and/or multiple resonances), number of protons, and coupling constant in hertz (Hz). High resolution mass spectra were obtained with a Synapt G2 instrument.

HPLC analysis. Hypersil C18, 4.6 mm X 250 mm (5 μm), λ = 250 nm, flow rate 1.0 mL/min, mobile phase (60:40) buffer/acetonitrile (buffer 5 mol% ammonium acetate aqueous solution).

Synthesis

4-(3-chloro-4-fluorophenylamino)-7-methoxyquinazolin-6-yl acetate hydrochloride (17). To a solution of dihydroquinazoline **15** (500.0 g, 2.135 mol) in toluene (5.0 L), were added triethylamine (324.0 g, 3.202 mol) and phosphoryl chloride (491.0 g, 3.202 mol). The reaction mixture was stirred at 60 °C for 5 hr and cooled to about 20 °C. Isopropylalcohol (3.5 L) and then 3-chloro-4-fluoroaniline (341.8 g, 2.348 mol) in isopropylalcohol (2.5 L) was slowly added. The reaction mixture was heated to 65 °C and stirred for 2 hr (completion of the reaction was confirmed by HPLC and TLC). The reaction mixture was cooled to 20 °C and stirred for 1 hr. The precipitate was collected by filtration, washed with isopropylalcohol

(2.5 L), and dried at 40 °C for 2 hr to give **17** as yellow powder (892.6 g, 100%). ^{1}H NMR (400MHz, DMSO-d_6): δ 2.40 (s, 3H), 4.03 (s, 3H), 7.53-7.59 (m, 2H), 7.72-7.78 (m, 1H), 8.02-8.07 (m, 1H), 8.84 (s, 1H), 8.97 (s, 1H). ^{13}C NMR (175 MHz, DMSO-d_6): δ 168.9, 159.3, 158.0, 156.3, 154.9, 151.5, 140.8, 134.6, 126.9, 125.6, 119.7, 119.6, 119.1, 117.5, 117.3, 107.6, 57.5, 45.8, 26.0, 20.7. HRMS: Calcd for $C_{17}H_{13}N_3O_3FCl$ [M+H]+ 362.0707; Found 362.0708. Elemental Anal. Calcd for $C_{17}H_{14}Cl_2FN_3O_3$: C, 51.28; H, 3.54; N, 10.55. Found: C, 51.91; H, 4.94; N, 10.57.

***O*-alkylation of 18 with an assistance of TMSI as a transient protection group (Table 3)**

***N*-(3-chloro-4-fluorophenyl)-7-methoxy-6-(3-morpholinopropoxy)-quinazoline-4-amine** (**1**, entry 1 in table 3). To a suspension of HCl salt of compound **18** (712.1 mg, 2.0 mmol) in dimethylsulfoxide (6.5 mL) were added potassium carbonate (975.9 mg, 7.0 mmol). To a reaction mixture was slowly added 4-(3-chloropropyl)morpholine (396.2 mg, 2.42 mol). The reaction mixture was heated to 80 °C and stirred for 2 hr (The termination of the reaction was confirmed using HPLC and TLC). The reaction mixture was cooled to 20 °C, and purified water (14.2 mL) was slowly added at this temperature and stirred for 30 min. The precipitate was collected by filtration, washed with purified water (14.2 mL), and dried at 50 °C for 3 hr to give gefitinib as pale yellow powder (576.5 mg, 64.5%).

***N*-(3-chloro-4-fluorophenyl)-7-methoxy-6-(3-morpholinopropoxy)-quinazoline-4-amine** (**1**, entry 2 in table 3). To a suspension of compound **18** (639.4 mg, 2.0 mmol) in dimethylsulfoxide (6.5 mL) were added *N*,*N*-dimethylaminopyridine (24.4 mg, 0.2 mmol) and potassium carbonate (975.9 mg, 7.0 mmol). To a reaction mixture was slowly added 4-(3-chloropropyl)morpholine (396.2 mg, 2.4 mmol). The reaction mixture was heated to 80 °C

and stirred for 2 hr (The termination of the reaction was confirmed using HPLC and TLC). The reaction mixture was cooled to 20 °C, and purified water (12.8 mL) was slowly added at this temperature and stirred for 30 min. The precipitate was collected by filtration, washed with purified water (12.8 mL), and dried at 50 °C for 3 hr to give gefitinib as pale yellow powder (550.6 mg, 61.6%).

***N*-(3-chloro-4-fluorophenyl)-7-methoxy-6-(3-morpholinopropoxy)-quinazoline-4-amine** (**1**, entry 3 in table 3). To a suspension of compound **18** (639.4 mg, 2.0 mmol) in dimethylsulfoxide (6.5 mL) were added potassium iodide (33.2 mg, 0.2 mmol) and potassium carbonate (975.9 mg, 7.0 mmol). To a reaction mixture was slowly added 4-(3-chloropropyl)morpholine (396.2 mg, 2.4 mmol). The reaction mixture was heated to 80 °C and stirred for 2 hr (The termination of the reaction was confirmed using HPLC and TLC). The reaction mixture was cooled to 20 °C, and purified water (12.8 mL) was slowly added at this temperature and stirred for 30 min. The precipitate was collected by filtration, washed with purified water (12.8 mL), and dried at 50 °C for 3 hr to give gefitinib as pale yellow powder (571.1 mg, 63.9%).

***N*-(3-chloro-4-fluorophenyl)-7-methoxy-6-(3-morpholinopropoxy)-quinazoline-4-amine** (**1**, entry 4 in table 3). To a suspension of compound **18** (639.4 mg, 2.0 mmol) in dimethylsulfoxide (6.5 mL) was potassium carbonate (975.9 mg, 7.0 mmol). The reaction mixture was cooled to -10 °C, and iodotrimethylsilane (400.2 mg, 2.0 mmol) was slowly added and stirred at 15 ℃ for 1 hr. To a reaction mixture was slowly added 4-(3-chloropropyl)morpholine (396.2 mg, 2.4 mmol). The reaction mixture was heated to 80 °C and stirred for 2 hr (The termination of the reaction was confirmed using HPLC and TLC).

The reaction mixture was cooled to 20 °C, and purified water (12.8 mL) was slowly added at this temperature and stirred for 30 min. The precipitate was collected by filtration, washed with purified water (12.8 mL), and dried at 50 °C for 3 hr to give gefitinib as pale yellow powder (701.6 mg, 78.5%).

***N*-(3-chloro-4-fluorophenyl)-7-methoxy-6-(3-morpholinopropoxy)quinazoline-4-amine** (**1**, entry 5 in table 3). To a suspension of compound **18** (645.0 g, 2.017 mol) in *N*,*N*-dimethylformamide (6.5 L) were added potassium carbonate (975.9 g, 7.061 mol) and *N*,*N*-dimethylaminopyridine (24.6 g, 0.202 mol). The reaction mixture was cooled to -10 °C, and iodotrimethylsilane (589.3 g, 2.017 mol) was slowly added and stirred at 15 °C for 1 hr. To a reaction mixture was slowly added 4-(3-chloropropyl)morpholine (396.2 g, 2.421 mol) in *N*,*N*-dimethylformamide (645.0 mL). The reaction mixture was heated to 80 °C and stirred for 2 hr (The termination of the reaction was confirmed using HPLC and TLC). The reaction mixture was cooled to 20 °C, and purified water (14.2 L) was slowly added and stirred for 30 min. The precipitate was collected by filtration, washed with purified water (645.0 mL), and dried at 50 °C for 3 hr to give gefitinib as pale yellow powder (811.4 g, 90.1%). HPLC purity: 99.21% (*N*-alkylated impurity : not detected). ^{1}H-NMR (400MHz, DMSO-d_6): δ 1.95-2.02 (m, 2H), 2.38 (br, 4H), 2.45-2.50 (m, 2H), 3.56-3.58 (m, 4H), 3.93 (s, 3H), 4.17 (t, 2H, J = 6.3 Hz), 7.19 (s, 1H), 7.44 (t, 1H, J = 9.1 Hz), 7.76-7.80 (m, 2H), 8.10 (dd, 1H, J = 4.2 Hz, 2.6 Hz), 8.49 (s, 1H), 9.57 (s, 1H). ^{13}C NMR (175 MHz, DMSO-d_6): δ 156.5, 155.0, 154.3, 153.1, 152.9, 148.8, 147.4, 137.3, 124.0, 122.8, 119.3, 119.2, 117.0, 109.2, 107.8, 103.0, 67.6, 66.7, 56.3, 55.4, 53.9, 26.3. HRMS: Calcd for $C_{22}H_{24}ClFN_4O_3$ [M+H]+ 447.1594; Found 447.1599. Elemental Anal. Calcd for $C_{22}H_{24}ClFN_4O_3$: C, 59.13; H, 5.41; N, 12.54. Found: C, 59.09; H, 5.48; N, 12.52.

Confirmation of 4-((3-chloro-4-fluorophenyl)(trimethylsilyl)amino)-7-methoxyquinazolin-6-ol, iodide (reaction intermediate 33). To a suspension of compound **18** (2.0 mmol) in dimethylsulfoxide-d_6 (5.0 mL) was added potassium carbonate (7.0 mmol). The reaction mixture was cooled to -10 °C, and iodotrimethylsilane (2.0 mmol) was slowly added and stirred at 15 °C for 1 hr. About 1.0 mL of the reaction sample was subjected to NMR analysis. ^{1}H NMR (400MHz, DMSO-d_6): δ 0.04 (s, 9H), 3.99 (s, 3H), 7.21 (s, 1H), 7.44 (t, 1H, J = 9.1 Hz), 7.76-7.81 (m, 1H), 8.14-8.16 (m, 1H), 8.58 (s, 1H), 9.85 (br, 1H), 9.94 (s, 1H).

Confirmation of *N*-(3-chloro-4-fluorophenyl)-7-methoxy-6-(3-morpholinopropoxy)-*N*-(trimethylsilyl)-quinazoline-4-amine, iodide (reaction intermediate 34). To a suspension of compound **18** (2.0 mmol) in dimethylsulfoxide-d_6 (5.0 mL) were added potassium carbonate (7.0 mmol) and *N*,*N*-dimethylaminopyridine (0.2 mmol). The reaction mixture was cooled to -10 °C, and iodotrimethylsilane (2.0 mmol) was slowly added and stirred at 15 °C for 1 hr. To a reaction mixture was slowly added 4-(3-chloropropyl)morpholine (2.4 mmol) in *N*,*N*-dimethylsulfoxide-d_6 (1.0 mL). The reaction mixture was heated to 80 °C and stirred for 2 hr. About 1.0 mL of the reaction sample was subjected to NMR analysis. ^{1}H-NMR (400MHz, DMSO-d_6): δ 0.41 (s, 9H), 2.28-2.32 (m, 2H), 3.14-3.21 (m, 2H), 3.38-3.41 (m, 2H), 3.55-3.70 (m, 4H), 3.98-4.09 (m, 5H), 4.28-4.33 (m, 2H), 7.28 (s, 1H), 7.57-7.68 (m, 2H), 7.96-7.98 (m, 1H), 8.09 (s, 1H), 8.95 (s, 1H), 9.50 (br, 1H).

***N*-(3-chloro-4-fluorophenyl)-7-methoxy-6-(3-morpholinopropoxy)-*N*-(3-morpholinopropyl)-quinazoline-4-amine (*N*-alkylated impurity, 19)**. ^{1}H-NMR (400MHz, DMSO-d_6): δ 1.85-1.94 (m, 4H), 2.26-2.44 (m, 12H), 3.92 (s, 3H), 4.06 (t, 2H, J = 6.5 Hz), 4.14 (t, 2H, J = 6.5 Hz), 6.90 (s, 1H), 6.92-6.96 (m, 1H), 7.17-7.25 (m, 2H), 7.65 (s, 1H), 7.98 (s, 1H).

Selective *O*-alkylation of 4-anilinoquinazoline moieties with an assistance of TMSI (Table 4)

General procedure 1 (without TMSI). To a suspension of 6-hydroxy quinazoline compound (2.0 mmol) in dimethylsulfoxide (6.0 mL) was potassium carbonate (7.0 mmol). To a reaction mixture was slowly added 4-(3-chloropropyl)morpholine (2.4 mmol). The reaction mixture was heated to 80 °C and stirred for 2 hr (The termination of the reaction was confirmed using HPLC and TLC). The reaction mixture was cooled to 20 °C, and purified water (12.0 mL) was slowly added and stirred for 30 min. The precipitate was collected by filtration, washed with purified water (12.0 mL) and dried at 50 °C for 3 hr to give 6-alkoxy quinazoline compound as pale yellow powder.

General procedure 2 (with TMSI). To a suspension of 6-hydroxy quinazoline compound (2.0 mmol) in dimethylsulfoxide (6.0 mL) was potassium carbonate (7.0 mmol). The reaction mixture was cooled to -10 °C, and iodotrimethylsilane (2.0 mmol) was slowly added and stirred at 15 °C for 1 hr. To a reaction mixture was slowly added 4-(3-chloropropyl)morpholine (2.4 mmol). The reaction mixture was heated to 80 °C and stirred for 2 hr (The termination of the reaction was confirmed using HPLC and TLC). The reaction mixture was cooled to 20 °C, and purified water (12.0 mL) was slowly added and stirred for 30 min. The precipitate was collected by filtration, washed with purified water (12.0 mL) and dried at 50 °C for 3 hr to give 6-alkoxy quinazoline compound as pale yellow powder.

7-methoxy-*N*-(4-methoxyphenyl)-6-(3-morpholinopropoxy)quinazolin-4-amine (35). ^{1}H-NMR (400MHz, DMSO-d_6): δ 1.95-2.01 (m, 2H), 2.38 (br, 4H), 2.45-2.51 (m, 2H), 3.57 (t, 4H, J = 4.5 Hz), 3.77 (s, 3H), 3.92 (s, 3H), 4.16 (t, 2H, J = 6.3 Hz) 6.94-6.98 (m, 2H), 7.15 (s, 1H), 7.59-7.63 (m, 2H), 7.83 (s, 1H), 8.37 (s, 1H), 9.45 (br, 1H). ^{13}C NMR (175 MHz, DMSO-d_6): δ 157.10, 156.12, 154.62, 153.50, 148.50, 147.18, 132.71, 124.96, 114.06, 109.20, 107.67, 103.27, 67.56, 66.65, 56.22, 55.65, 55.45, 53.90. HRMS: Calcd for $C_{23}H_{28}N_4O_4$ [M+H]+ 425.2189; Found 425.2189.

***N*-(3-iodo-4-methoxyphenyl)-7-methoxy-6-(3-morpholinopropoxy)quinazoline-4-amine (36)**. ^{1}H-NMR (400MHz, DMSO-d_6): δ 1.95-2.02 (m, 2H), 2.38 (br, 4H), 2.42-2.51 (m, 2H), 3.59 (t, 4H, J = 4.5 Hz), 3.81 (s, 3H), 3.92 (s, 3H), 4.16 (t, 2H, J = 6.4 Hz) 7.04 (d, 1H, J = 8.9 Hz), 7.16 (s, 1H), 7.80-7.83 (m, 2H), 8.15 (s, 1H), 8.42 (s, 1H), 9.43 (br, 1H). ^{13}C NMR (175 MHz, DMSO-d_6): δ 156.74, 154.73, 154.53, 153.32, 148.61, 147.23, 134.24, 133.26, 124.46, 123.56, 111.53, 109.19, 107.70, 103.10, 85.54, 67.54, 66.65, 57.01, 56.28, 55.44, 53.91, 26.34. HRMS: Calcd for $C_{23}H_{27}IN_4O_4$ [M+H]+ 551.1151; Found 551.1155.

6,7-dimethoxy-*N*-(4-methoxyphenyl)quinazoline-4-amine (37). ^{1}H-NMR (400MHz, DMSO-d_6): δ 3.78 (s, 3H), 3.93 (s, 3H), 3.95 (s, 3H), 6.97 (d, 2H, J = 7.4 Hz), 7.17 (s, 1H), 7.62 (d, 2H, J = 7.6 Hz), 7.83 (s, 1H), 8.38 (s, 1H), 9.41 (br, 1H). ^{13}C NMR (175 MHz, DMSO-d_6): δ 157.10, 156.14, 154.51, 153.53, 149.18, 147.23, 132.67, 124.93, 114.11, 109.14, 107.62, 102.38, 56.64, 56.23, 55.68. HRMS: Calcd for $C_{17}H_{17}N_3O_3$ [M+H]+ 312.1344; Found 312.1348.

***N*-(3-iodo-4-methoxyphenyl)-6,7-dimethoxyquinazolin-4-amine (38)**. ^{1}H-NMR (400MHz, DMSO-d_6): δ 3.84 (s, 3H), 3.93 (s, 3H), 3.95 (s, 3H), 7.05 (d, 2H, J = 8.7 Hz), 7.17 (s, 1H), 7.80-7.84 (m, 2H), 8.15 (s, 1H), 8.43 (s, 1H), 9.42 (br, 1H). ^{13}C NMR (175 MHz, DMSO-d_6): δ 170.81, 156.73, 154.62, 154.55, 153.36, 149.30, 147.30, 134.21, 133.19, 124.39, 111.57, 109.14, 107.65, 102.22, 85.57, 60.23, 57.01, 56.64, 56.26. HRMS: Calcd for $C_{17}H_{16}IN_3O_3$ [M+H]+ 438.0318; Found 438.0315.

Alkylation of amino alcohols (Table 5)

General procedure. To a suspension of amino alcohol compound (2.0 mmol) in dimethylsulfoxide (6.0 mL) was potassium carbonate (7.0 mmol). The reaction mixture was cooled to -10 °C, and iodotrimethylsilane (2.0 mmol) was slowly added and stirred at 15 °C for 1 hr. To a reaction mixture was slowly added 4-(3-chloropropyl)morpholine (2.4 mmol). The reaction mixture was heated to 80 °C and stirred for 2 hr (The termination of the reaction was confirmed using HPLC and TLC). The reaction mixture was cooled to 20 °C, and purified water (12.0 mL) was slowly added and stirred for 30 min. The precipitate was collected by filtration, washed with purified water (12.0 mL) and dried at 50 °C for 3 hr to give alkylated amino alcohol compound as pale yellow powder.

3-(3-morpholinopropoxy)-*N*-(3-morpholinopropyl)aniline (39). ^{1}H-NMR (400MHz, DMSO-d_6): δ 1.83-1.90 (m, 2H), 2.35-2.51 (m, 6H), 3.56 (br, 4H), 3.93-4.00 (m, 2H), 6.38 (d, 1H, J = 8.1 Hz), 6.60-6.66 (m, 2H), 6.81-6.89 (m, 1H), 7.07-7.13 (m, 3H), 7.22-7.28 (m, 2H), 8.15 (s, 1H). ^{13}C NMR (100 MHz, DMSO-d_6): δ 160.03, 158.03, 145.83, 145.22, 143.62, 143.02, 139.14, 130.36, 129.71, 129.62, 120.90, 120.32, 118.05, 117.62, 110.89, 109.41, 106.08, 103.02, 101.60, 73.40, 66.96, 66.65, 65.94, 55.36, 55.31, 53.87, 53.83, 26.35, 26.18. MS (*m/z*): 313 $(M+H)^+$.

4-(3-morpholinopropoxy)-*N*-(3-morpholinopropyl)aniline (40). ^{1}H-NMR (400MHz, DMSO-d_6): δ 1.62-1.66 (m, 2H), 2.24-2.44 (m, 6H), 3.28 (t, 2H, J = 6.8 Hz), 3.55 (br, 4H), 4.38 (br, 2H), 6.58 (s, 4H), 7.18-7.22 (m, 3H), 7.27-7.31 (m, 2H), 8.56 (s, 1H). ^{13}C NMR (100 MHz, DMSO-d_6): δ 149.17, 142.13, 140.29, 128.72, 127.40, 126.94, 116.11, 115.36, 115.31, 66.69, 56.07, 55.28, 53.82, 49.94, 24.15. MS (*m/z*): 327 $(M+H)^+$.

4-(3-morpholinopropoxy)-*N*-phenylaniline (41). ^{1}H-NMR (400MHz, DMSO-d_6): δ 1.83-1.90 (m, 2H), 2.35-2.51 (m, 6H), 3.56 (br, 4H), 3.93-4.00 (m, 2H), 6.38 (d, 1H, J = 8.1 Hz), 6.60-6.66 (m, 2H), 6.81-6.89 (m, 1H), 7.07-7.13 (m, 3H), 7.22-7.28 (m, 2H), 8.15 (s, 1H). ^{13}C NMR (100 MHz, DMSO-d_6): δ 160.03, 158.03, 145.83, 145.22, 143.62, 143.02, 139.14, 130.36, 129.71, 129.62, 120.90, 120.32, 118.05, 117.62, 110.89, 109.41, 106.08, 103.02, 101.60, 73.40, 66.96, 66.65, 65.94, 55.36, 55.31, 53.87, 53.83, 26.35, 26.18. MS (*m/z*): 313 $(M+H)^+$.

3-(benzyl(3-morpholinopropyl)amino)phenol (42). ^{1}H-NMR (400MHz, DMSO-d_6): δ 1.62-1.66 (m, 2H), 2.24-2.44 (m, 6H), 3.28 (t, 2H, J = 6.8 Hz), 3.55 (br, 4H), 4.38 (br, 2H), 6.58 (s, 4H), 7.18-7.22 (m, 3H), 7.27-7.31 (m, 2H), 8.56 (s, 1H). ^{13}C NMR (100 MHz, DMSO-d_6): δ 149.17, 142.13, 140.29, 128.72, 127.40, 126.94, 116.11, 115.36, 115.31, 66.69, 56.07, 55.28, 53.82, 49.94, 24.15. MS (*m/z*): 327 $(M+H)^+$.

Examination of deacetylation conditions for the preparation of intermediate 18 (Table 6)

4-(3-chloro-4-fluorophenylamino)-7-methoxyquinazolin-6-ol (**18**, entry 1 in table 6). To a reaction flask were added compound **17** (30.0 g, 0.075 mol), and methanol (1,050 mL). To a reaction mixture was added 30% (w/w%) aqueous ammonia (37.6 mL) and then stirred at room temperature for 17 hr, and refluxed for 1.5 hr (The termination of the reaction was confirmed using HPLC). The reaction mixture was cooled to 20 °C and stirred for 30 min. The precipitate was collected by flitration, washed with methanol (150.0 mL) and dried at 40 °C for 3 hr to give compound **18** as pale yellow powder (22.6 g, 93.7%). Unreacted residue : 2.0% (compound **17**).

4-(3-chloro-4-fluorophenylamino)-7-methoxyquinazolin-6-ol (**18**, entry 2 in table 6). In the same manner as in preparation of compound **18** (entry 4 in table 6), with replacement of LiOH with NaOH. Unreacted residue : 0.1% (compound **17**).

4-(3-chloro-4-fluorophenylamino)-7-methoxyquinazolin-6-ol (**18**, entry 3 in table 6). In the same manner as in preparation of compound **18** (entry 4 in table 6), with replacement of LiOH with KOH. Unreacted residue : 0.1% (compound **17**).

4-(3-chloro-4-fluorophenylamino)-7-methoxyquinazolin-6-ol (**18**, entry 4 in table 6). To a reaction flask were added compound **17** (892.6 g, 2.241mol), methanol (8.9 L) and water (8.9 L). To a reaction mixture was added lithium hydroxide (161.1 g, 6.724 mol) and then vigorously stirred for 30 min. (The termination of the reaction was confirmed using HPLC and TLC). The reaction mixture was cooled to 20 °C and adjusted to pH 7.0 with 20% (v/v%)

acetic acid (5.4 L), and then stirred at 20 °C for 1 hr. The precipitate was collected by filtration, washed with methanol (4.5 L) and dried at 40 °C for 3 hr to give compound **18** as pale yellow powder (645.0 g, 90.0%). ^{1}H NMR (400MHz, DMSO-d_6): δ 4.02 (s, 3H), 7.41 (s, 1H), 7.51 (t, 1H, J = 9.1 Hz), 7.69-7.73 (m, 1H), 8.00-8.03 (m, 1H), 8.06 (s, 1H), 8.85 (s, 1H), 10.59 (br, 1H), 11.15 (br, 1H). ^{13}C NMR (175 MHz, DMSO-d_6): δ 156.32, 154.42, 154.01, 152.64, 152.38, 147.28, 146.69, 137.67, 137.66, 123.23, 122.17, 122.14, 119.18, 119.07, 116.98, 116.85, 110.02, 107.66, 105.74, 56.40. HRMS: Calcd for $C_{15}H_{12}ClFN_3O_2$ [M+H]+ 320.0602; Found 320.0602. Elemental Anal. Calcd for $C_{15}H_{11}ClFN_3O_2$: C, 56.35; H, 3.47; N, 13.14. Found: C, 55.81; H, 3.43; N, 13.01.

V. References

1. Sawyers, C. *Nature*, **2004**, 432, 294-297.

2. Li, J.; Chen, F.; Cona, M. M.; Feng, Y.; Himmelreich, U.; Oyen, R.; Verbruggen, A.; Ni, Y. *Targeted Oncology*, **2012**, 7, 69-85.

3. Flaherty, K. T.; Infante, J. R.; Daud, A.; Gonzalez, R.; Kefford, R. F.; Sosman, J; Hamid, O.; Schuchter, L.; Cebon, J.; Ibrahim, N.; Kudchadkar, R.; Burris III, H. A.; Falchook, G.; Algazi, A.; Lewis, K.; Long, G. V.; Puzanov, I.; Lebowitz, P.; Singh, A.; Little,S.; Sun, P.; Allred, A.; Ouellet, D.; Kim, K. B.; Patel, K.; Weber, J.*New England Journal of Medicine*, **2012**, 367, 1694-1703.

4. Zhang H.; Berezov A.; Wang Q.; Zhang G.; Drebin J.; Murali R.; Greene M. I. *Journal of Clinical Investigation*, **2007**, 117(8), 2051-2058

5. Earp H. S.; Dawson T.L.; Li X. et al. *Breast Cancer Research and Treatment*, **1995**, 35, 115-132

6. Schlessinger J. *Cell*, **2000**, 103(2), 211-225

7. Yarden Y.; Schlessinger J. *Biochemistry*, **1987**, 26(5) 1443–1451

8. Hsuan J. J. *Anticancer Research*, **1993**, 13, 2521-2522

9. Soler C.; Beguinot L.; Carpenter G. *Journal of Biological Chemistry*, **1994**, 269, 12320-12324

10. Yarden Y.; Sliwkowski M. X. *Nature Reviews Molecular Cell Biology*, **2001**, 2(2), 127-137

11. Salomon D. S.; Brandt R.; Ciardiello F. et al. *Critical Reviews in Oncology/Hematology*, **1995**, 19, 183-232

12. Xi, L.; Zhang, J. Q.;, Liu, Z. C.; Zhang, J. H.; Yan, J. F.; Jin, Y.; Lin, J. *Org. Biomol. Chem.*, **2013**, 11, 4367-4378.

13. Fry, D. W.; Kraker, A. J.; McMichael, A.; Ambroso, L. A.; Nelson, J. M.; Leopold, W.

R.; Connors, R. W.; Bridges, A. J. *Science*, **1994**, 265, 1093-1095.

14. Zhang, Y.; Huang, Y. J.; Xiang, H. M.; Wang, P. Y.; Hu, D. Y.; Xue, W.; Song, B. A.; Yang, S. *Eur. J. Med. Chem.*, **2014**, 78, 23-34.

15. Huang, Y.; Liu, G.; Hu, X.; Liu, H.; Hu, J.; Feng, Z.; Tang, B.; Qian, J.; Wang, Q.; Long, X. *Lett. Drug Des. Discov.*, **2014**, 11, 731-735.

16. Zhang, Y.; Chen, Z.; Lou, Y.; Yu, Y. *Eur. J. Med. Chem.*, **2009**, 44, 448-452.

17. Huang, Y.; Xie, H.; Liu, G.; Hu, X.; Su, L.; Hu, J.; Wang, Q.; Ding, Y. *Lett. Drug Des. Discov.*, **2014**, 11, 1090-1095.

18. Paul, K.; Sharma, A.; Luxami, V. *Bioorg. Med. Chem. Lett.*, **2014**, 24, 624-629.

19. Garofalo, A.; Goossens, L.; Six, P.; Lemoine, A.; Ravez, S.; Farce, A.; Depreux, P. *Bioorg. Med. Chem. Lett.*, **2011**, 21, 2106-2112.

20. Xu, Y. Y.; Li, S. N.; Yu, G. J.; Hub, Q. H.; Li, H. Q. *Bioorg. Med. Chem.*, **2013**, 21, 6084-6091.

21. Zhang, H. Q.; Gong, F. H.; Li, C. G.; Zhang, C.; Wang, Y. J.; Xu, Y. G.; Sun, L. P. *Eur. J. Med. Chem.*, **2016**, 109, 371-379.

22. Cheng, W.; Zhu, S.; Ma, X.; Qiu, N.; Peng, P.; Sheng, R.; Hu, Y. *Eur. J. Med. Chem.*, **2015**, 89, 826-834.

23. Cheng, W.; Yuan, Y.; Qiu, N.; Peng, P.; Sheng, R.; Hu, Y. *Bioorg. Med. Chem.*, **2014**, 22, 6796–6805.

24. Zhao, F.; Lin, Z.; Wang, F.; Zhao, W.; Dong, X. *Bioorg. Med. Chem. Lett.*, **2013**, 23, 5385–5388.

25. Li, R. D.; Zhang, X.; Li, Q. Y.; Ge, Z. M.; Li, R. T. *Bioorg. Med. Chem. Lett.*, **2011**, 21, 3637–3640.

26. Chandregowda, V.; Kush, A.K.; Reddy, G. C. *Eur. J. Med. Chem.*, **2009**, 44, 3046–3055.

27. Barbosa, M. L. C.; Lima, L. M.; Tesch, R.; Sant'Anna, C. M. R.; Totzke, F.; Kubbutat, M. H. G.; Schächtele, C.; Laufer, S. A.; Barreiro, E. J. *Eur. J. Med. Chem.*, **2014**, 71, 1-14.

28. Pham, H. T.; Hanson, R. N.; Olmsted, S. L.; Kozhushnyan, A.; Visentin, A.; Weglinsky, P. J.; Massero, C.; Bailey, K. *Tetrahedron Lett.*, **2011**, 52, 1053–1056.

29. Zhao, F.; Lin, Z.; Wang, F.; Zhao, W.; Dong, X. *Bioorg. Med. Chem. Lett*., **2013**, 23, 5385-5388.

30. Conconi, M.T.; Marzaro, G.; Urbani, L.; Zanusso, I.; Di Liddo, R.; Castagliuolo, I.; Brun, P.; Tonus, F.; Ferrarese, A.; Guiotto, A.; Chilin, A. *Eur. J. Med. Chem*., **2013**, 67, 373-383.

31. Zhang, X.; Su, M.; Chen, Y.; Li, J.; Lu, W. *Molecules*, **2013**, 18, 6491-6503.

32. Lü, S.; Zheng, W.; Ji, L.; Luo, Q.; Hao, X.; Li, X.; Wang, F. *Eur. J. Med. Chem*., **2013**, 61, 84-94.

33. Ban, H.S.; Tanaka, Y.; Nabeyama, W.; Hatori, M.; Nakamura, H. *Bioorg. Med. Chem*., **2010**,

18, 870-879.

34. Zhang, Q. W.; Diao, Y. Y.; Wang, F.; Fu, Y.; Tang, F.; You, Q. D.; Zhou, H. Y. *Med. Chem. Commun*., **201**3, 4, 979-986.

35. Cai, X.; Zhai, H. X.; Wang, J.; Forrester, J.; Qu, H.; Yin, L.; Lai, C. J.; Bao, R.; Qian, C. J. *Med. Chem*., **2010**, 53, 2000-2009.

36. Mowafy, S.; Farag, N. A.; Abouzid, K. A. *Eur. J. Med. Chem*., **2013**, 61, 132-145.

37. Rao, G. W.; Xu, G. J.; Wang, J.; Jiang, X. L.; Li, H. B. *Chem. Med. Chem*., **2013**, 8, 928-933.

38. Li, S.; Guo, C.; Sun, X.; Li, Y.; Zhao, H.; Zhan, D.; Lan, M.; Tang, Y. *Eur. J. Med. Chem*., **2012**, 49, 271-278.

39. Hamed, M. M.; Abou El Ella, D. A.; Keeton, A. B.; Piazza, G. A.; Abadi, A. H.; Hartmann, R. W.; Engel, M. *Chem. Med. Chem*., **2013**, 8, 1495-1504.

40. Xu, Y. Y.; Li, S. N.; Yu, G. J.; Hub, Q. H.; Li, H. Q. *Bioorg. Med. Chem*., **2013**, 21, 6084-6091.

41. Li, H. Q.; Li, D. D.; Lu, X.; Xu, Y. Y.; Zhu, H. L. *Bioorg. Med. Chem*., **2012**, 20, 317-323.

42. Li, D. D.; Fang, F.; Li, J. R.; Du, Q. R; Sun, J.; Gong, H. B.; Zhu, H. L. *Bioorg. Med. Chem. Lett*., **2012**, 22, 5870-5875.

43. Ban, H. S.; Usui, T.; Nabeyama, W.; Morita, H.; Fukuzawa, K.; Nakamura, H. *Org. Biomol. Chem*., **2009**, 7, 4415-4427.

44. Beckers, T.; Mahboobi, S.; Sellmer, A.; Winkler, M.; Eichhorn, E.;Pongratz, H.; Maier, T.; Ciossek, T.; Baer, T.; Kelter, G.; Fiebig, H.; Schmidt, M. *Med. Chem. Commun*., **2012**, 3, 829-835.

46. Gibson, K. H. PCT INt Appl. WO 1996/033980.

47. Gilday, J. P.; Moody, D. PCT INt Appl. WO 2004/024703.

48. Gilday, J. P.; Welham, M. J. PCT INt Appl. WO 2005/023783.

49. Kumar, N.; Chowdhary, A.; Gudaparthi, O.; Patel, N. G.; Soni, S. K.; Sharma, P. *Indian J. Chem., Sect. B*, **2014**, 1269-1274.

50. Lee, S. U.; Woo, D. G.; Kang, S. K.; Kim, D. J.; Park, D. J. PCT INt Appl. WO 2013/180403.

51. The chemical shift of ^{1}H NMR spectra for N-H and O-H of **18** is 10.58 ppm (N-H) and 11.15 ppm (O-H), respectively. Acid-amine salt **34** was obtained when **18** was treated with K_2CO_3, DMAP, and TMSI. Comparison of spectra obtained from intermediate **18** and **34** revealed the change of chemical shift from 10.59 ppm to 9.85 ppm for O-H and from 11.15 to 9.94 ppm for N-H, respectively. Upon completion of reaction of the C-6 hydroxyl group with morpholino propyl chloride, the resonance for O-H of intermediate **35** in ^{1}H NMR spectra disappeared whereas the resonance for N-H remained. The ^{1}H NMR spectra of gefitinib clearly showed the resonance for N-H at 9.56 ppm.

52. Qian, C.; Cai, X. PCT INt Appl. WO 2008/033748.

VI. Appendix

4-(3-chloro-4-fluorophenylamino)-7-methoxyquinazolin-6-yl acetate, hydrochloride.

▼ ^{1}H-NMR (DMSO-d_6, 400 MHz)

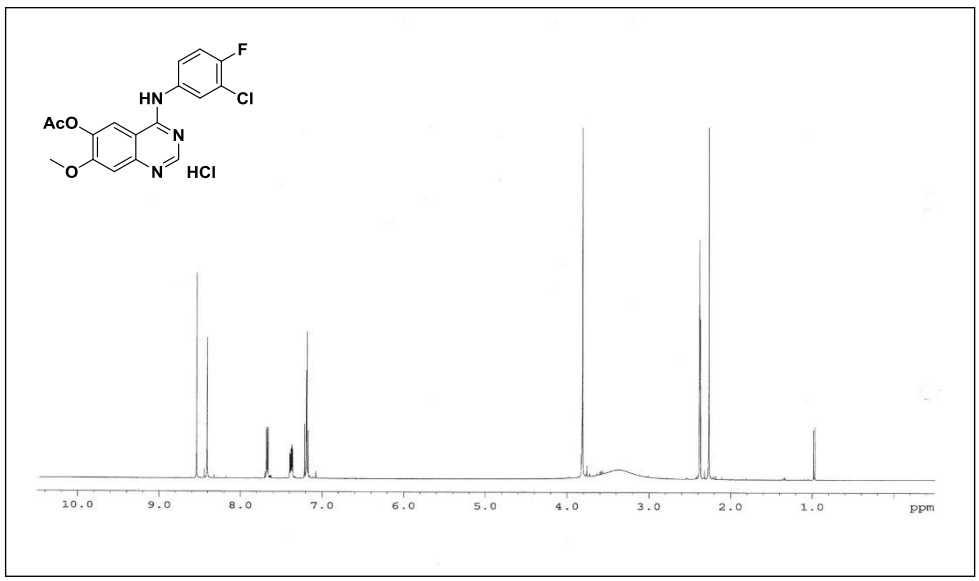

▼ ^{13}C-NMR (DMSO-d_6, 175 MHz)

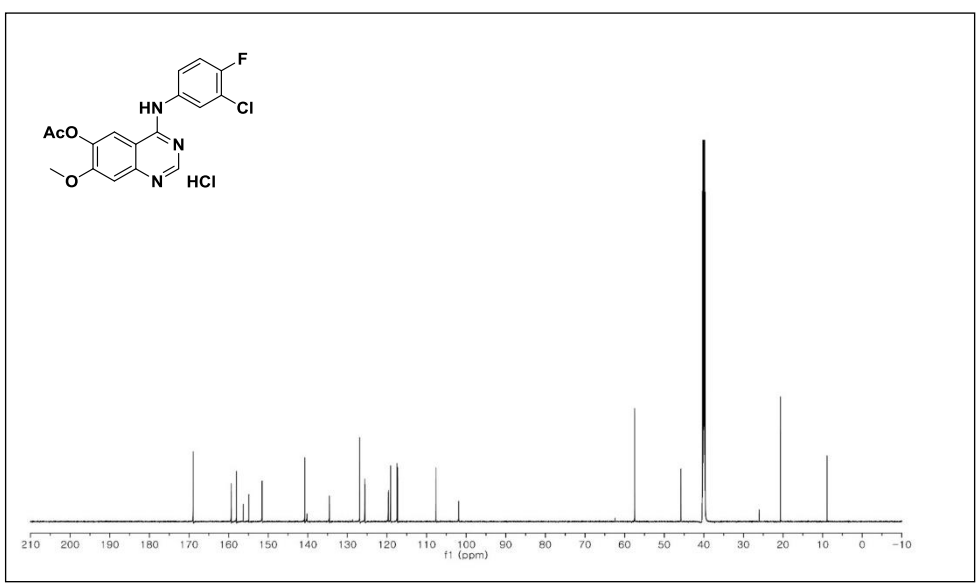

▼ High-Resolution Mass

Data of High-Resolution Mass Spectrum

Elemental Composition Report

Single Mass Analysis
Tolerance = 1.0 PPM / DBE: min = -1.5, max = 50.0
Element prediction: Off
Number of isotope peaks used for i-FIT = 3

Monoisotopic Mass, Even Electron Ions
162 formula(e) evaluated with 1 results within limits (all results (up to 1000) for each mass)
Elements Used:
C: 1-20 H: 1-20 N: 1-5 O: 1-5 F: 1-2 Cl: 1-2

Mass	Calc. Mass	mDa	PPM	DBE	i-FIT	Norm	Conf(%)	Formula
362.0707	362.0708	-0.1	-0.3	11.5	284.6	n/a	n/a	C17 H14 N3 O3 F Cl

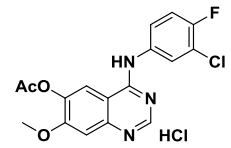

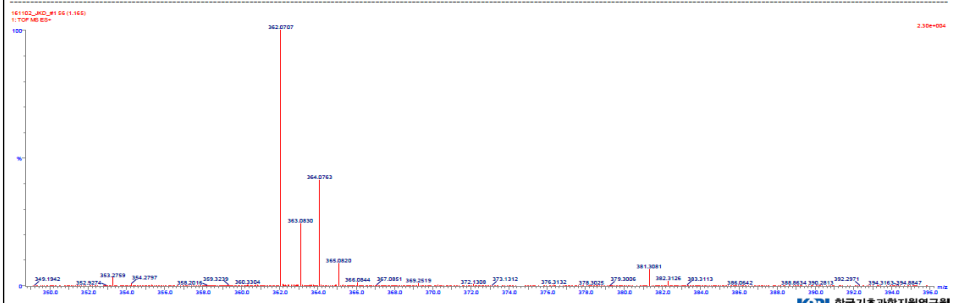

▼ Elemental analysis

Operator ID:	SNU-EA2000
Company name:	ThermoFinnigan
Method name:	CHN-S
Printed:	2012-12-28 15:38
Elemental Analyser method:	
Sampler method:	
Sample ID:	AcQA (# 13)
Analysis type:	UnkNown
Calibration method:	K Factors
Sample weight:	1.667
Protein factor:	6.25

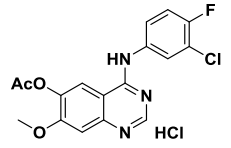

Element Name		Ret.Time	Area	BC	Area ratio	K factor
Nitrogen	10.5699	52	367473	RS	11.706620	.208554E+07
Carbon	51.9065	76	4301868	RS	1.000000	.496719E+07
Hydrogen	4.9378	209	1280559	RS	3.359367	.155065E+08
Totals	67.4142		5949900			

***N*-(3-chloro-4-fluorophenyl)-7-methoxy-6-(3-morpholinopropoxy)-quinazoline-4-amine**

▼ ^{1}H-NMR (DMSO-d_6, 400 MHz)

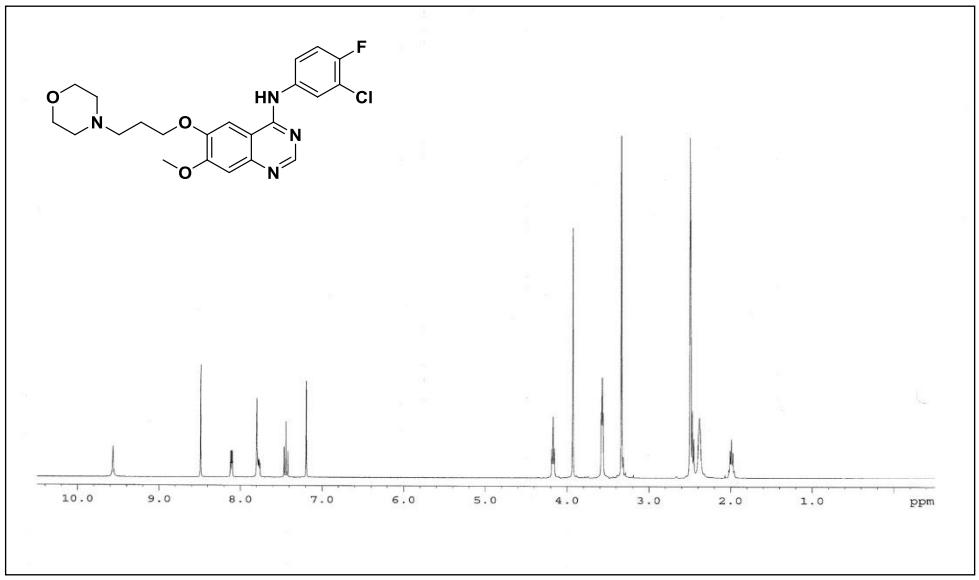

▼ ^{13}C-NMR (DMSO-d_6, 175 MHz)

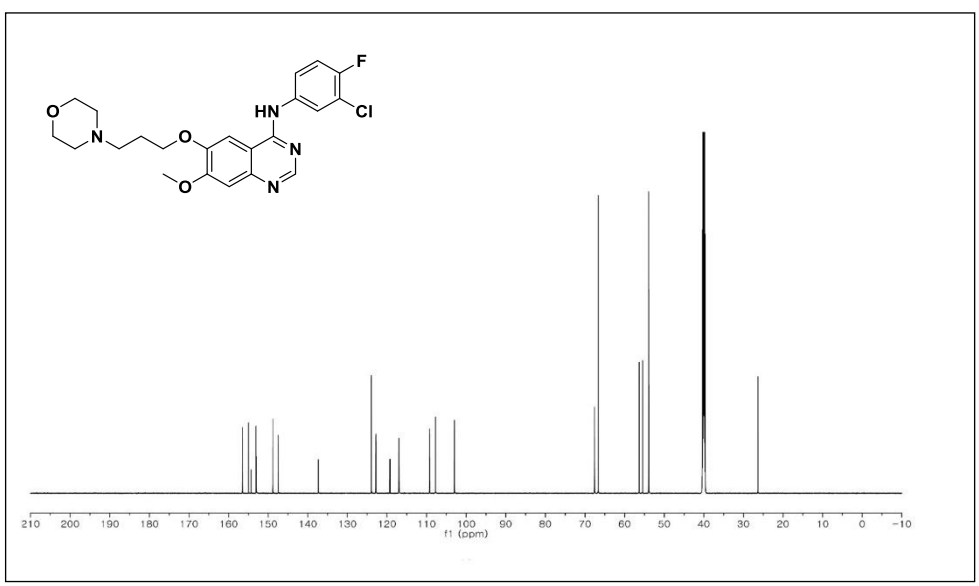

▼ High-Resolution Mass

Data of High-Resolution Mass Spectrum

Elemental Composition Report

Single Mass Analysis
Tolerance = 2.0 PPM / DBE: min = -1.5, max = 50.0
Element prediction: Off
Number of isotope peaks used for i-FIT = 3

Monoisotopic Mass, Even Electron Ions
248 formula(e) evaluated with 1 results within limits (all results (up to 1000) for each mass)
Elements Used:
C: 1-30 H: 1-30 N: 1-5 O: 1-5 F: 1-2 Cl: 1-2

Mass	Calc. Mass	mDa	PPM	DBE	i-FIT	Norm	Conf(%)	Formula
447.1594	447.1599	-0.5	-1.1	11.5	134.5	n/a	n/a	C22 H25 N4 O3 F Cl

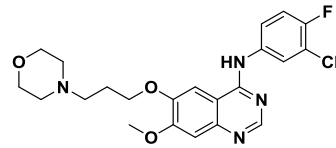

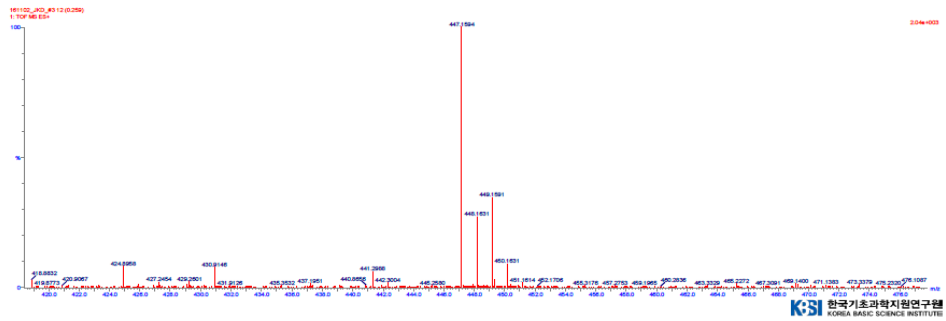

▼ Elemental analysis

Operator ID: SNU-EA2000
Company name: ThermoFinnigan
Method name: CHN-S
Printed: 2012-12-28 15:32
Elemental Analyser method:
Sampler method:
Sample ID: Gefitinib (# 9)
Analysis type: UnkNown
Calibration method: K Factors
Sample weight: 2.154
Protein factor: 6.25

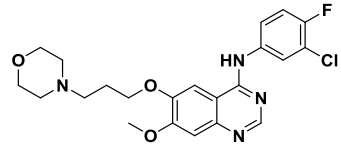

Element Name		Ret.Time	Area	BC	Area ratio	K factor
Nitrogen	12.5189	51	565046	RS	11.195220	.209543E+07
Carbon	59.0874	74	6325811	RS	1.000000	.496719E+07
Hydrogen	5.4755	219	1817697	FU	3.480124	.153765E+08
Totals	77.0818		8708554			

▼ HPLC

```
Acq. Operator   : Cheon Mi Hee                    Seq. Line :   2
Acq. Instrument : S-5                             Location : Vial 82
Injection Date  : 2013-01-31 오후 3:55:51          Inj :   1
                                                  Inj Volume : 5.000 µl
Acq. Method     : C:\CHEM32\1\DATA\GEFITINIB-ORIGINAL\GEFITINIB-ORIGINAL 2013-01-31 14-
                  51-10\GEFITINIB-ORIGINAL.M
Last changed    : 2013-01-31 오후 2:51:10 by Cheon Mi Hee
Analysis Method : C:\CHEM32\1\DATA\GEFITINIB-ORIGINAL\GEFITINIB-ORIGINAL 2013-01-31 14-
                  51-10\GEFITINIB-ORIGINAL.M (Sequence Method)
Last changed    : 2013-02-01 오전 11:17:33 by Cheon Mi Hee
                  (modified after loading)
Method Info     : 2013. 01. 31. 126 bar

Sample Info     : 7mg / 20ml 0.2%TFA, 60%ACN
```

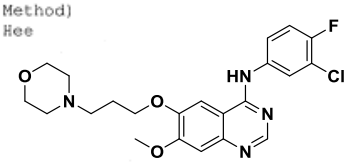


```
Additional Info : Peak(s) manually integrated
```

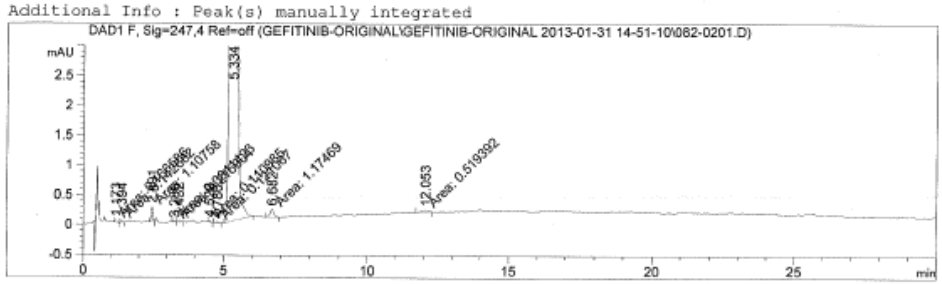


```
                          Area Percent Report

Sorted By             :      Signal
Multiplier:                   :      1.0000
Dilution:                     :      1.0000
Do not use Multiplier & Dilution Factor with ISTDs


Signal 1: DAD1 F, Sig=247,4 Ref=off

Peak RetTime Type  Width     Area      Height     Area
  #   [min]        [min]    [mAU*s]    [mAU]       %
----|-------|----|-------|----------|----------|--------|
   1   1.173 MM    0.0775 1.66586e-1 3.58435e-2 2.267e-3
   2   1.394 MM    0.0674 1.42682e-1 3.52814e-2 1.942e-3
   3   2.491 MM    0.0729    1.10758 2.53164e-1   0.0151
   4   3.286 MF    0.1057 8.11423e-2 1.27958e-2 1.104e-3
   5   3.432 FM    0.1209 2.15904e-1 2.97648e-2 2.938e-3
   6   4.520 MM    0.0909 1.10985e-1 2.03462e-2 1.510e-3
   7   4.780 MM    0.1373 1.21067e-1 1.46952e-2 1.648e-3
   8   5.334 BB    0.1203 7344.86279  948.79309  99.9505
   9   6.682 MM    0.1556    1.17469 1.25817e-1   0.0160
  10  12.053 MM    0.2874 5.19392e-1 3.01226e-2 7.068e-3

Totals :                  7348.50282  949.35092


                          *** End of Report ***
```

4-((3-chloro-4-fluorophenyl)(trimethylsilyl)amino)-7-methoxyquinazolin-6-ol, iodide

▼ ^{1}H-NMR (DMSO-d_6, 400 MHz)

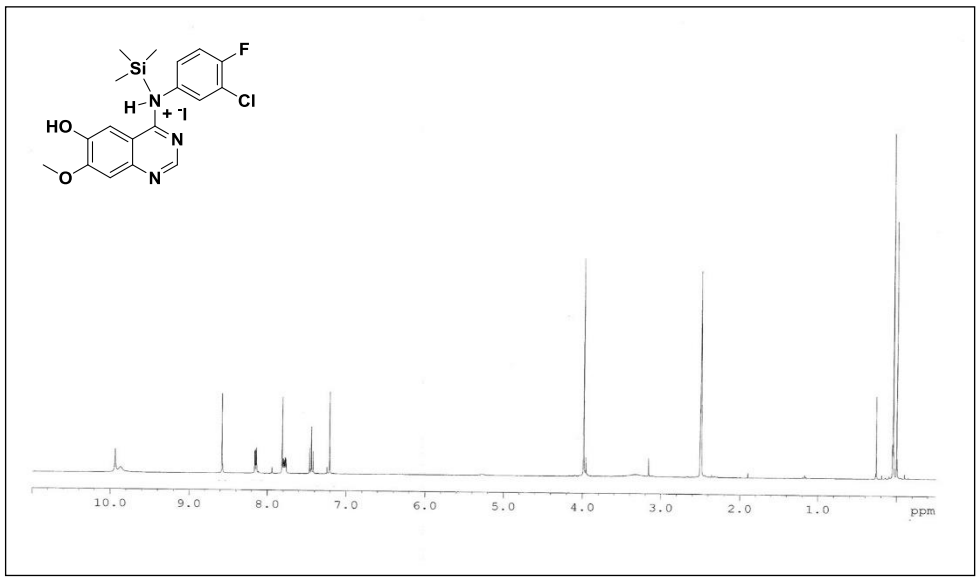

***N*-(3-chloro-4-fluorophenyl)-7-methoxy-6-(3-morpholinopropoxy)-*N*-(trimethylsilyl)-quinazoline-4-amine, iodide**

▼ ^{1}H-NMR (DMSO-d_6, 400 MHz)

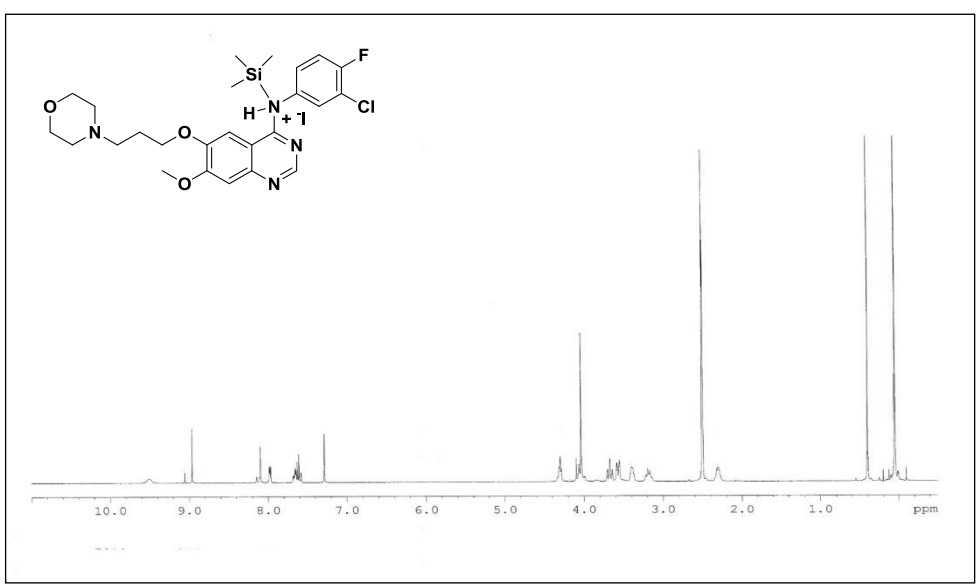

***N*-(3-chloro-4-fluorophenyl)-7-methoxy-6-(3-morpholinopropoxy)-*N*-(3-morpholinopropyl)-quinazoline-4-amine**

▼ ^{1}H-NMR (DMSO-d_6, 400 MHz)

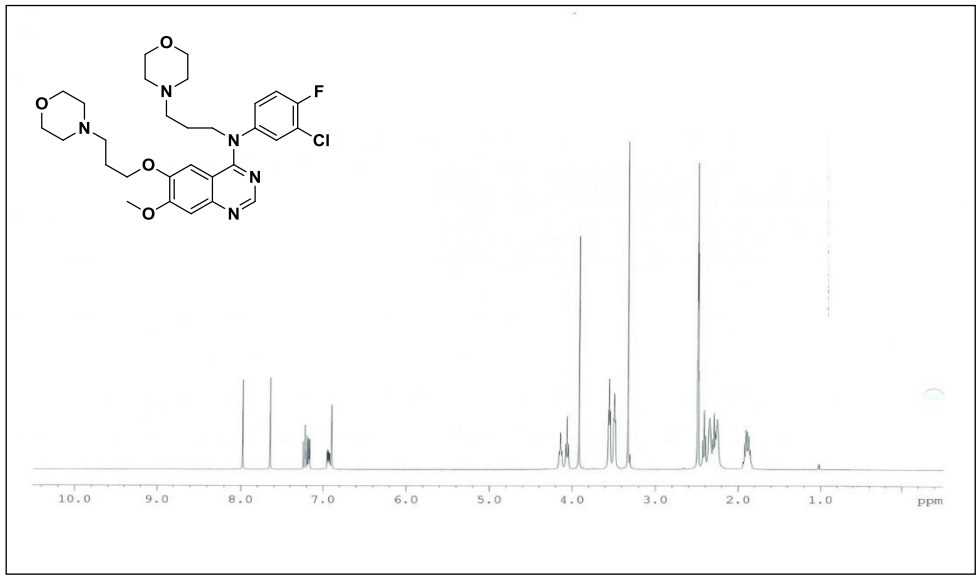

Selective *O*-alkylation of 4-anilinoquinazoline moieties with an assistance of TMSI (Table 4)

▼ HPLC (entry 1)

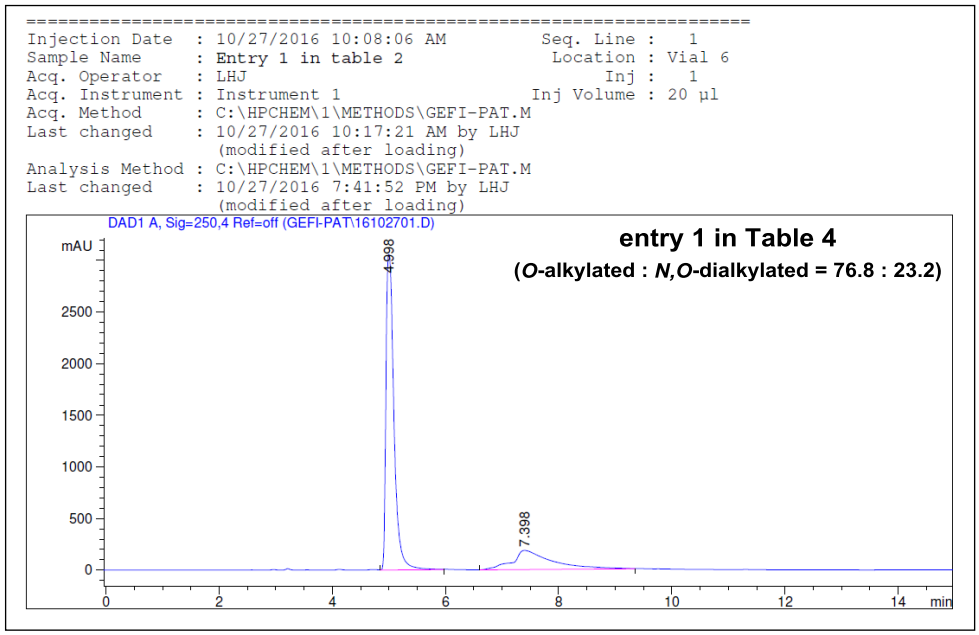

▼ HPLC (entry 2)

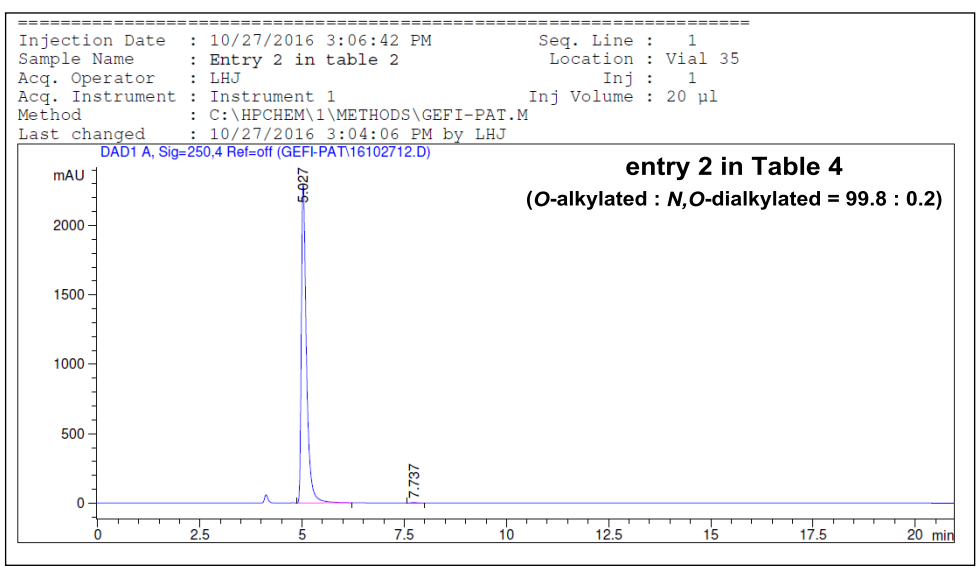

▼ HPLC (entry 3)

```
==========================================================================
Injection Date  : 10/27/2016 10:42:35 AM          Seq. Line :   3
Sample Name     : Entry 3 in table 2               Location : Vial 8
Acq. Operator   : LHJ                                  Inj :   1
Acq. Instrument : Instrument 1                   Inj Volume : 20 µl
Acq. Method     : C:\HPCHEM\1\METHODS\GEFI-PAT.M
Last changed    : 10/27/2016 11:03:56 AM by LHJ
                  (modified after loading)
Analysis Method : C:\HPCHEM\1\METHODS\GEFI-PAT.M
Last changed    : 10/27/2016 7:41:52 PM by LHJ
                  (modified after loading)
```

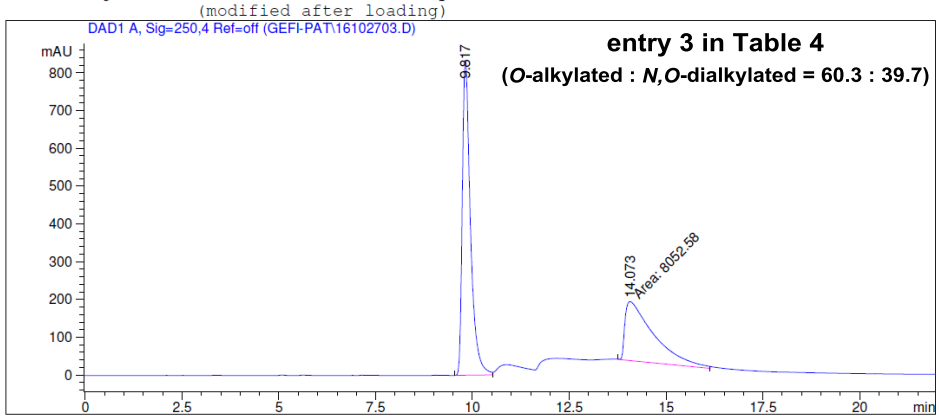

▼ HPLC (entry 4)

```
==========================================================================
Injection Date  : 10/27/2016 6:14:27 PM           Seq. Line :   2
Sample Name     : Entry 4 in Table 2               Location : Vial 20
Acq. Operator   : LHJ                                  Inj :   1
Acq. Instrument : Instrument 1                   Inj Volume : 20 µl
Method          : C:\HPCHEM\1\METHODS\GEFI-PAT.M
Last changed    : 10/27/2016 3:04:06 PM by LHJ
```

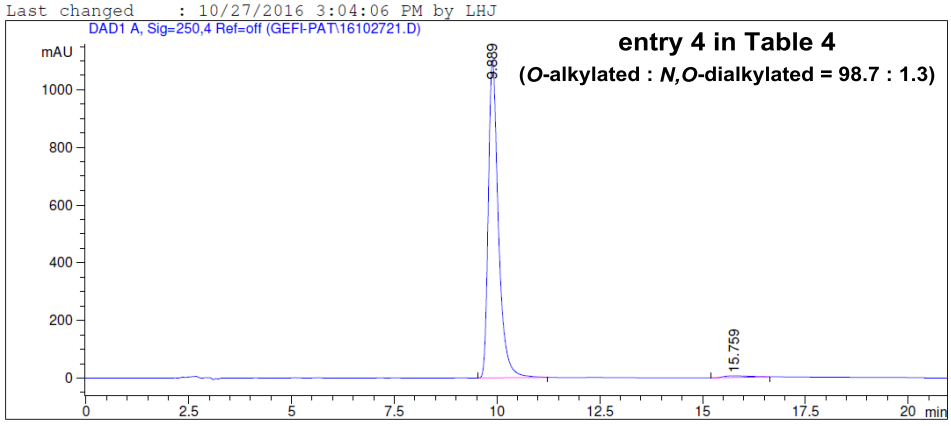

▼ HPLC (entry 5)

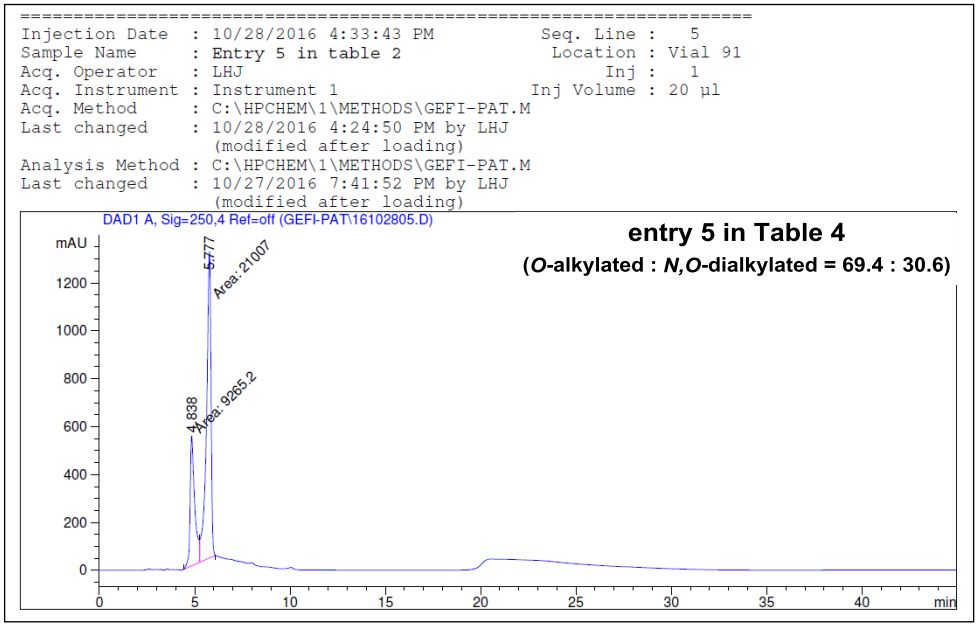

▼ HPLC (entry 6)

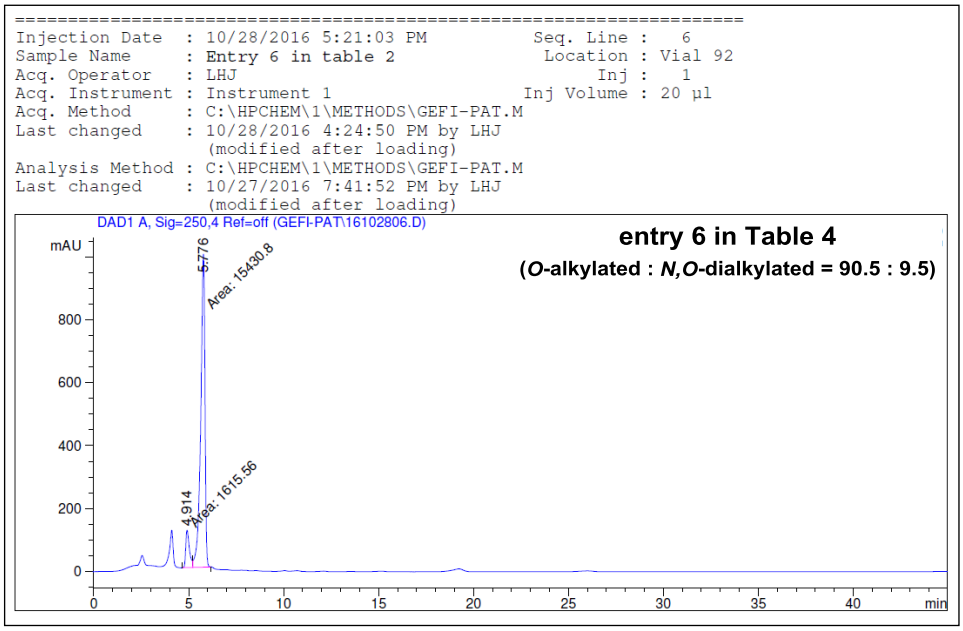

▼ HPLC (entry 7)

```
==========================================================================
Injection Date  : 10/28/2016 6:55:31 PM          Seq. Line :   8
Sample Name     : Entry 7 in table 2              Location : Vial 94
Acq. Operator   : LHJ                                 Inj :   1
Acq. Instrument : Instrument 1                 Inj Volume : 20 µl
Acq. Method     : C:\HPCHEM\1\METHODS\GEFI-PAT.M
Last changed    : 10/28/2016 4:24:50 PM by LHJ
                  (modified after loading)
Analysis Method : C:\HPCHEM\1\METHODS\GEFI-PAT.M
Last changed    : 10/27/2016 7:41:52 PM by LHJ
                  (modified after loading)
```

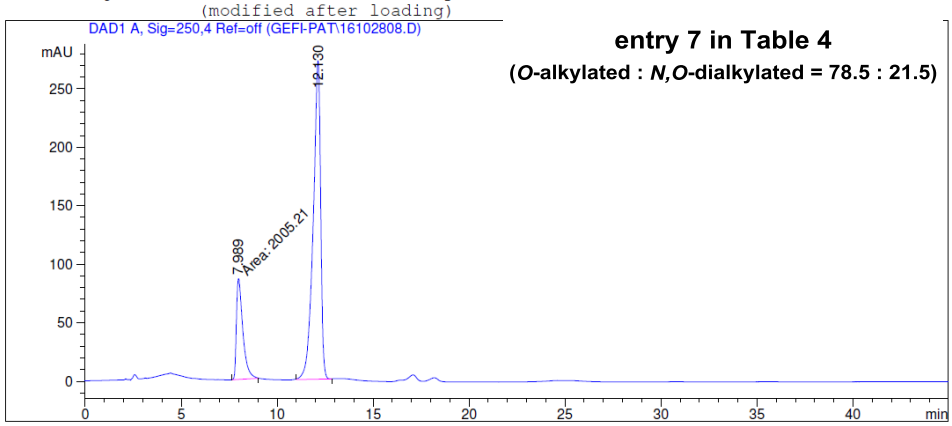

▼ HPLC (entry 8)

```
==========================================================================
Injection Date  : 10/28/2016 7:42:37 PM          Seq. Line :   9
Sample Name     : Entry 8 in table 2              Location : Vial 95
Acq. Operator   : LHJ                                 Inj :   1
Acq. Instrument : Instrument 1                 Inj Volume : 20 µl
Acq. Method     : C:\HPCHEM\1\METHODS\GEFI-PAT.M
Last changed    : 10/28/2016 4:24:50 PM by LHJ
                  (modified after loading)
Analysis Method : C:\HPCHEM\1\METHODS\GEFI-PAT.M
Last changed    : 10/27/2016 7:41:52 PM by LHJ
                  (modified after loading)
```

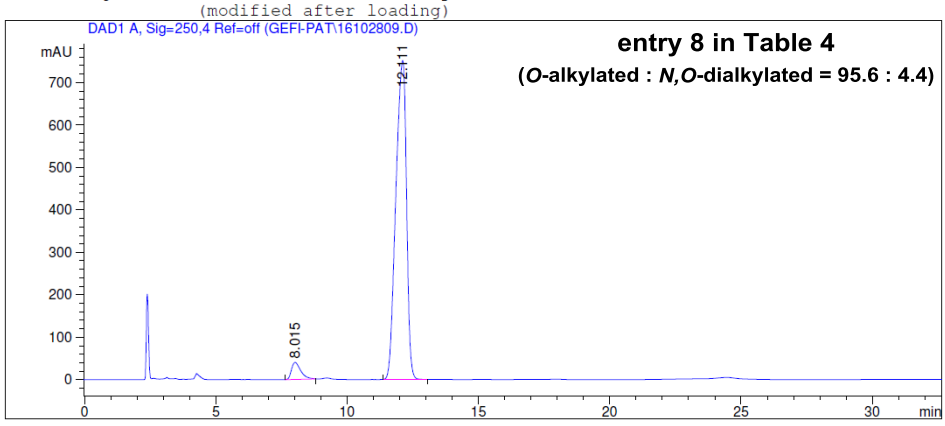

7-methoxy-*N*-(4-methoxyphenyl)-6-(3-morpholinopropoxy)quinazolin-4-amine

▼ ^{1}H-NMR (DMSO-d_6, 400 MHz)

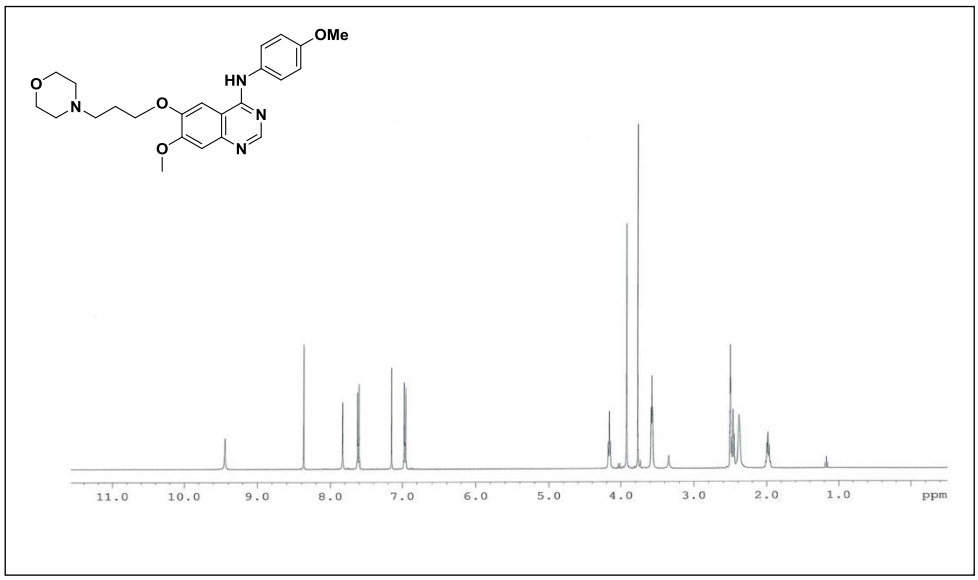

▼ ^{13}C-NMR (DMSO-d_6, 175 MHz)

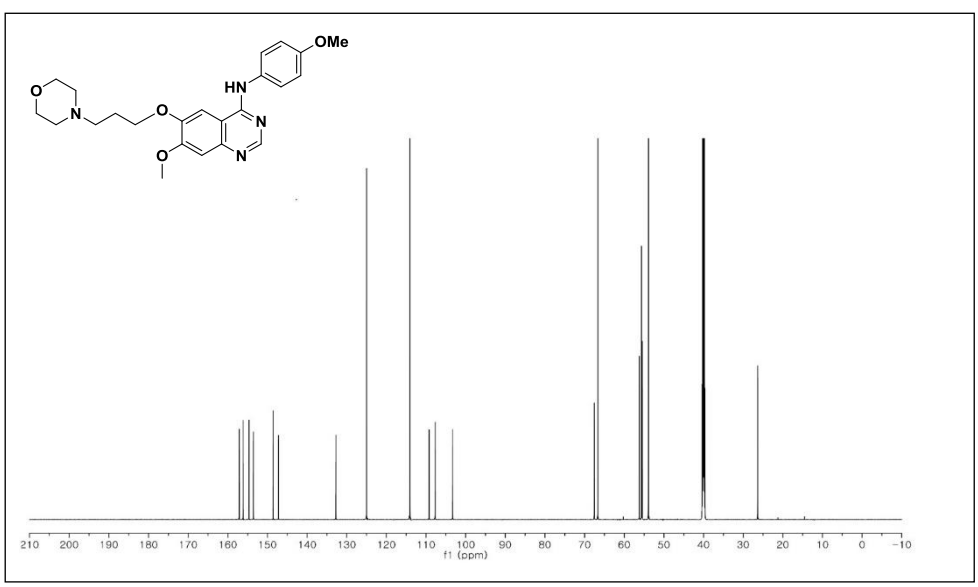

▼ High-Resolution Mass

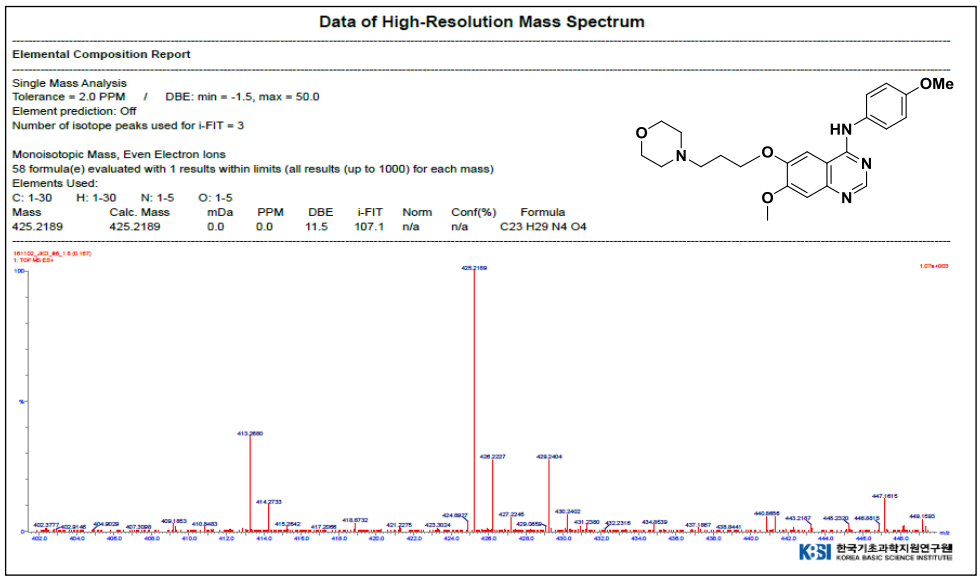

***N*-(3-iodo-4-methoxyphenyl)-7-methoxy-6-(3-morpholinopropoxy)quinazoline-4-amine**

▼ ^{1}H-NMR (DMSO-d_6, 400 MHz)

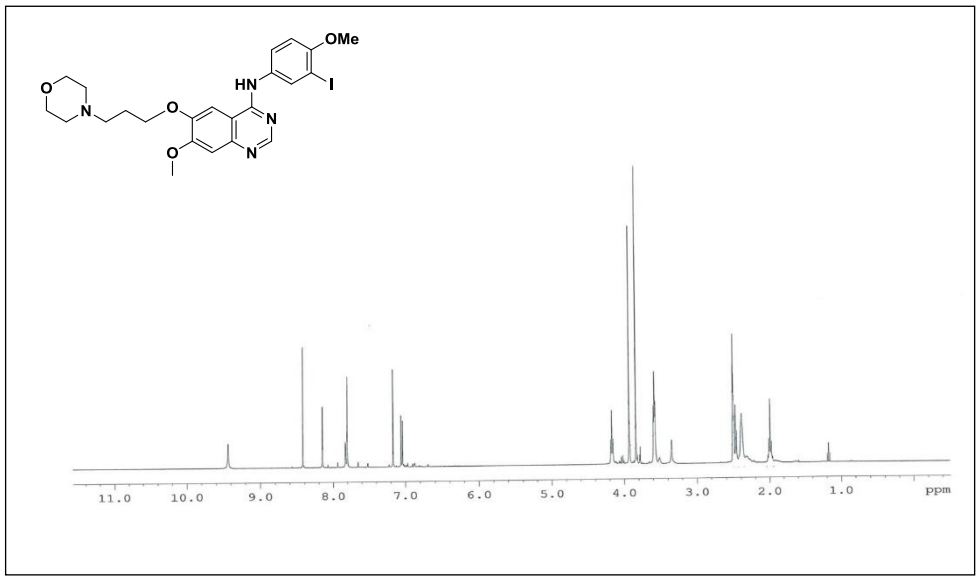

▼ ^{13}C-NMR (DMSO-d_6, 175 MHz)

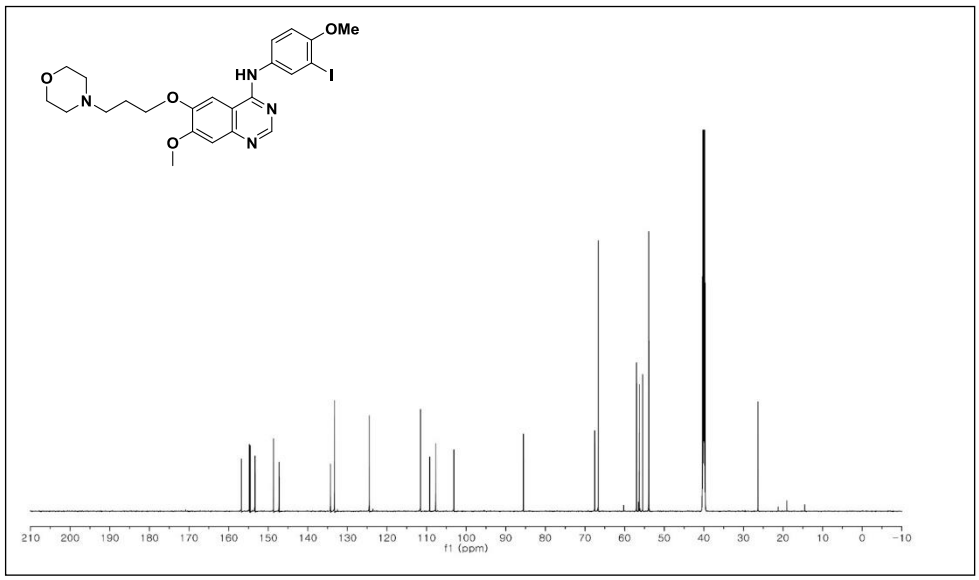

▼ High-Resolution Mass

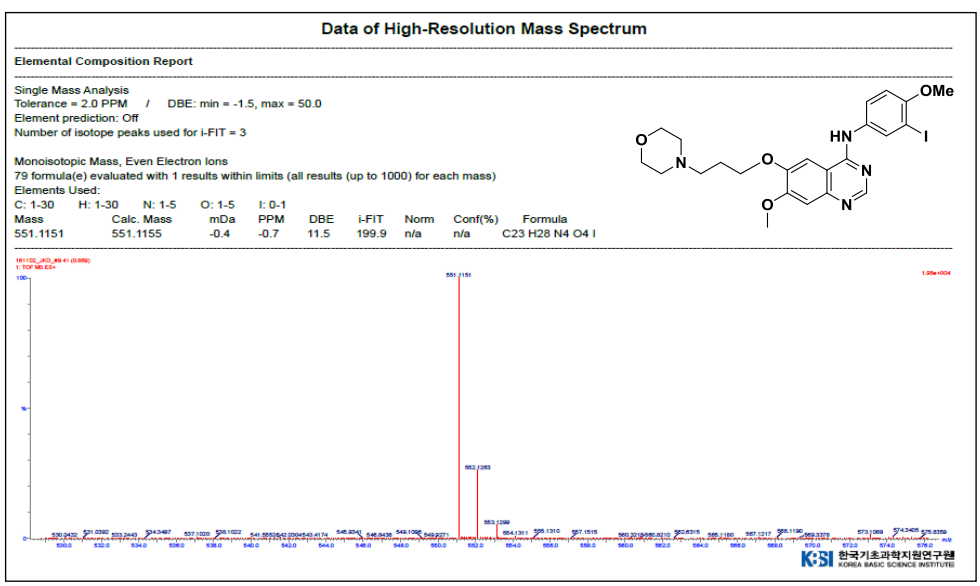

6,7-dimethoxy-*N*-(4-methoxyphenyl)quinazoline-4-amine

▼ ^{1}H-NMR (DMSO-d_6, 400 MHz)

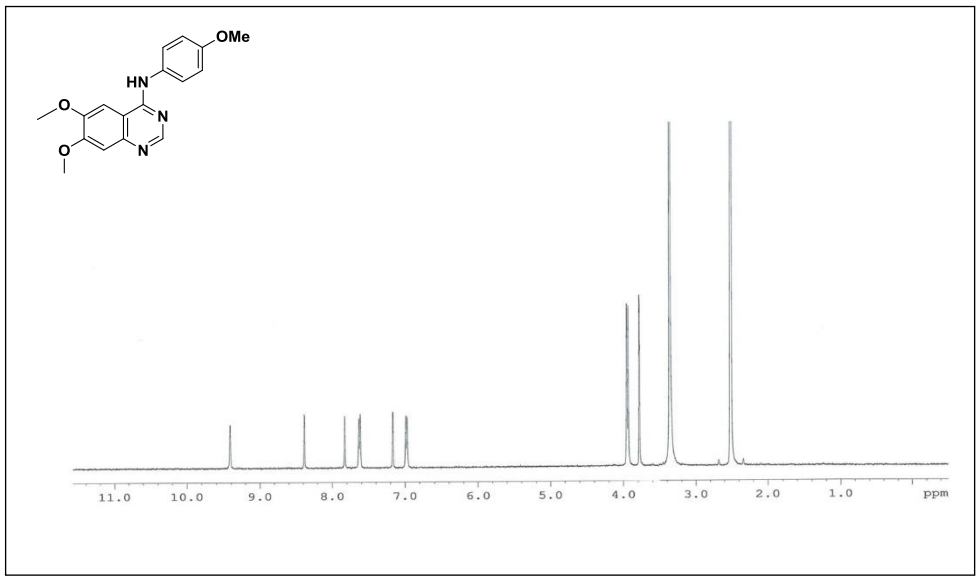

▼ ^{13}C-NMR (DMSO-d_6, 175 MHz)

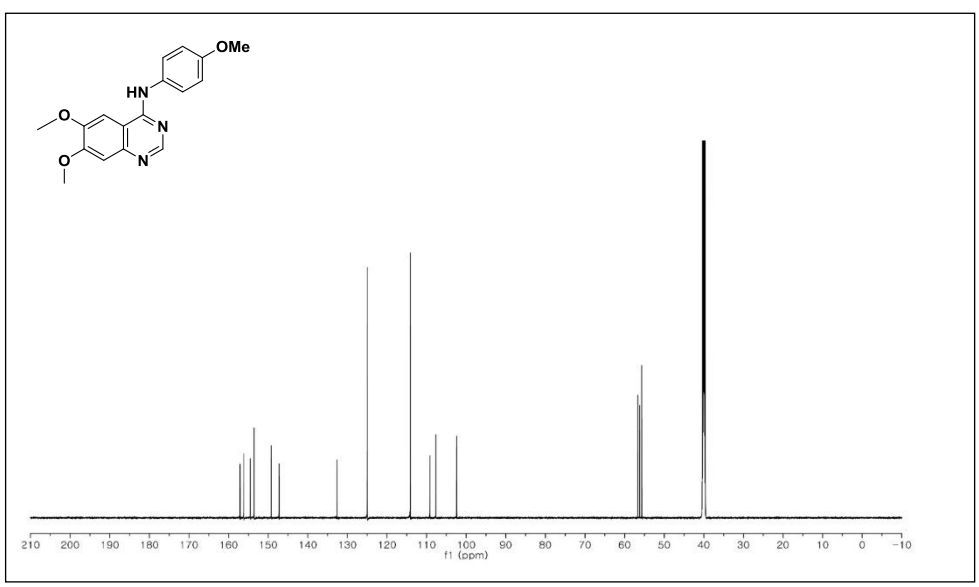

▼ High-Resolution Mass

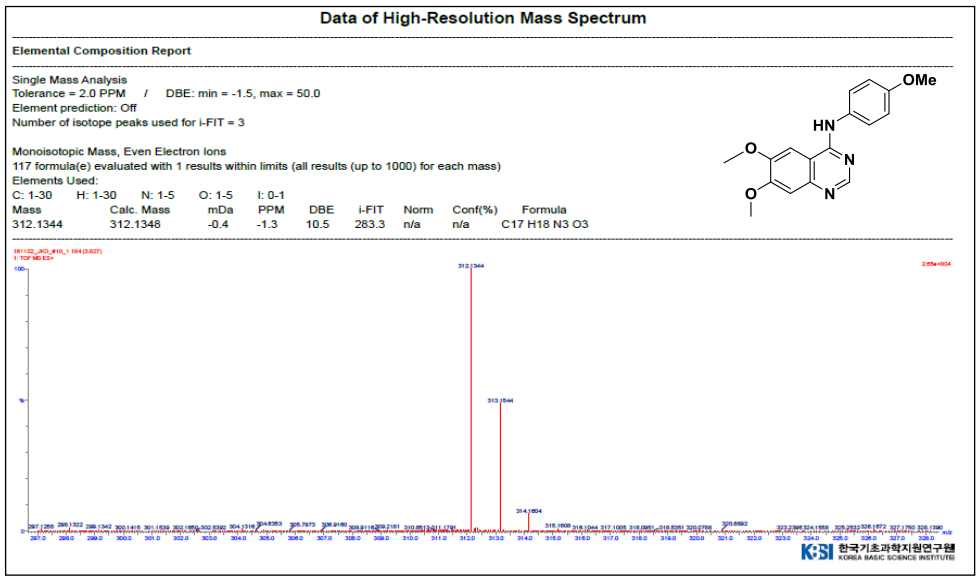

***N*-(3-iodo-4-methoxyphenyl)-6,7-dimethoxyquinazolin-4-amine**

▼ ^{1}H-NMR (DMSO-d_6, 400 MHz)

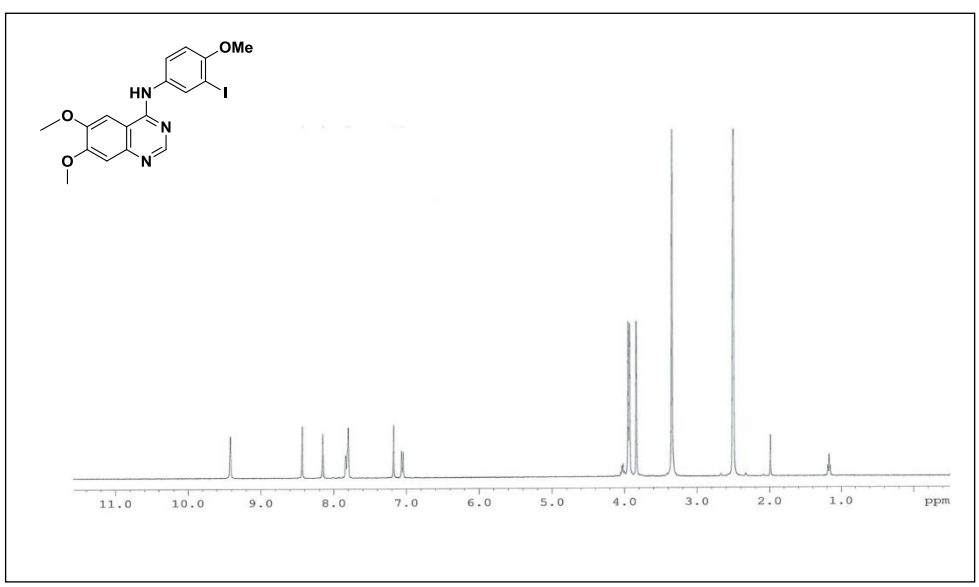

▼ ^{13}C-NMR (DMSO-d_6, 175 MHz)

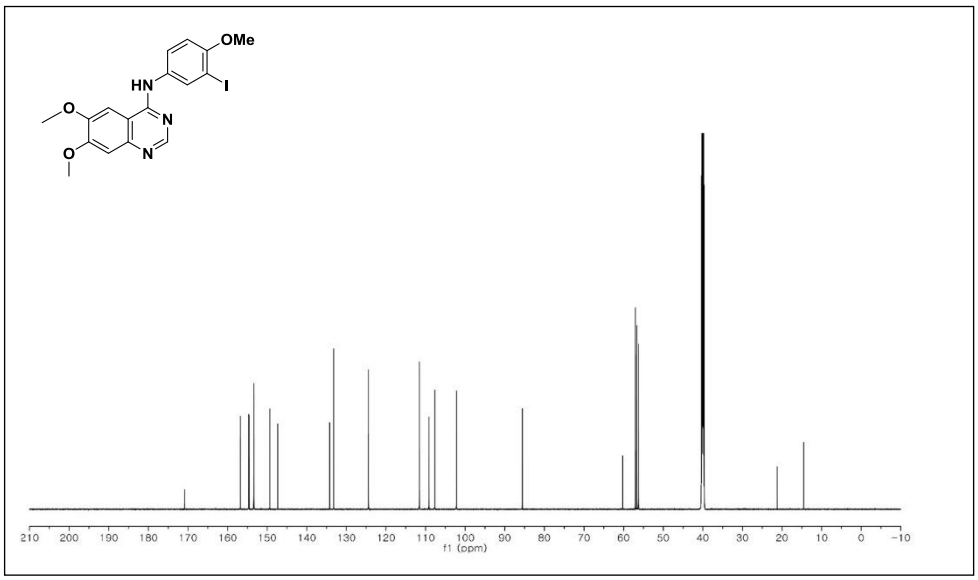

▼ High-Resolution Mass

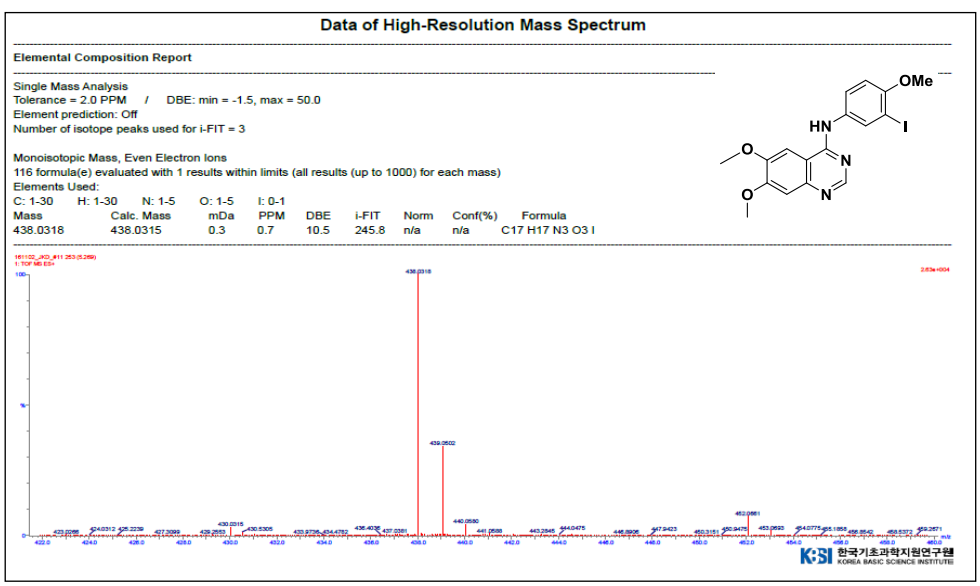

3-(3-morpholinopropoxy)-*N*-(3-morpholinopropyl)aniline

▼ ^{1}H-NMR (DMSO-d_6, 400 MHz)

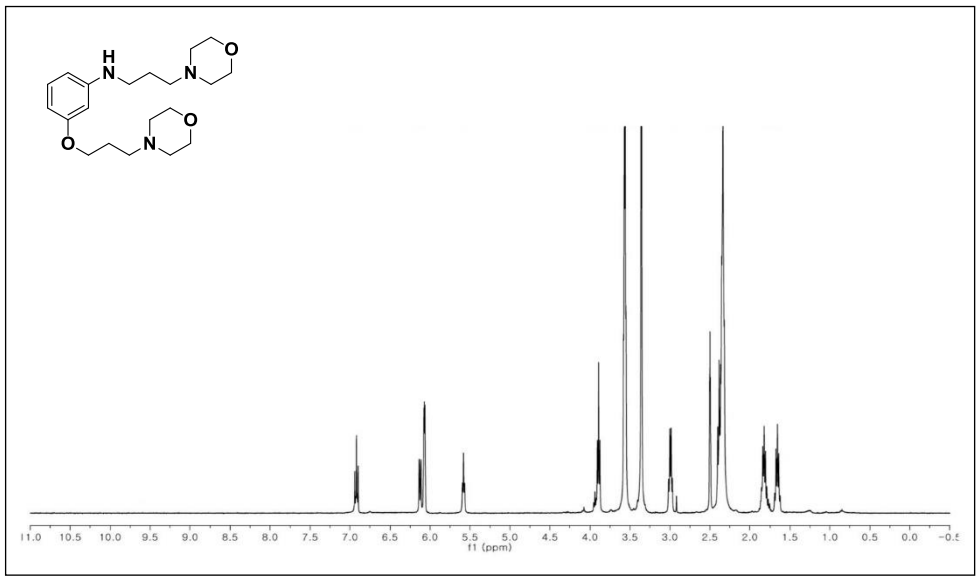

▼ ^{13}C-NMR (DMSO-d_6, 100 MHz)

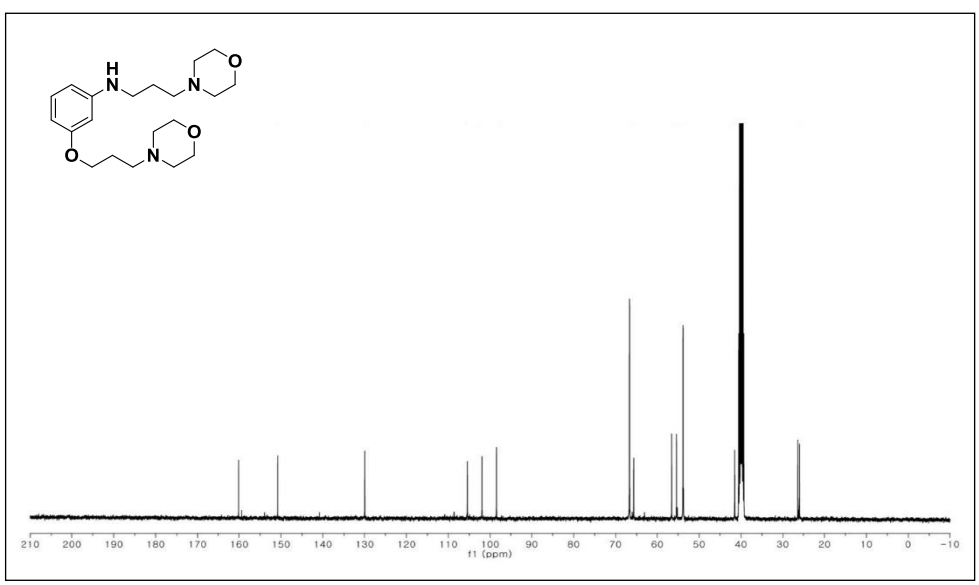

4-(3-morpholinopropoxy)-*N*-(3-morpholinopropyl)aniline

▼ ^{1}H-NMR (DMSO-d_6, 400 MHz)

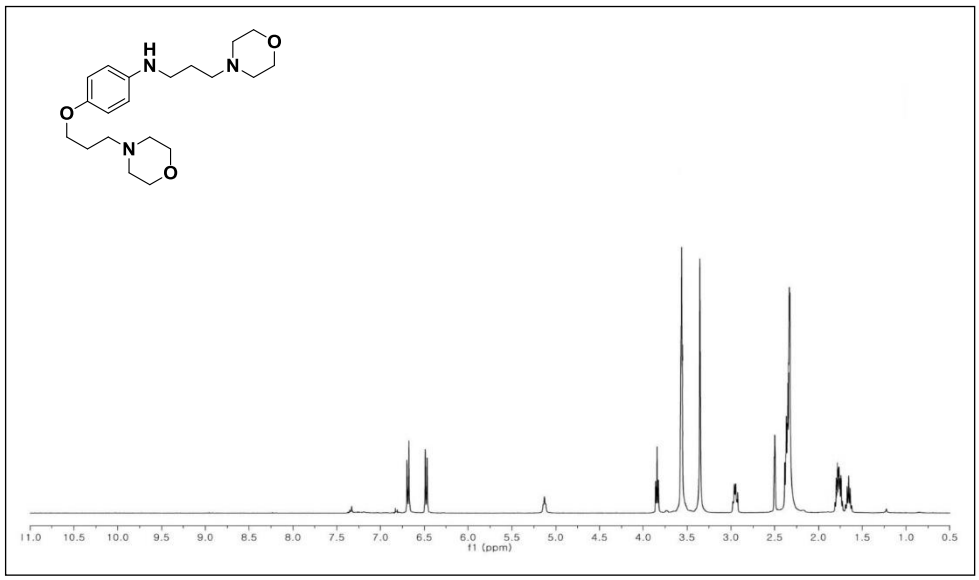

▼ ^{13}C-NMR (DMSO-d_6, 100 MHz)

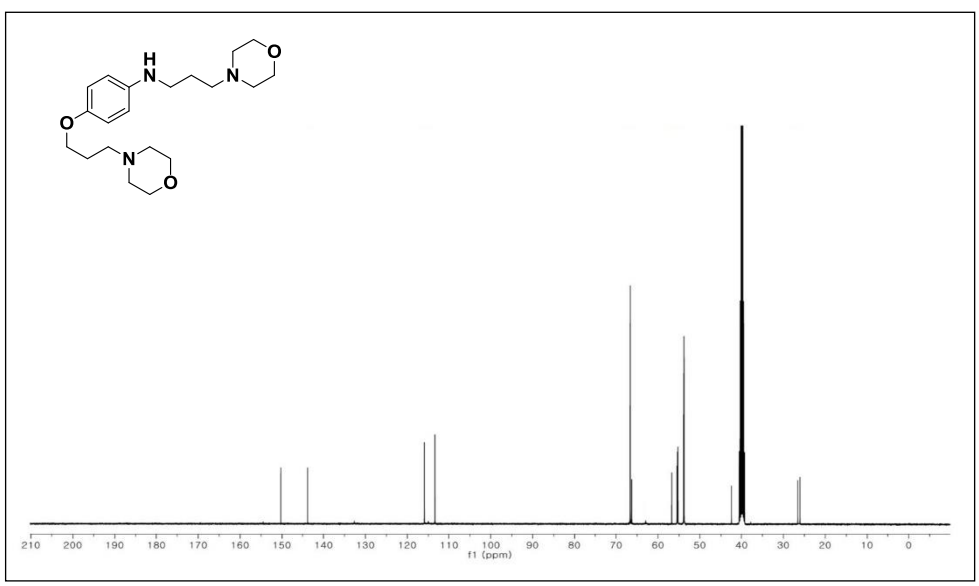

4-(3-morpholinopropoxy)-*N*-phenylaniline

▼ ^{1}H-NMR (DMSO-d_6, 400 MHz)

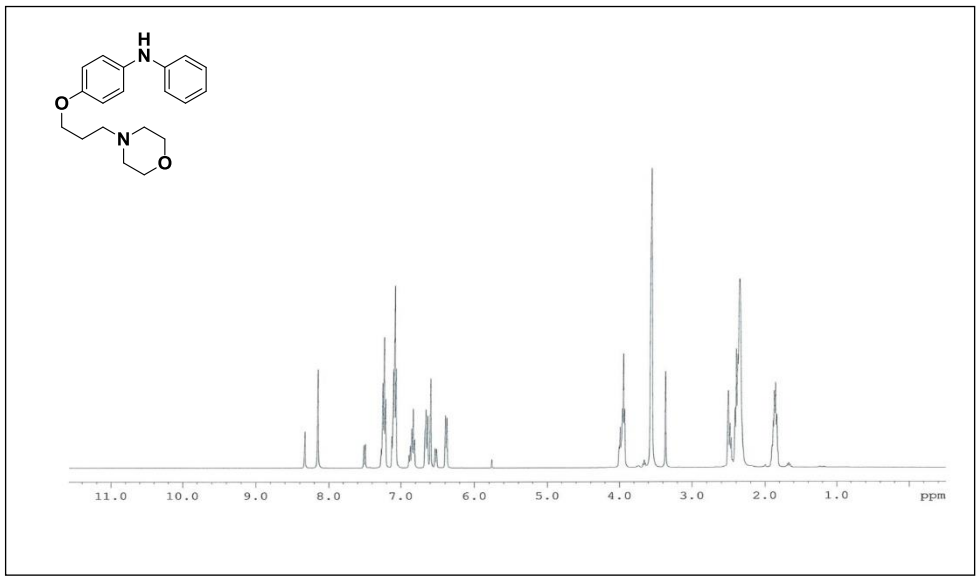

▼ ^{13}C-NMR (DMSO-d_6, 100 MHz)

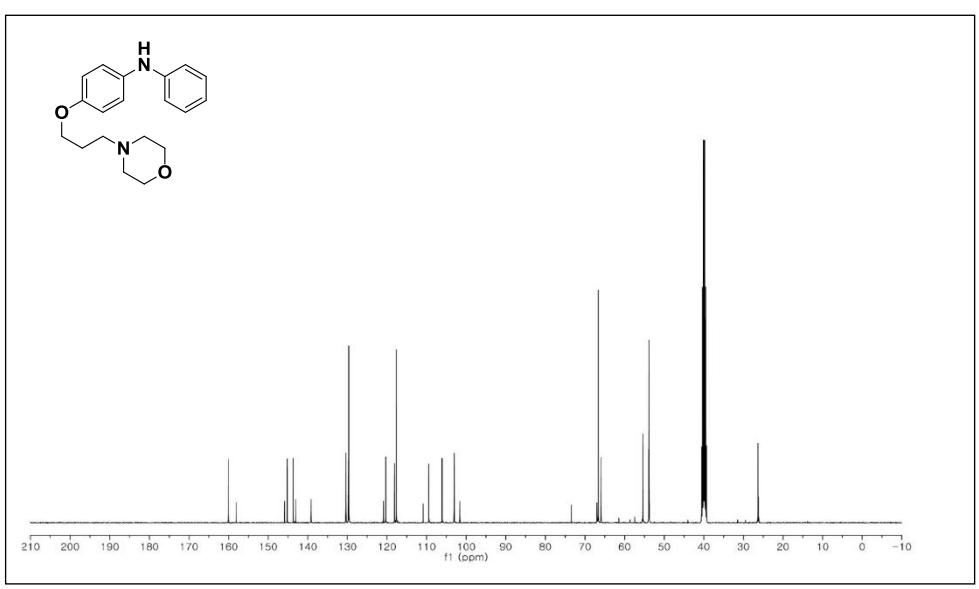

3-(benzyl(3-morpholinopropyl)amino)phenol

▼ ^{1}H-NMR (DMSO-d_6, 400 MHz)

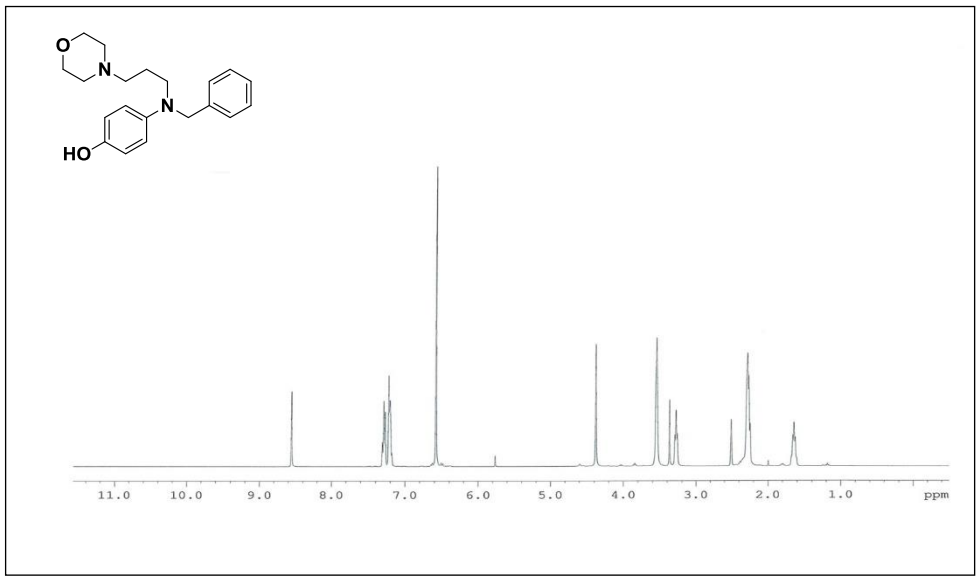

▼ ^{13}C-NMR (DMSO-d_6, 100 MHz)

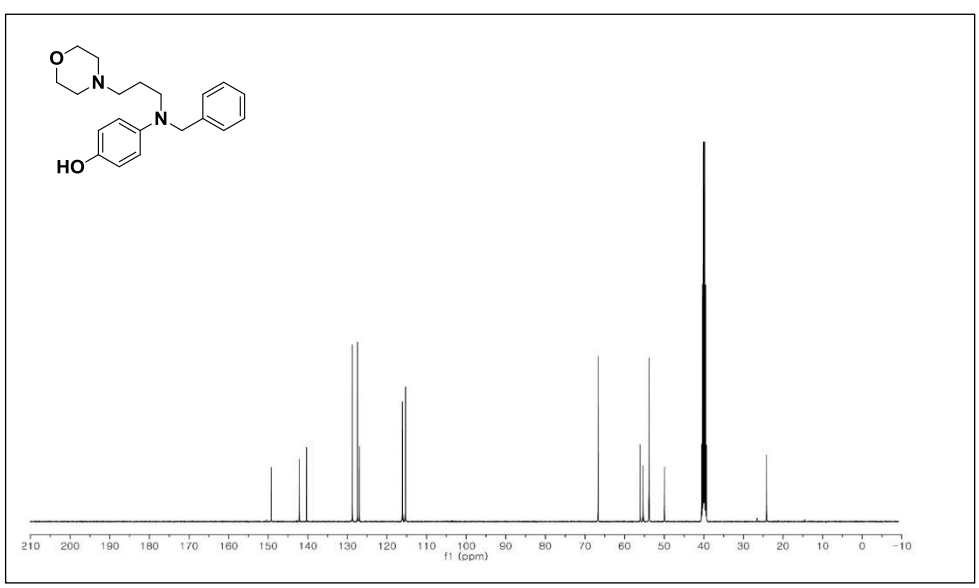

4-(3-chloro-4-fluorophenylamino)-7-methoxyquinazolin-6-ol

▼ ^{1}H-NMR (DMSO-d_6, 400 MHz)

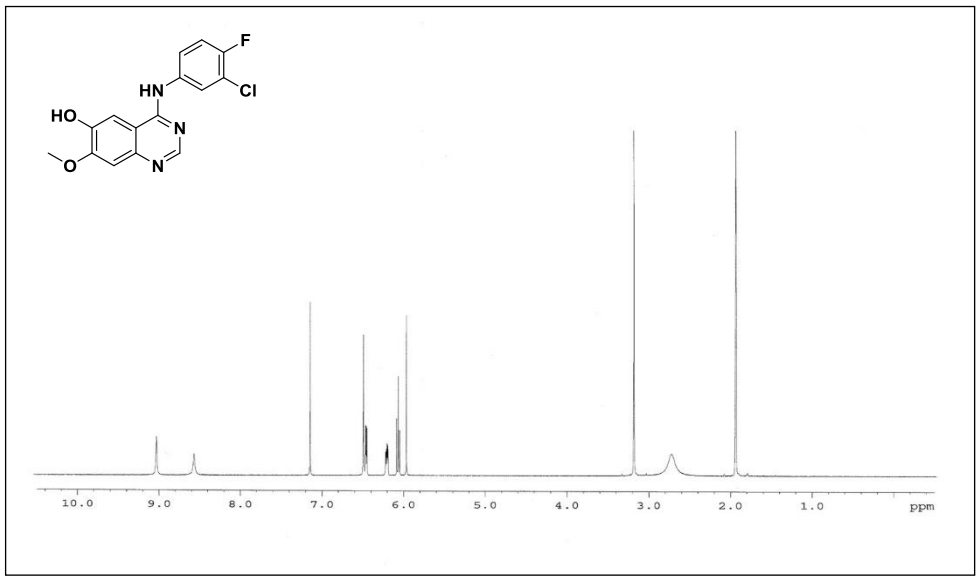

▼ ^{13}C-NMR (DMSO-d_6, 175 MHz)

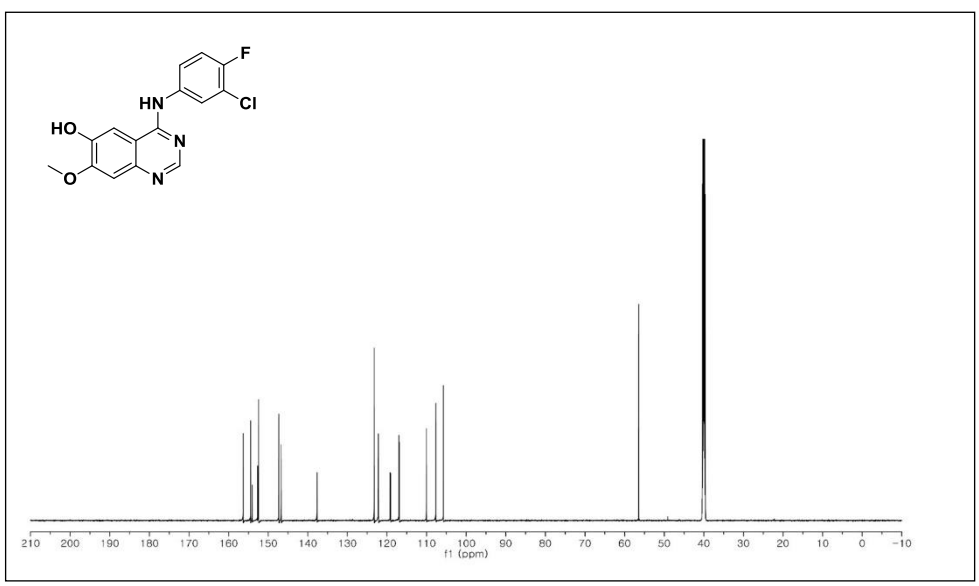

▼ High-Resolution Mass

Data of High-Resolution Mass Spectrum

Elemental Composition Report

Single Mass Analysis
Tolerance = 1.0 PPM / DBE: min = -1.5, max = 50.0
Element prediction: Off
Number of isotope peaks used for i-FIT = 3

Monoisotopic Mass, Even Electron Ions
168 formula(e) evaluated with 1 results within limits (all results (up to 1000) for each mass)
Elements Used:
C: 1-20 H: 1-20 N: 1-5 O: 1-5 F: 1-2 Cl: 1-2

Mass	Calc. Mass	mDa	PPM	DBE	i-FIT	Norm	Conf(%)	Formula
320.0602	320.0602	0.0	0.0	10.5	302.8	n/a	n/a	C15 H12 N3 O2 F Cl

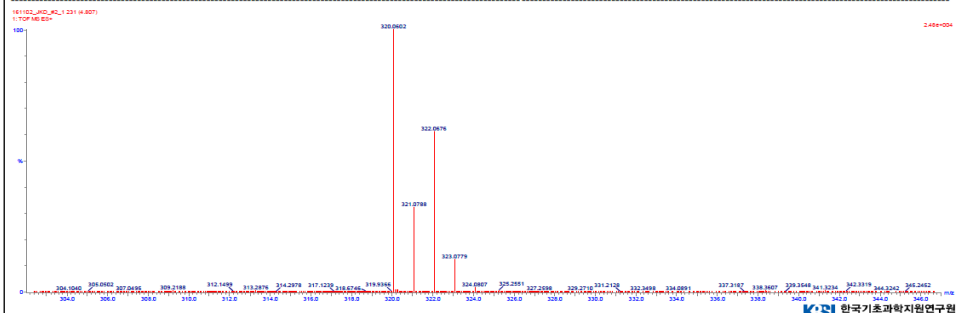

▼ Elemental analysis

Operator ID:	SNU-EA2000
Company name:	ThermoFinnigan
Method name:	CHN-S
Printed:	2012-12-28 15:35
Elemental Analyser method:	
Sampler method:	
Sample ID:	OHQA (# 11)
Analysis type:	UnkNown
Calibration method:	K Factors
Sample weight:	1.453
Protein factor:	6.25

Element Name		Ret.Time	Area	BC	Area ratio	K factor
Nitrogen	13.0053	51	394098	RS	10.230210	.208554E+07
Carbon	55.8080	75	4031699	RS	1.000000	.496719E+07
Hydrogen	3.4316	202	770852	RS	5.230186	.153765E+08
Totals	72.2449		5196649			

VII. Abstract

4-Anilinoquinazolines, have been prevalent motifs for pharmaceutical molecules in recent years, notably as EGFR inhibitors. Many novel EGFR inhibitors have been designed and synthesized through incorporating an alkoxy moiety *via* *O*-alkylation of hydroxyl group at the C-6 or C-7 position of the 4-anilinoquinazoline scaffold. However, in most case of alkylation of anilinoquinazolines with alkyl halide, a mixture of *O*- and *N*-alkylated, and *N*,*O*-dialkylated derivatives were generated without decent selectivity. It is a tedious work to separate and purify them. Thus, the development of new synthetic strategies which allow access to selective *O*-alkylation of 4-anilinoquinazolines is of interest to both laboratory and industry preparation of EGFR inhibitors. Gefitinib (marketed by AstraZeneca) is the first selective inhibitor of EGFR kinase domain and was approved in May 2003 for treatment of recurrent NSCLC (Non Small Cell Lung Cancer). Since then, it has been widely used worldwide and synthetic methods for gefitinib consisting of 4-anilinoquinazoline moiety have been continuously reported. According to the procedure described in previous reports, the generation of an excess of an *N*-alkylated impurity is an inevitable hurdle for the preparation of gefitinib. We introduced a novel concept, that trimethylsilyl (TMS) group was used as a transient protection group capable of significantly suppressing the *N*-alkylated impurity generation. The TMS group was quite attractive to us in terms of highly *N*-alkylation suppressing effect and facile removable character by a simple work-up. Indeed, this new and unique process minimized the generation of the *N*-alkylated side product. We also confirmed that our process is well applicable to a variety of 4-anilinoquinazolines.

Keyword : Gefitinib, EGFR inhibitor, Anilinoquinazoline, Transient protection group

Student Number : 2009-31060

Part Ⅱ: Practical synthesis of Levocabastine, a H_1 receptor antagonist

Part Ⅱ. H_1 receptor antagonist인 Levocabastine의 실용적인 합성법 개발

국문초록

레보카바스틴(Levocabastine)은 Janssen에 의해개발된 H_1 receptor antagonist 계열의 항히스타민제로써, 1979년 알레르기성 결막염 및 비염적응증에 대해 리보스틴(Livostin)라는 제품명으로 허가받았다. Levocabastine은 또한 뉴로텐신수용체 NTS_2 대해서도 강력하고 선택적인 길항제로서 작용하는 것으로 밝혀졌다.

Levocabastine은 phenyl이 치환된 piperidine과 cyclic hexane이 연결되어 있으며, 3개의 chiral center가 도입되어 있는 구조를 가지고있다. 현재까지 알려져 있는 Levocabastine의 제조방법은 1980년에 Janssen에 의해 출원된 특허가 유일하다. 상기의 제법은 chiral center 도입을 위한 chiral resolution, 전기분해를 이용한 탈술폰화 및 백금촉매를 이용하는 환원반응 등이 이용되어, 실용적인 생산제법 으로 이용하기에는 어려움이 따른다. 이에 본 연구진은 상기의 문제점들을 해결하면서 상업적으로 이용가능한 효율적인 제법을 연구하였다. 본합성의 핵심 반응은 chiral compound를 출발물질로 이용하여 입체이성질체 도입 및 재결정을 통한 입체이성질체분리, 전기분해를 대체할 수 있는 탈술폰화 반응등이며, 이를 이용하여 Levocabastine을 고순도로 제조할 수 있는 상업적인 제조방법 개발을 완료하였다.

주요어: Levocabastine, chiral resolution, electrosysis

학번: 2009-31060

Table of Contents

List of Tables

List of Figures

List of Schemes

Abbreviations

AcOH : Acetic acid

ADHS : Attention-deficit/hyperactivity disorder

AIBN :Azobisisobutyronitrile

ATPases :adenosine triphosphatase

CNS : Central nervous system

DAO :Diamine oxidase

DMSO: Dimethylsulfoxide

dr :Diastereomeric ratio

ECL cell :Enterochromaffin-like cell

GPCR : G protein-coupled receptors

HDC :Histidine decarboxylase

HMT :Histamine *N*-methyltransferase

HPLC :High-performance liquid chromatography

HRMS : High-resolution mass spectrometry

hr : Hour

$KPPh_2$: Potassium diphenylphosphide

MS: Mass spectrometry

$NaBH(OAc)_3$: Sodium triacetoxyborohydride

$NaCNBH_3$:Sodium cyanoborohydride

n-Bu3SnH :Tributyltin hydride

NMR : Nuclear magnetic resonance spectroscopy

NF-κB : nuclear factor kappa-light-chain-enhancer of activated B cells

pKa : Acid dissociation constant

PLP :pyridoxal 5′-phosphate

r.t. : Room temperature

TBAF :Tetra-*n*-butylammonium fluoride

THF :Tetrahydrofuran

TMSI :Trimethylsilyl iodide

TLC : Thin layer chromatography

SAM :S-adenosyl-L-methionine

I. Introduction

1. Histamine

Histamine [2-(4-Imidazolyl)-ethylamine] is an important mediator of many biological processes including inflammation, gastric acid secretion, neuromodulation, and regulation of immune function. Due to its potent pharmacological activity even at very low concentrations, the synthesis, transport, storage, release and degradation of histamine have to be carefully regulated to avoid undesirable reactions.[1] Histamine has two basic centers, namely the aliphatic amino group and nitrogen atom of the imidazole ring (**Figure 1**). Under physiological conditions, the aliphatic amino group (having a pK_a around 9.4) will be protonated, whereas the second nitrogen of the imidazole ring ($pK_a \approx 5.8$) will not be protonated.[2] Thus, histamine is normally protonated to a singly charged cation.

Figure 1. The structure of histamine

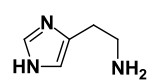

The best characterized roles of histamine are those in inflammation, gastric acid secretion and as a neurotransmitter (**Figure 2**). During inflammation, histamine is released from preformed stores in mast cells and basophils. Histamine acts on vascular smooth muscle cells and endothelial cells, leading to vasodilation and an increase in vascular permeability. In the skin, this results in the 'triple response', which is an immediate local reddening due to vasodilation, a wheal due to increased vascular permeability and a flare response due to indirect vasodilation *via* the stimulation of axonal reflexes (**Figure 2. a.**). In the gastrointestinal system, histamine is essential for gastric acid secretion.[3] Gastrin and vagal

stimulation induce enterochromaffinlike cells in the gut to release histamine. This histamine can then act on parietal cells to stimulate H+, K+ ATPases, leading to the secretion of H+ and subsequent acidification that assists in digestive processes (**Figure 2. b.**). Histamine is also a neurotransmitter in the CNS with a role in sleep–wake cycles, appetite, learning and memory.[4] It is produced in a subset of neurons in the tuberomammillary nucleus of the hypothalamus and its effects are ransmitted widely to other regions of the brain (**Figure 2. c.**).

Figure 2. The major classical physiological roles of histamine

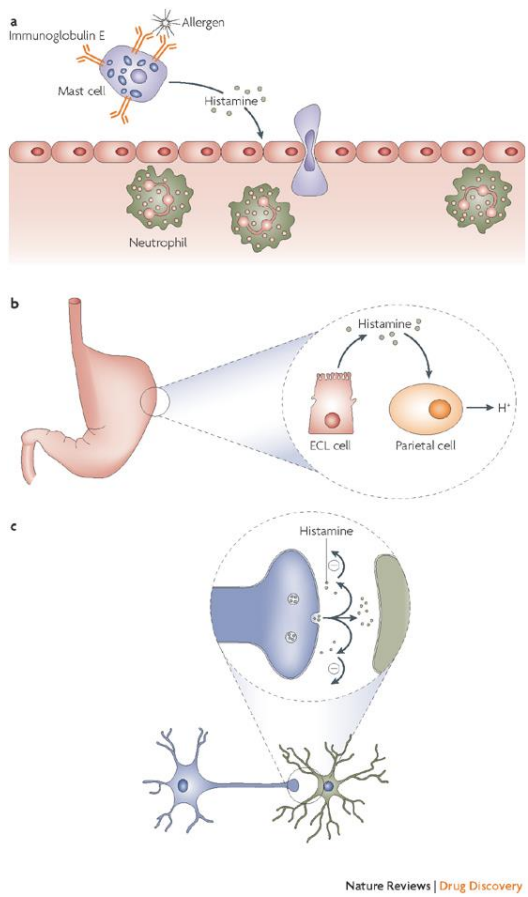

1-1. Synthesis and Metabolism of histamine

Histamine is derived from the decarboxylation of the amino acid histidine, a reaction catalyzed by the enzyme L-histidine decarboxylase (**Figure 3**). Histidine decarboxylase (HDC) is an enzyme that is expressed in various cells throughout the body, including central nervous system, neurons, gastric-mucosa, parietal cells, mast cells, and basophils. This homodimeric enzyme is a pyridoxal phosphate (PLP)-dependent decarboxylase and is highly specific for its histidine substrate.[5-7]

Figure 3. The biosynthesis of histamine

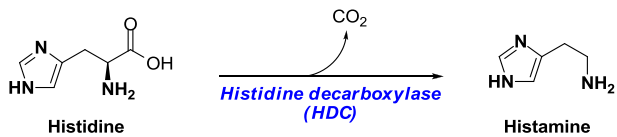

The major routes of histamine inactivation in mammals are methylation of the imidazole ring, catalyzed by histamine *N*-methyltransferase, and oxidative deamination of the primary amino group, catalyzed by diamine oxidase.[1] (**Figure 4**)

Figure 4. The two primary degradation pathways of histamine

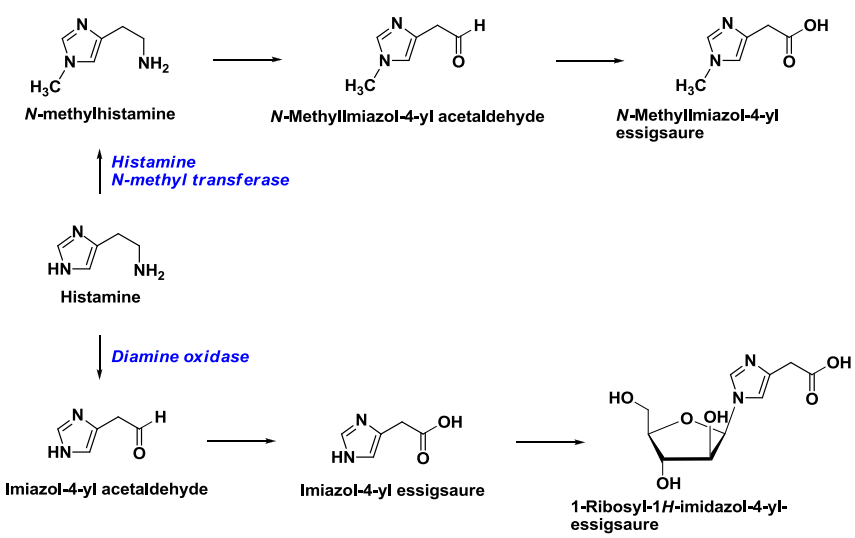

Histamine *N*-methyltransferase (HMT) catalyzes the transfer of a methyl group from *S*-adenosyl-*L*-methionine (SAM) to the secondary amino group of the imidazole ring forming *N*-methylhistamine.[8] HMT is a cytosolic protein that is highly specific for histamine and does not show significant methylation of other substrates. HMT is present in most tissues of mammals but the enzyme is absent from body fluids. HMT is responsible for the inactivation of intracellular histamine that is either synthesized in the cell or taken up from the extracellular space, likely after binding to one of its receptors present on the cell surface. Diamine oxidase (DAO) uses molecular oxygen to oxidatively deaminate histamine to imidazole acetaldehyde, ammonia and hydrogen peroxide.[9] DAO is a member of the class of copper-containing amine oxidases that have in their active-sites a copper ion bound by three conserved histidine residues and the cofactor 2,4,5-trihydroxyphenylalanine quinone, formed post-translationally from a conserved tyrosine residue. DAO is expressed mainly in intestinal and kidney epithelial cells where the enzyme is stored in secretory vesicles at the basolateral plasma membrane and released into the extracellular space upon stimulation. The best characterised DAO release stimulator is heparin that is released together with histamine by activated mast cells. Apparently, DAO is released locally to inactivate the excess of extracellular histamine to terminate its action.

1-2. Histamine receptors

Histamine In the human organism, histamine fulfils various functions as tissue hormone, neurotransmitter and messenger substance (biochemical signal transduction), which have only been insufficiently studied so far. At a molecular level, histamine exerts its actions *via* an activation of histamine receptors H_1, H_2, H_3 and H_4, which are part of the family of G protein-coupled receptors (GPCR). In 1966, histamine receptors were first differentiated into H_1 and H_2,[10] and it was reported that some responses to histamine were inhibited by low doses

of mepyramine (pyrilamine), whereas others were unsympathetic. In 1999, a third histamine receptor subtype was cloned and termed as H_3.[11] Subsequently in 2000, the fourth histamine receptor subtype was reported which was termed as H_4[12] and introduced a significant chapter in the story of histamine effects. Histamine acts by binding to target receptors according to the lock and key model and modulating intracellular signal cascades.

1-2-1. H_1 receptors

Histamine An activation of H_1 receptors is primarily responsible for the allergy symptoms triggered by histamine. These include itching and pain, contractions of smooth muscle tissue in the bronchial tubes and large blood vessels (diameter of more than 80 µm) as well as dilation of smaller blood vessels with hives and flush. In the central nervous system, histamine is involved in triggering vomiting and the regulation of the sleep-wake cycle *via* an activation of H_1 receptors. H_1 receptors also play a part in regulating the release of hormones such as adrenaline. Histamine is a messenger substance active in inflammatory processes and burns, and furthermore boosts the release of additional inflammatory mediators. Besides, it seems to play a part in the regulation of body temperature, the central control of blood pressure and pain perception.

1-2-2. H_2 receptors

H_2 receptors are involved in the regulation of gastric acid production and bowel movements (motility, peristalsis). An increase of gastric acid production may be interpreted as a component of histamine-induced immune reaction. An accelerated onward transport of the intestinal contents leads to diarrhea and may also be seen as an immune response. A stimulation of H_2 receptors also leads to an accelerated or stronger heart beat as well as dilation of smaller blood vessels.

1-2-3. H_3 receptors

In the human body the H_3 receptors are primarily found presynaptically on cells of the central and peripheral nervous systems. As autoreceptors, they play a role when negative feedback prevents additional histamine release. Via presynaptic receptors (in particular H_2 receptors), histamine has a regulatory influence on noradrenergic, serotoninergic, cholinergic, dopaminergic and glutaminergic neurons by blocking the release of neurotransmitters in the central and peripheral nervous systems. Thus it inhibits the release of the neurotransmitters acetylcholine, noradrenalin and serotonin as heteroreceptor. In this way, histamine influences indirectly the activity of these neurotransmitters. Through these mechanisms, the H_3 receptors play a role in the central regulation of hunger and thirst, the circadian rhythm, body temperature and blood pressure. Furthermore, these receptors are said to be directly or indirectly implicated in the pathophysiology of neurological pain, schizophrenia, Parkinson's disease and ADHS.

1-2-4. H_4 receptors

H_4 receptors are involved in the targeted migration of immune cells such as eosinophil granulocytes, T lymphocytes and monocytes to sources of histamine. This is why it is assumed that these receptors play an important role in the recruitment of leukocytes during immune responses, in particular in allergic reactions.

1-3. Antihistamines

An antihistamine is a type of pharmaceutical drug that opposes the activity of histamine receptors in the body. Antihistamines are subclassified according to the histamine receptor that they act upon: the two largest classes of antihistamines are H_1-antihistamines and H_2-antihistamines. Antihistamines that target the histamine H_1-receptor are used to treat allergic

reactions in the nose (e.g., itching, runny nose, and sneezing) as well as for insomnia. They are sometimes also used to treat motion sickness caused by problems with the inner ear. Antihistamines that target the histamine H_2-receptor are used to treat gastric acid conditions (e.g., peptic ulcersand acid reflux). H_1-antihistamines work by binding to histamine H_1 receptors in mast cells, smooth muscle, and endothelium in the body as well as in the tuberomammillary nucleus in the brain; H_2-antihistamines bind to histamine H_2 receptors in the upper gastrointestinal tract, primarily in the stomach.

1-3-1. H_1 Antihistamines; H_1 receptor antagonist

H_1-antihistamines refer to compounds that inhibit the activity of the H_1 receptor.[13] Since the H_1 receptor exhibits constitutive activity, H_1-antihistamines can be either neutral receptor antagonists or inverse agonists. Normally, histamine binds to the H_1 receptor and heightens the receptor's activity; the receptor antagonists work by binding to the receptor and blocking the activation of the receptor by histamine; by comparison, the inverse agonists bind to the receptor and reduce its activity, an effect which is opposite to histamine's. The vast majority of marketed H_1-antihistamines are receptor antagonists and only a minority of marketed compounds are inverse agonists at the receptor. Clinically, H_1-antihistamines are used to treat allergic reactions and mast cell-related disorders. Sedation is a common side effect of H_1-antihistamines that readily cross the blood-brain barrier; some of these drugs, such as diphenhydramine and doxylamine, are therefore used to treat insomnia. H_1-antihistamines can also reduce inflammation, since the expression of NF-κB, the transcription factor regulating inflammatory processes, is promoted by both the receptor's constitutive activity and agonist (i.e., histamine) binding at the H_1 receptor. Second-generation antihistamines cross the blood–brain barrier to a much lower degree than the first-generation antihistamines. Their main benefit is that they primarily affect peripheral histamine receptors

and therefore are less sedating. However, high doses can still induce the central nervous system drowsiness.

Figure 5. Representative histamine H_1-receptor antagonists

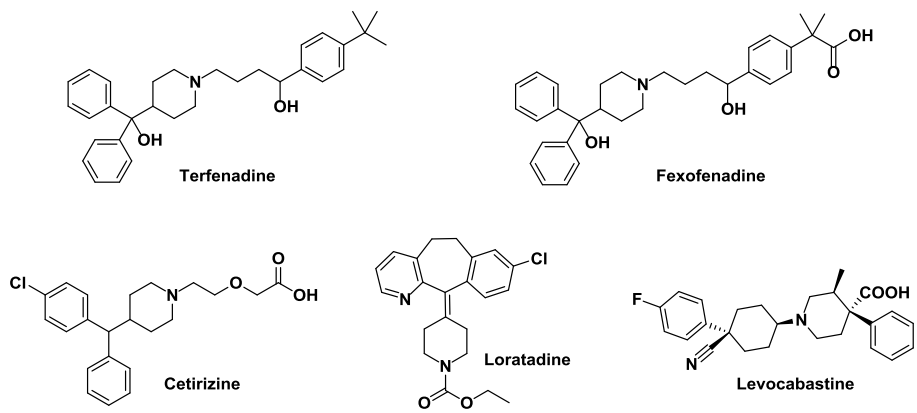

1-3-2. H_2 Antihistamines; H_2 receptor antagonist

H_2-antihistamines, like H_1-antihistamines, occur as inverse agonists and neutral antagonists. They act on H_2 histamine receptors found mainly in the parietal cells of the gastric mucosa, which are part of the endogenous signaling pathway for gastric acid secretion. Normally, histamine acts on H_2 receptor to stimulate acid secretion, drugs that inhibit H_2 receptor signaling thus reduce the secretion of gastric acid. H_2-antihistamines are among first-line therapy to treat gastrointestinal conditions including peptic ulcers and gastroesophageal reflux disease. Most side effects are due to cross-reactivity with unintended receptors.

Figure 6. Representative histamine H_2-receptor antagonists

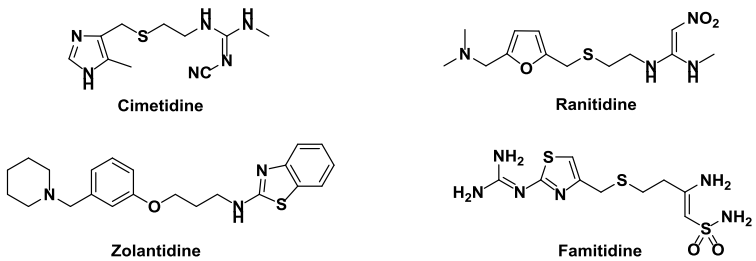

1-3-3. H_3 Antihistamines; H_3 receptor antagonist

An H_3-antihistamine is a classification of drugs used to inhibit the action of histamine at the H_3 receptor. H_3 receptors are primarily found in the brain and are inhibitory autoreceptors located on histaminergic nerve terminals, which modulate the release of histamine. Histamine release in the brain triggers secondary release of excitatory neurotransmitters such as glutamate and acetylcholine *via* stimulation of H_1 receptors in the cerebral cortex. Consequently, unlike the H_1-antihistamines which are sedating, H_3-antihistamines have stimulant and cognition-modulating effects.

Figure 7. Representative histamine H_3-receptor antagonists

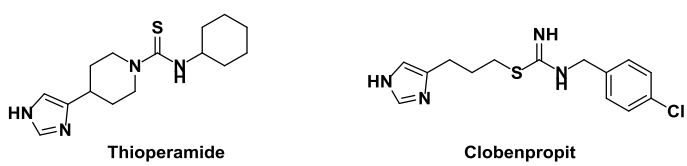

1-3-4. H_4 Antihistamines; H_4 receptor antagonist

H_4 receptor is intimately linked to many functional inflammatory responses mediated by histamine, including chemotaxis and cell recruitment, upregulation of adhesion molecule expression and modulation of cytokine and chemokine release. H_4-antihistamine have shown efficacy in a variety of inflammatory animal models, including peritonitis, colitis, and airway

inflammation models. These data suggest that the H_4 receptor is an attractive target for possible treatment of inflammation, allergy, and asthma.

2. Previous synthesis

According to the procedure (**Scheme 1**) described in a previous report,[14] piperidine intermediate **9** was synthesized using *N*,*N*-bis(2-chloroethyl)-4-methylbenzene-sulfonamide as a starting material in a sequence of piperidine ring formation, the chiral resolution of intermediate **5**, esterification of intermediate **6**, and detosylation with electrolysis. Subsequently, reductive amination with cyclic hexanone ring, hydrolysis, and salt formation afford to levocabastine hydrochloride **1**.

Scheme 1. Janssen′s route for levocabastine synthesis

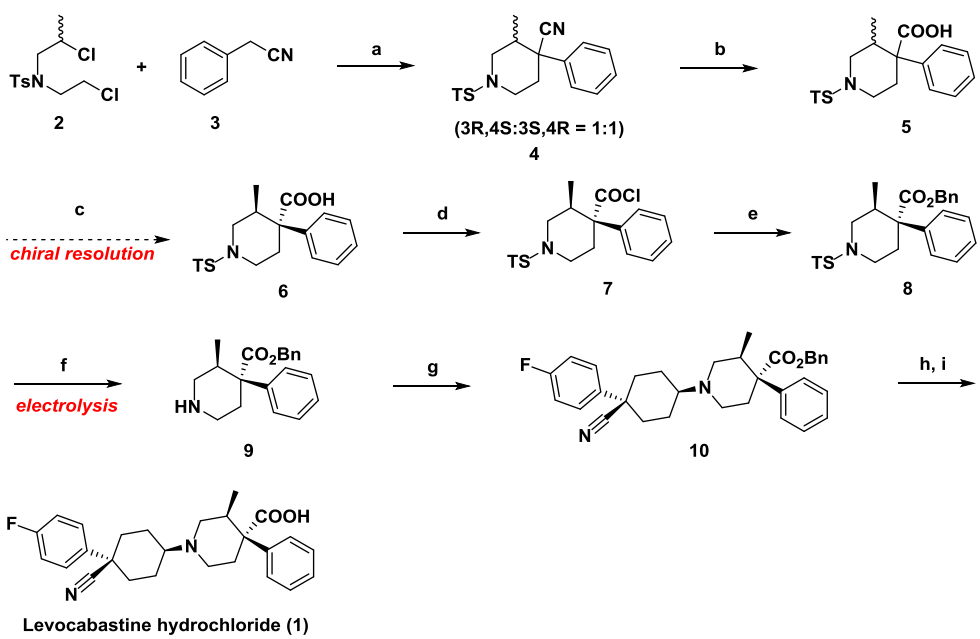

Reagents and conditions: (a) lithium amide, toluene, reflux, 20.0%; (b) potassium hydroxide, ethylene glycol, quantitative; (c) chiral resolution, 25.3%; (d) thionyl chloride, benzene, reflux, quantitative; (e) benzyl alcohol, toluene, r.t., 90.0%; (f) tetraethylammonium bromide, ethanol, 85.2%; (g) 1-(4-fluorophenyl)-4-oxo cyclohexanecarbonitrile, platinum, hydrogen gas, 2-propanol, 46.5%; (h) palladium, tetrahydrofuran, r.t.; (i) Methanolic HCl, 73.0% (for 2 steps)

However, this procedure is considered not industrially suitable because it requires a chiral resolution, which lowered the yield and limited the utility of this synthesis in an economical process. Furthermore, the use of expensive platinum catalyst for reductive amination and electrolysis for detosylation remained as drawbacks for the commercial production.

II. Results and Discussion

1. Synthetic strategy for levocabastine synthesis

Levocabastine is a synthetic piperidine derivative which is distinguished by 3 stereocenters, functionalized piperidine ring, and cyclic hexane ring containing geometric center (**Figure 8**).

Figure 8. Characterization of structure of levocabastine

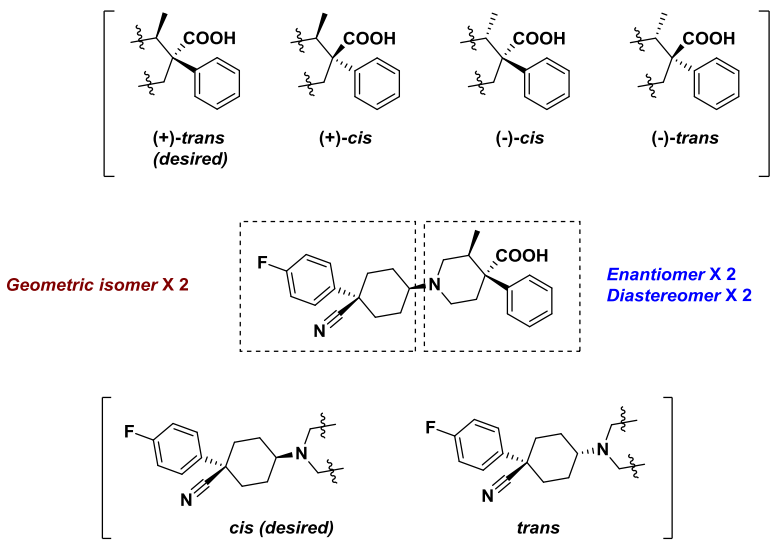

Synthetic strategy for the successful synthesis of levocabastine are as follows, outlined in **Figure 9**. The key part of our strategy involves an introduction of chiral starting material, (*S*)-propylene oxide **11**, to afford an optically pure key intermediate **8** (> 99% dr), replacement of electrolysis for detosylation to improve the commercial applicability, and removal of the use of platinum catalyst for reductive amination to obtain an intermediate **10**. Moreover, we tried to establish a production method reliable through process development of reaction step.

Figure 9. Synthetic strategy for the synthesis of levocabastine

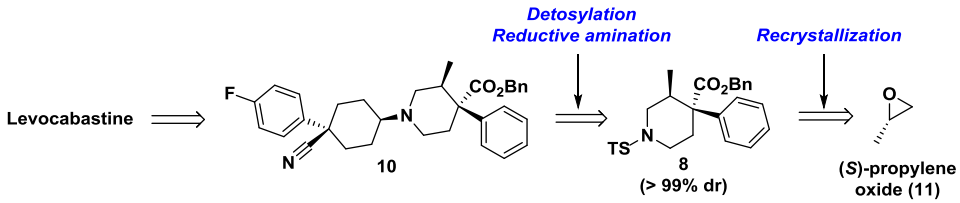

2. Synthesis of key intermediate

2-1. Synthesis of optically pure key intermediate 8

We used chiral starting material to introduce the two chiral centers present in key intermediate **8**. The optically pure diol **12**, prepared by *N*-alkylation to commercially available (*S*)-propylene oxide **11** with ethanolamine, was subjected to global tosylation to provide tosylate **13**. Facile cyclization with benzyl cyanide afforded cyanide **14** with 1:1 diastereomeric mixture. Hydrolysis of cyanide **14** with potassium hydroxide produced acid **15** with 1:1 diastereomeric mixture. Finally, esterification of acid **15**, followed by recrystallization afforded key intermediate **8** with a diastereomeric purity of more than 99% dr.

Scheme 2. Synthesis of the key intermediate 8 in an optically active form

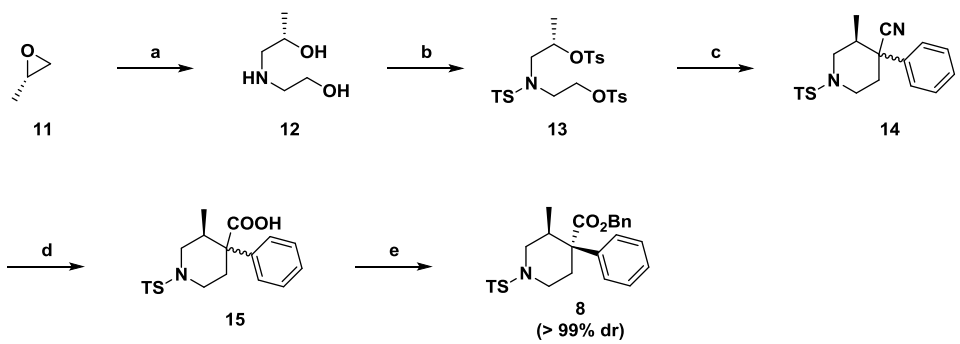

Reagents and conditions: (a) ethanolamine, H_2O, 0 °C to r.t., quantitative; (b) tosyl chloride, pyridine, 0 °C, 95.5%; (c) benzyl cyanide, sodium amide, tetrahydrofuran, 40°C, 70.8%; (d) potassium hydroxide, ethylene glycol, 170 °C, quantitative; (e) benzyl bromide, potassium carbonate, dimethylformamide, r.t., 41.5%

At this stage, we attempted the facile separation of desired intermediate **8** by simple recrystallization of the diastereomeric mixture, (instead of a delicate chiral resolution), based on the distinct physical properties of the diastereomers, particularly solubility. We thoroughly explored recrystallization of a number of intermediates (**14**, **15**, and **8**; **Figure 10**) and the results are summarized in **Table 1**.

Figure 10. Diastereomeric mixture of intermediate 14, 15, and 8

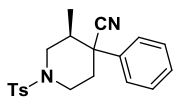

Diastereomeric mixture of 14

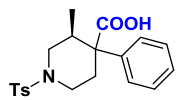

Diastereomeric mixture of 15

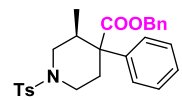

Diastereomeric mixture of 8

Table 1. Recrystallization of intermediate 14, 15, and 8

Entry	Intermediate	Temperature	Time (hr)	Solvent	Diastereomeric ratios of **14**, **15**, and **8**[a]	Diastereomeric ratios of **12**, **13**, and **5** after recrystallization[a]	Yield (%)[b]
1	14	reflux to r.t.	1	MeOH	40 : 60	53 : 47	70.8
2	14	reflux to r.t.	1	MeOH/$CHCl_3$	40 : 60	48 : 52	68.3
3	14	reflux to r.t.	1	Acetone	40 : 60	50 : 50	66.5
4	14	r.t.	6	ACN/ MeOH	40 : 60	46 : 54	71.2
5	15	reflux to r.t.	1	IPE	50 : 50	98 : 2	23.0
6	15	40 °C	1.5	IPE	50 : 50	95 : 5	22.9
7	8	r.t. to 0 °C	16	MeOH/IPE	52 : 48	99 : 1	41.5
8	8	r.t. to 0 °C	16	MeOH/HEX/IPE	52 : 48	98 : 2	38.2

[a] Diastereoselectivity was determined by HPLC. [b] Isolated yield.

Recrystallization of the diastereomeric mixture of cyanide **14** only slightly improved the diastereomeric ratio (less than 53% dr) regardless of temperature, time, or solvent (entries 1-4). In the case of acid **15**, the diastereomeric ratio was greatly improved to more than 95% dr (entries 5 and 6); however, the low yield limits the utility of this procedure. Fortunately, recrystallization of ester **8** provided a good diastereomeric ratio (over 98% dr) and a good yield (41.5%, entries 7 and 8). Accordingly, the overall yield for the preparation of ester intermediate **8** was improved by approximately 24.8% (from 4.6% to 29.4%).

2-2. Synthesis of optically pure key intermediate 10

2-2-1. Deprotection of ester intermediate 8

Although intermediate **9** was obtained by electrolysis of **8** in a good yield according to the procedure described in a previous report,[14] electrolysis requires special equipment. Thus, we looked for a convenient and economical process for detosylation under the conditions shown in **Table 2**.[15-21] Treatment of intermediate **8** with TBAF, thiophenol, and trimethylsilane did not provide the desired product (entries 1-4). Detosylation with low-valent titanium prepared from $Ti(OiPr)_4$/Mg powder was also not successful (entry 5). Interestingly, the reaction of **8** with potassium diphenylphosphide[22] provided desired product 9 in 68% yield (entry 6). We further optimized the detosylation conditions (entries 7 - 9) based on entry 6. Finally, the reaction of **8** with potassium diphenylphosphide in THF at -40 °C for 3 hours afforded free amine **9** in the best yield (69.5%) although the yield was still not ideal.

Table 2. Convenient detosylation of intermediate 8

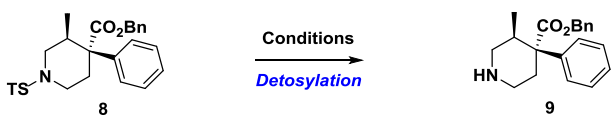

Entry	Reagents (eq.)	Temp.	Reaction time (hr)	Solvent	Yield (%)[a]
1	TBAF (10.0)	reflux	5	THF	No reaction
2	Thiophenol (1.3)/K_2CO_3 (2.0)	reflux	21	DMF/ACN	No reaction
3	TMSCl (1.5)/NaI (1.5)	reflux	17	ACN	No reaction
4	TMSI (neat)	80 °C	1	-	No reaction
5	Mg (5.0)/$Ti(OiPr)_4$ (1.0)	50 °C	21	THF	No reaction
6	0.5 M $KPPh_2$ in THF (1.3)	-78 °C	24	THF	68.0
7	0.5 M $KPPh_2$ in THF (1.3)	-40 °C	3	THF	69.5
8	0.5 M $KPPh_2$ in THF (1.3)	-20 °C	3	THF	43.7
9	0.5 M $KPPh_2$ in THF (1.3)	0 °C	3	THF	30.4

[a] Isolated yield.

2-2-2. Reductive amination for the preparation of intermediate 10

Next, we investigated the reductive amination of intermediate **9** to avoid the use of the expensive platinum catalyst. The reductive amination of amine **9** with cyclohexanone is an essential step prior to preparing the final target compound, levocabastine. Especially, it was inevitable for formation of geometric isomer **16** in addition to the desired compound **10** during the reductive amination reaction. To develop a sustainable and economical process, we explored the effect of reducing agent, temperature, and reaction time (**Table 3**).

Table 3. Modification of reductive amination for the preparation of intermediate 10

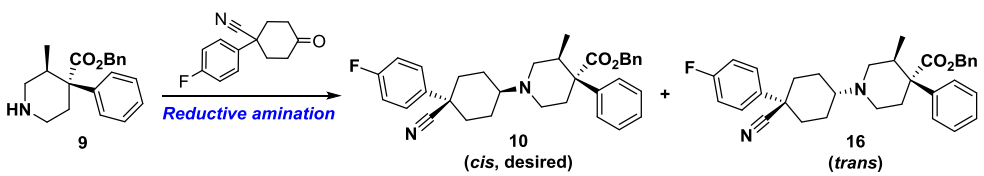

Entry	Reducing agents	Catalyst	Temperature (°C)	Reaction time (hr)	Conversion[a] (%)[a]	Ratio (*cis* : *trans*)
1	H_2	Pt	r.t.	3	91	90 : 10
2	$NaCNBH_3$	AcOH	40	24	74	72 : 28
3	$NaCNBH_3$	AcOH	40	48	83	67 : 33
4	$NaCNBH_3$	AcOH	40	72	95	66 : 34
5	$NaCNBH_3$	AcOH	60	24	93	62 : 38
6	$NaCNBH_3$	AcOH	0	6	75	68 : 32
7	$NaCNBH_3$	AcOH	r.t.	6	77	65 : 35
8	$NaCNBH_3$	AcOH	60	6	83	70 : 30
9	$NaBH(OAc)_3$	AcOH	r.t.	21	55	-
10	$NaBH(OAc)_3$	-	r.t.	24	95	83 : 17

[a] Determined by HPLC analysis.

We first explored the effect of reaction time on conversions of the substrate using established condtions (40 °C, $NaCNBH_3$, AcOH). The reactivity of the substrates improved depending

on the reaction time and reaction temperature (entries 2 – 4). About 95% conversion was the best result, when the reaction time was 72 hr (entry 4). However, a low selectivity was the drawback for preparation of the desired compound. Further screening revealed that the selectivity generally showed poor results regardless of temperature and reaction time (entries 5 - 8). Upon use of $NaBH(OAc)_3$ as a reducing agent without catalyst, the geometric isomer of 17.0% (entry 10) was observed after completion of the reaction. On the other hand, in the reaction using $NaBH(OAc)_3$ with AcOH as a catalyst, the reactivity was lowered due to partial reduction of the cyclohexanone intermediate (entry 9).

3. Final optimized synthesis of levocabastine hydrochloride

Cyanide intermediate **14** was prepared using (S)-propylene oxide **11** as a starting material in a sequence of *N*-alkylation, tosylation, and the piperidine ring cyclization with benzyl cyanide. Hydrolysis of Cyanide compound **14** followed by esterification with benzyl bromide afforded **8** with an excellent diastereoselectivity of >99% dr. Detosylation of the sulfonamide with $KPPh_2$ solution in THF afforded amino ester **9** without special equipment. The cyclohexanone was then coupled to free amine **9** at room temperature using $NaBH(OAc)_3$, followed by hydrolysis of benzyl ester and salt formation with 3 M HCl provided pure levocabastine hydrochloride **1** with more than 99.5% purity by HPLC. Our optimal synthetic route was shown in **Scheme 3**.

Scheme 3. Optimal synthesis of levocabastine hydrochloride

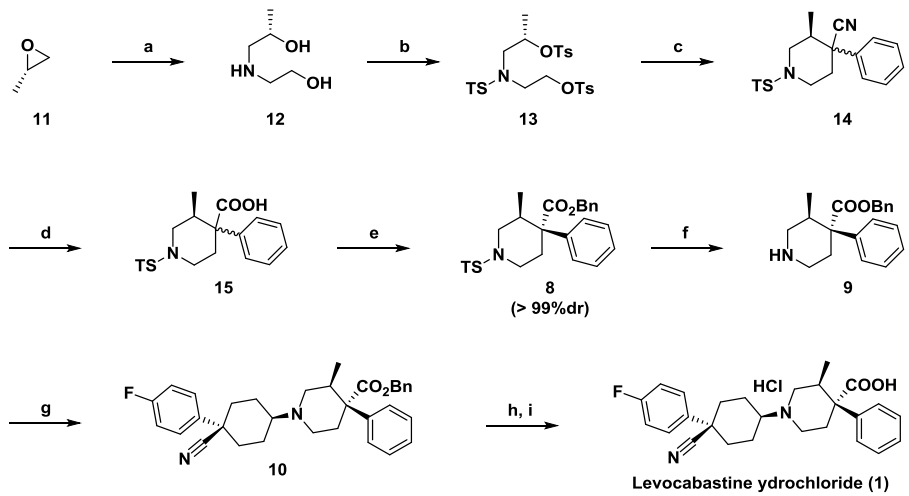

Reagents and conditions: (a) ethanolamine, H_2O, 0 °C to r.t.; (b) tosyl chloride, pyridine, 0 °C; (c) benzyl cyanide, sodium amide, tetrahydrofuran, 40°C, 70.8% (for 3 steps); (d) potassium hydroxide, ethylene glycol, 170 °C; (e) benzyl bromide, potassium carbonate, dimethylformamide, r.t., 41.5% (for 2 steps), (f) potassium diphenylphosphide solution (0.5 M in THF), 2 M HCl, -40 °C,; (g) 1-(4-fluorophenyl)-4-oxo cyclohexanecarbonitrile, sodium triacetoxyborohydride, dichloromethane, 51.5% (for 2 steps); (h) ammonium formate, palladium hydroxide; (i) 3 M HCl, MeOH, 93.8% (for 2 steps)

III. Conclusion

In summary, a practical and sustainable synthesis of levocabastine hydrochloride with high purity (> 99.5% by HPLC) was accomplished in 14.2% overall yield through 9 steps from commercially available and optically pure epoxide **11**. The high optical purity was achieved *via* simple recrystallization without chiral resolution. Our synthetic procedure enabled us to replace the previous process for detosylation by electrolysis and reductive amination using expensive metal catalyst with convenient and economical methods, respectively. Our synthetic procedure seems industrially quite suitable and widely utilized to secure pharmaceutically useful molecules.

IV. Experimental

General experimental

^{1}H spectra and ^{13}C spectra were recorded using a Bruker DPX 400 Spectrometer. All purity values were obtained by HPLC analysis using HPLC 1200 Series from Agilent Technologies. All NMR spectra were measured using 400 UltraShield NMR. Chemical shifts are expressed in parts per million (ppm, δ) downfield from tetramethylsilane, and were referenced to the DMSO-d_6 (2.49 ppm for ^{1}H and 39.5 ppm for ^{13}C, respectively), $CDCl_3$ (7.26 ppm for ^{1}H and 77.0 ppm for ^{13}C, respectively) and CD_3OD (4.87 ppm for ^{1}H and 49.2 ppm for ^{13}C, respectively). ^{1}H-NMR data are reported in the order of chemical shift, multiplicity (s, singlet; d, doublet; t, triplet; q, quartet; m, multiplet and/or multiple resonances), number of protons, and coupling constant in hertz (Hz). High resolution mass spectra were obtained with a Synapt G2 instrument.

HPLC analysis (compound 13, 14) : YMC-Pack ODS AQ, 4.6 mm X 250 mm (3 ㎛), λ = 220 nm, flow rate 0.5 mL/min, column temperature: 37 °C, mobile phase (30 : 70 = H_2O : MeOH).

HPLC analysis (compound 15, 8) : YMC-Pack ODS AQ, 4.6 mm X 250 mm (3 ㎛), λ = 220 nm, flow rate 0.5 mL/min, column temperature: 37 °C, mobile phase (20 : 80 = buffer : MeOH; buffer : 0.024 M Bu_4NHSO_4 solution).

HPLC analysis (compound 9, 10, 1) : . Acquity UPLC BEH Phenyl, 2.1 mm X 100 mm (1.7 ㎛), λ = 210 nm, flow rate 0.5 mL/min, column temperature: 60 °C, mobile phase (20 : 80 = buffer : acetonitrile; buffer : 0.05 M Bu_4NHSO_4 solution).

Synthesis

(*S*)-1-((2-hydroxyethyl)amino)propan-2-ol (12). To a stirred solution of ethanolamine (800.0 g, 13.10 mol) in purified water (1,640 mL) was slowly added (*S*)-propylene oxide (115 mL, 1.64 mol) at 0 °C. The mixture was stirred for 1 hr at the same temperature and stirred for 4 hr at room temperature. The reaction mixture was concentrated under reduced pressure at 90 °C. Diol **12** was obtained as yellow oil (207.0g, quantitative, 75.0% purity). This product was used in the next step without further purification; ^{1}H NMR (400 MHz, D_2O): δ 1.15 (d, 3H, J = 6.4 Hz), 2.57-2.59 (m, 2H), 2.70-2.73 (m, 2H), 3.66 (td, 2H, J = 5.7 Hz, 2.1 Hz), 3.91 (dd, 1H, J = 6.4 Hz, 5.9 Hz). ^{13}C NMR (100 MHz, $CDCl_3$): δ 64.8, 59.6, 56.1, 50.9, 21.0. HRMS: Calcd for $C_5H_{13}NO_2$ [M+H]+120.1025; Found 120.1025.

(*S*)-1-((4-methyl-*N*-(2-(tosyloxy)ethyl)phenyl)sulfonamido)propan-2-yl-4-methyl benzenesulfonate (13). To a stirred solution of *p*-toluenesulfonylchlrode (260.0 g, 1.36 mol) in pyridine (75 mL) was slowly added diol **12** (50.0 g, 0.42 mol, 75.0% purity) in pyridine (200 mL) at 0 °C. The mixture was stirred for 48 hr at the same temperature and quenched with H_2O (700 mL) and DCM (700 mL) at room temperature. The reaction slurry was washed with 4.0 M HCl solution (700 mL), 10% NaCl solution (900 mL), and concentrated *in vacuo* to afford tosylate **13** as yellow oil (233.0g, 95.5%, 76.3% purity). This product was used in the next step without further purification; ^{1}H NMR (400 MHz, $CDCl_3$): δ 1.21 (d, 3H, J = 6.4 Hz), 2.43 (s, 3H), 2.45 (s, 3H), 2.46 (s, 3H), 3.15-3.28 (m, 3H), 3.33-3.39 (m, 1H), 4.06-4.13 (m, 2H), 4.77 (q, 1H, J = 6.2 Hz), 7.26-7.36 (m, 6H), 7.61 (d, 2H, J = 8.3 Hz), 7.73-7.78 (m, 4H). ^{13}C NMR (100 MHz, $CDCl_3$): δ 145.3, 145.1, 144.3, 135.0, 133.7, 132.5, 130.1, 128.1, 128.0, 127.5, 77.8, 68.2, 54.4, 49.0, 25.5, 21.8, 21.7, 18.3. HRMS: Calcd for $C_{26}H_{31}NO_8S_3$ [M+Na]+604.1110; Found 604.1111.

(3*S*)-3-methyl-4-phenyl-1-tosylpiperidine-4-carbonitrile (14). To a suspension of sodium amide (48.5 g, 1.24 mol) in THF (675 mL) was slowly added a solution of benzyl cyanide (115 mL, 1.64 mol) in THF (460 mL) at 0 °C. The mixture was stirred for 1 hr at room temperature and a solution of tosylate **13** (233.0 g, 0.40 mol, 76.3% purity) in THF was added dropwise for 1 hr at 0 °C. The reaction mixture was stirred for 2 hr at 40 °C, cooled to 0 °C, and 15% NH_4Cl solution (140 mL) was added. The reaction slurry was distilled until THF was completely removed. To the concentrated mixture was added purified water (1,000 mL) and DCM (1,000 mL) and the reaction slurry was stirred for 30 mins. The organic layer was washed with 10% NaCl solution (1,000 mL) and concentrated under reduced pressure. The residue was dissolved with MeOH (230 mL). The resulting solution was stirred for 1 hr at 75 °C, stirred for 30 mins at room temperature, and stirred for 1 hr at 0 °C. The precipitate was filtered and then dried to afford cyanide **14** as white solid (80.3 g, 70.8% for 3 steps); ^{1}H NMR (400 MHz, $CDCl_3$): δ 0.81-0.85 (m, 3H), 2.09-2.13 (m, 1H), 2.26-2.44 (m, 2H), 2.48-2.49 (m, 3H), 2.58-3.04 (m, 2H), 3.74-3.91 (m, 1H), 3.96-4.09 (m, 1H), 7.28-7.46 (m, 7H), 7.68-7.72 (m, 2H). ^{13}C NMR (100 MHz, $CDCl_3$): δ 144.2, 144.1, 137.8, 137.6, 133.2, 133.0, 130.1, 129.3, 128.6, 127.7, 127.6, 126.3, 126.0, 122.6, 119.2, 50.0, 49.7, 49.5, 44.2, 44.0, 43.8, 39.1, 38.3, 37.8, 26.6, 21.7, 14.2, 12.4. HRMS: Calcd for $C_{20}H_{22}N_2O_2S$ [M+H]+ 355.1480; Found 355.1481. dr = 53.1 : 46.9.

(3*S*)-3-methyl-4-phenyl-1-tosylpiperidine-4-carboxylic acid (15). To a stirred solution of cyanide **14** (80.3 g, 0.23 mol) in ethylene glycol (400 mL) was added potassium hydroxide (89.0 g, 1.59 mol). The reaction mixture was stirred for 44 hr at 170 °C, cooled to room temperature, and DCM (562 mL) was added. The reaction slurry was slowly quenched with 2.0 M HCl solution (900 mL) at 0 °C. The organic layer was washed with 10% NaCl solution (800 mL) and concentrated *in vacuo* to afford acid **15** as yellow oil (92.3g, quantitative, 91.7%

purity). This product was used in the next step without further purification; ^{1}H NMR (400 MHz, $CDCl_3$): δ 0.78-1.14 (m, 3H), 2.28-2.39 (m, 2H), 2.41-2.45 (m, 3H), 2.53-2.90 (m, 2H), 3.00-3.18 (m, 2H), 3.62-3.95 (m, 1H), 7.25-7.38 (m, 8H), 7.58-7.66 (m, 2H). ^{13}C NMR (100 MHz, $CDCl_3$): δ 179.3, 179.0, 143.6, 140.3, 139.0, 133.8, 129.9, 129.8, 129.0, 128.9, 127.7, 127.6, 127.5, 127.0, 126.1, 52.8, 52.1, 50.1, 48.5, 44.4, 43.1, 34.4, 25.9, 21.7, 21.6, 14.8, 13.5. HRMS: Calcd for $C_{20}H_{23}NO_4S$ [M+H]+374.1426; Found 374.1423.

(3*S*,4*R*)-Benzyl-3-methyl-4-phenyl-1-tosylpiperidine-4-carboxylate (8). To a stirred solution of acid **15** (92.3 g, 0.25 mol, 91.7% purity) in DMF (320 mL) were added potassium carbonate (37.6 g, 0.27 mol) and benzyl bromide (32.4 g, 0.27 mol). The reaction mixture was stirred for 3 hr at room temperature, cooled to 0 °C, and quenched with 10% NH_4Cl solution (600 mL) and ethyl acetate (500 mL). The organic layer was washed with 10% NaCl solution (500 mL) and concentrated under reduced pressure. The residue was clearly dissolved with MeOH (60 mL). To the resulting solution was added IPE (360 mL), and stirred for 15 hr at room temperature, and stirred for 1 hr at 0 °C. The precipitate was filtered and then dried to afford ester **8** as white solid (42.9 g, 41.5% for 2 step); ^{1}H NMR (400 MHz, $CDCl_3$): δ 0.79 (d, 3H, J = 7.0 HZ), 2.19-2.29 (m, 2H), 2.46 (s, 3H), 2.56-2.62 (m, 2H), 2.92-2.95 (m, 1H), 3.57-3.61 (m, 1H), 3.87-3.90 (m, 1H), 4.93 (dd, 2H, J = 21.2 Hz, 12.3 Hz), 6.96-6.98 (m, 2H), 7.17-7.21 (m, 2H), 7.23-7.33 (m, 8H), 7.57-7.60 (m, 2H). ^{13}C NMR (100 MHz, $CDCl_3$): δ 173.8, 143.4, 140.6, 135.5, 133.4, 129.8, 128.8, 128.5, 128.2, 127.9, 127.6, 127.5, 126.0, 66.8, 52.4, 50.2, 44.5, 34.5, 25.9, 21.7, 13.5. HRMS: Calcd for $C_{27}H_{29}NO_4S$ [M+H]+464.1896; Found 464.1894. dr = 99.4 : 0.6.

Convenient detosylation of intermediate 8 (Table 2)

(3*S*,4*R*)-Benzyl-3-methyl-4-phenylpiperidine-4-carboxylate (**9**, entry 1 in table 2). To a stirred solution of **8** (46 mg, 0.10 mmol) in THF (10 mL) was added TBAF in THF (1.00 mmol) at room temperature. The reaction mixture was stirred for 5 hr under refluxing condition. No reaction (by TLC).

(3*S*,4*R*)-Benzyl-3-methyl-4-phenylpiperidine-4-carboxylate (**9**, entry 2 in table 2). To a stirred solution of **8** (46 mg, 0.10 mmol) in THF (10 mL) and ACN (10 mL) were added potassium carbonate (28 mg, 0.20 mmol) and thiophenol (14 mg, 0.13 mmol) at room temperature. The reaction mixture was stirred for 21 hr under refluxing condition. No reaction (by TLC).

(3*S*,4*R*)-Benzyl-3-methyl-4-phenylpiperidine-4-carboxylate (**9**, entry 3 in table 2). To a suspension of sodium iodide (23 mg, 0.15 mmol) in ACN (10 mL) was slowly added trimethylsilyl chloride (16 mg, 0.15 mmol) at 0 °C. To the mixture was added **8** (46 mg, 0.10 mmol). The reaction mixture was stirred for 17 hr under refluxing condition. No reaction (by TLC).

(3*S*,4*R*)-Benzyl-3-methyl-4-phenylpiperidine-4-carboxylate (**9**, entry 4 in table 2). To a reaction flask were added **8** (49 mg, 0.11 mmol) and iodotrimethylsilane (1 mL, 0.75 mmol). The reaction mixture was stirred for 1 hr at 80 °C. No reaction (by TLC).

(3*S*,4*R*)-Benzyl-3-methyl-4-phenylpiperidine-4-carboxylate (**9**, entry 5 in table 2). To a stirred solution of **8** (100 mg, 0.22 mmol) in THF (10 mL) was added Mg (26 mg, 1.08 mmol) at room temperature. The mixture was stirred for 30 mins at the same temperature and titanium isopropoxide (61 mg, 0.22 mmol) and trimethylsilyl chloride (35 mg, 0.32 mmol) were added. The reaction mixture was stirred 21 hr at 50 °C. No reaction (by TLC).

(3*S*,4*R*)-Benzyl-3-methyl-4-phenylpiperidine-4-carboxylate (**9**, entry 7 in table 2). To a stirred solution of ester **8** (50.0 g, 0.11 mol) in THF (500 mL) was added dropwise 0.5 M potassium diphenylphosphide solution (280 mL, 0.14 mol) at -40 °C. The mixture was stirred for 3 hr at the same temperature. To the reaction slurry was added 2.0 M HCl solution (250 mL), and stirred for 2 hr at room temperature. The reaction mixture was quenched with 10% $NaHCO_3$ solution (1,000 mL) and ethyl acetate (800 mL). The organic layer was concentrated under reduced pressure to afford piperidine **9** as yellow oil (67.5 g, quantitative, 34.3% purity). This product was used in the next step without further purification; ^{1}H NMR (400 MHz, CD_3OD): δ 0.75 (d, 3H, J = 7.4 Hz), 2.27 (td, 1H, J = 13.7 Hz, 4.2 Hz), 2.59-2.63 (m, 1H), 2.75 (td, 1H, J = 13.4 Hz, 2.8 Hz), 2.97-3.00 (m, 1H), 3.09-3.24 (m, 2H), 3.31-3.35 (m, 1H), 5.12 (dd, 2H, J = 12.2 Hz, 5.8 Hz), 7.13-7.15 (m, 2H), 7.24-7.37 (m, 8H). ^{13}C NMR (100 MHz, CD_3OD): δ 174.8, 141.7, 137.1, 129.9, 129.5, 129.3, 129.2, 128.6, 126.9, 68.1, 53.1, 43.8, 34.5, 25.5, 13.4. HRMS: Calcd for $C_{20}H_{23}NO_2$ [M+H]+310.1807; Found 310.1811.

(3*S*,4*R*)-benzyl-1-((1*S*,4*R*)-4-cyano-4-(4-fluorophenyl)cyclohexyl)-3-methyl-4-henylpiperidine-4-carboxylate (10). To a suspension of piperidine **9** (67.5 g, 0.22 mol, 34.3% purity) in DCM (400 mL) were added cyclohexanone (56.2 g, 0.26 mol) and $NaBH(OAc)_3$ (57.2 g, 0.27 mol) at room temperature. The reaction mixture was stirred for 24 hr, and quenched with 10% $NaHCO_3$ solution (700 mL) at the same temperature. The organic layer was washed with 10% NaCl solution (600 mL), and concentrated *in vacuo*. The residue was clearly dissolved with methanol (500 mL) at 60 °C. The resulting solution was stirred 2 hr at room temperature. The precipitate was filtered and then dried to afford tertiary amine **10** as off-white solid (28.4 g, 51.5% for 2 steps); ^{1}H NMR (400 MHz, $CDCl_3$): δ 0.76 (d, 3H, J =

7.0 Hz), 1.76-1.91 (m, 6H), 2.19-2.24 (m, 3H), 2.32-2.38 (m, 2H), 2.57-2.60 (m, 1H), 2.65-2.71 (m, 2H), 2.94 (d, 2H, *J* = 9.2 Hz), 5.11 (dd, 2H, *J* = 24.6 Hz, 12.4 Hz), 7.08-7.12 (m, 2H), 7.17-7.20 (m, 2H), 7.24-7.39 (m, 8H), 7.46-7.49 (m, 2H). ^{13}C NMR (100 MHz, $CDCl_3$): δ 174.8, 163.5, 161.1, 141.9, 136.6, 136.1, 128.6, 128.5, 128.1, 127.5, 127.4, 127.0, 126.3, 122.4, 116.0, 115.8, 66.6, 62.3, 53.2, 53.0, 48.2, 43.8, 37.2, 35.1, 27.2, 26.2, 25.0, 14.6. HRMS: Calcd for $C_{33}H_{35}N_2O_2F$ [M+H]+511.2761; Found 511.2762. HPLC purity: 99.5%. Geometric isomer < 0.1%.

(3*S*,4*R*)-1-(*cis*-4-cyano-4-(4-fluorophenyl)cyclohexyl)-3-methyl-4-phenyl-4-piperidinecarboxylic acid, hydrochloride (1, levocabastine hydrochloride). To a stirred solution of tertiary amine **10** (51.3 g, 0.10 mol) in DCM (210 mL) and MeOH (420 mL) were added ammonium formate (12.7 g, 0.20 mol) and palladium hydroxide (5.1 g, 10 wt% of compound **10**) at room temperature. The reaction mixture was stirred for 3 hr at the same temperature and 7.0 M ammonia in methanol (500 mL) was slowly added. The reaction slurry was concentrated under reduced pressure. To the concentrated mixture was added MeOH (255 mL) and IPE (1,020 mL) and the reaction slurry was stirred for 1 hr at room temperature. The precipitate was filtered. The obtained solid was suspended with MeOH (208 mL). To a suspended solution was slowly added 3.0 M HCl solution in MeOH (165 mL) and then the reaction mixture was stirred for 30 mins at room temperature. To the reaction slurry was added IPE (754 mL) and the mixture was stirred for 1 hr at room temperature. The solid was filtered and then washed with IPE (500 mL). The residue was suspended with EtOH (132 mL) and MeOH (132 mL) for 6 hr at 50 °C, and cooled to room temperature. The solid was filtered, washed with ethanol (264 mL), and then dried to afford Levocabastine hydrochloride **1** as white solid (43.1 g, 93.8% for 2 steps); $[\alpha]_D^{20}$ = -104.02 (c = 1, MeOH). ^{1}H NMR (400 MHz, CD_3OD): δ 0.86 (d, 3H, *J* = 7.6 Hz), 1.97-2.13 (m, 4H), 2.35-2.54 (m, 5H), 2.83 (dd,

1H, *J* = 12.6 Hz, 2.0 Hz), 3.12 (td, 1H, *J* = 13.3 Hz, 2.6 Hz), 3.21-3.23 (m, 1H), 3.41-3.45 (m, 2H), 3.70-3.74 (m, 1H), 3.82-3.85 (m, 1H), 7.16-7.21 (m, 2H), 7.31-7.35 (m, 1H), 7.38-7.42 (m, 4H), 7.58-7.62 (m, 2H). ^{13}C NMR (100 MHz, CD_3OD): δ 176.1, 165.1, 162.7, 141.0, 137.0, 136.9, 130.0, 128.9, 128.8, 126.9, 122.7, 117.0, 116.8, 65.4, 54.9, 52.0, 50.0, 44.1, 36.5, 35.0, 25.9, 25.5, 25.4, 13.9. HRMS: Calcd for $C_{26}H_{29}N_2O_2F$ [M+H]+ 421.2291; Found 421.2292. HPLC purity: 99.7%. Optical purity > 99.9%.

V. References

1. Maslinski, C.; Fogel, W. A. *Handbook of experimental pharmacology*, **1991**, 97, 165-189.

2. Paiva, T. B.; Tominaga, M.; Paiva, A. C. M. *Journal of Medicinal Chemistry*, 1970, 13, 689–692.3. Moessner, J.; Caca, K. *Eur. J. Clin. Invest.* **2005**, 35, 469–475.

4. Haas, H.; Panula, P. *Nature Rev. Neurosci.* **2003**, 4, 121–130.5. Gale, E. F. *Biochem. J.* 1945, 39, 42–46.

6. Tudball, N.; Thomas, J. H. *Biochemistry*, **1968**, 7, 3520–3528.

7. Rosenthaler J.; Guirard B. M.; Chang G. W.; Snell E. E. *Proc. Natl. Acad. Sci.* U.S.A. **1965**, 54, 152–158.

8. Schwelberger, H. G. *Histamine : Biology and Medical Aspects*, **2004**, 53-59.

9. Schwelberger, H. G. *Histamine : Biology and Medical Aspects*, **2004**, 43-52.

10. Ash, A. S.; Schild, H. O. *Br. J. Pharmacol*. **1966**, 27, 427-439.

11. Lovenberg, T. W.; Roland, B. L.; Wilson, S. J. *Mol. Pharmacol*. **1999**, 55, 1101-1107.

12. Oda, T.; Morikawa, N.; Saito, Y.; Masuho, Y.; Matsumoto, S. *J. Biol. Chem*. **2000**, 275, 36781-36786.

13. Leurs, R.; Church, M. K.; Taglialatela, M. *Clinical and Experimental Allergy*, **2002**, 32, 489–498.

14. Raymond, A. Stokbroekx; Marcel, G. M. Luyckx; Joannes, J. M. Willems. US 4369184.

15. Senboku, H.; Nakahara, K.; Fukuhara, T.; Hara, S. *Tetrahedron Lett.* **2010**, 51, 435-437.

16. Yasuhara, A.; Kameda, M.; Sakamoto, T. *Chem. Pharm. Bull*. **1999**, 47, 809-812.

17. Sophia, S.; Michaelidou; Panayiotis, A.; Koutentis, *Tetrahedron*, **2010**, 66, 3016–3023.

18. Knowles, H. S.; Parsons, A. F.; Pettifer, R. M.; Rickling, S. *Tetrahedron*, **2000**, 56, 979-988.

19. Shohji, N.; Kawaji, T.; Okamoto, S. *Org. Lett.* **2011**, 13, 2626–2629.

20. Sridhar, M.; Kumar, B. A.; Narender, R. Tetrahedron Lett. 1998, 39, 2847. Nyasse, B.; Ragnarsson, U. *Chem. Commun*. **1997**, 1017-1018.

21. Sabitha, G.; Reddy, B. V. S.; Abraham, S.; Yadav, J. S. *Tetrahedron Lett*. **1999**, 40, 1569-1571.

22. Yoshida, S.; Igawa, K.; Tomooka, K. *J. Am. Chem. Soc.* **2012**, 134, 19358-19361.

VI. Appendix

(*S*)-1-((2-hydroxyethyl)amino)propan-2-ol

▼^{1}H-NMR ($CDCl_3$, 400 MHz)

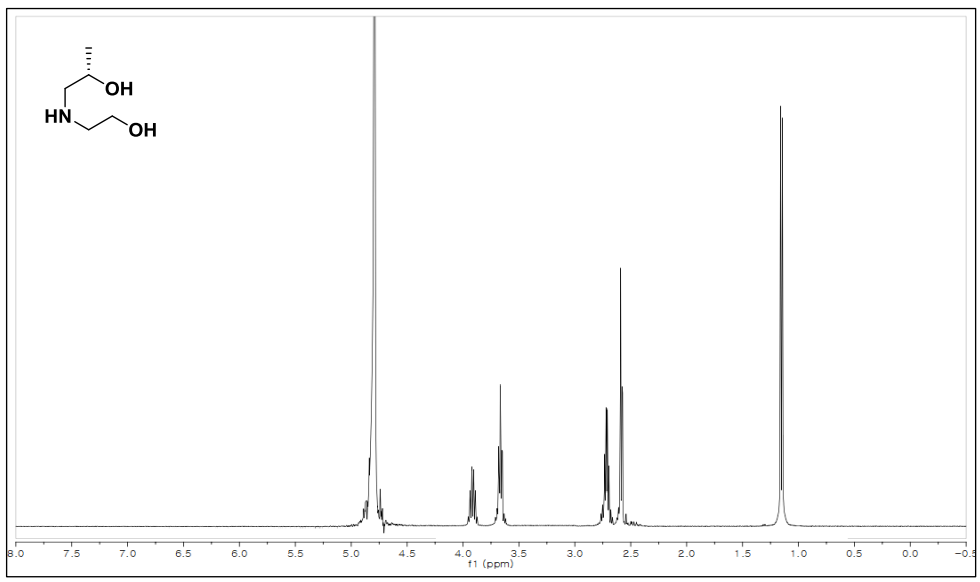

▼^{13}C-NMR ($CDCl_3$, 100 MHz)

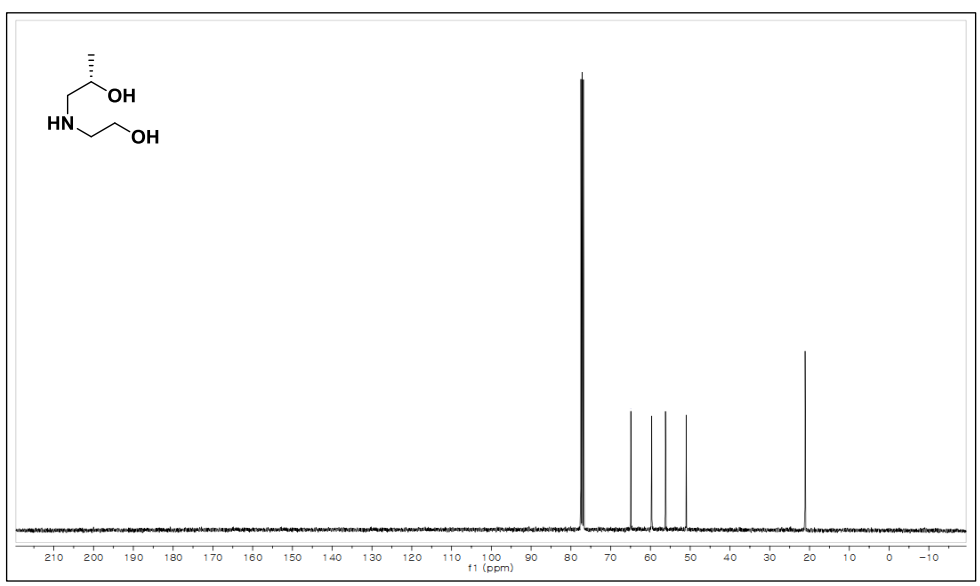

▼High-Resolution Mass

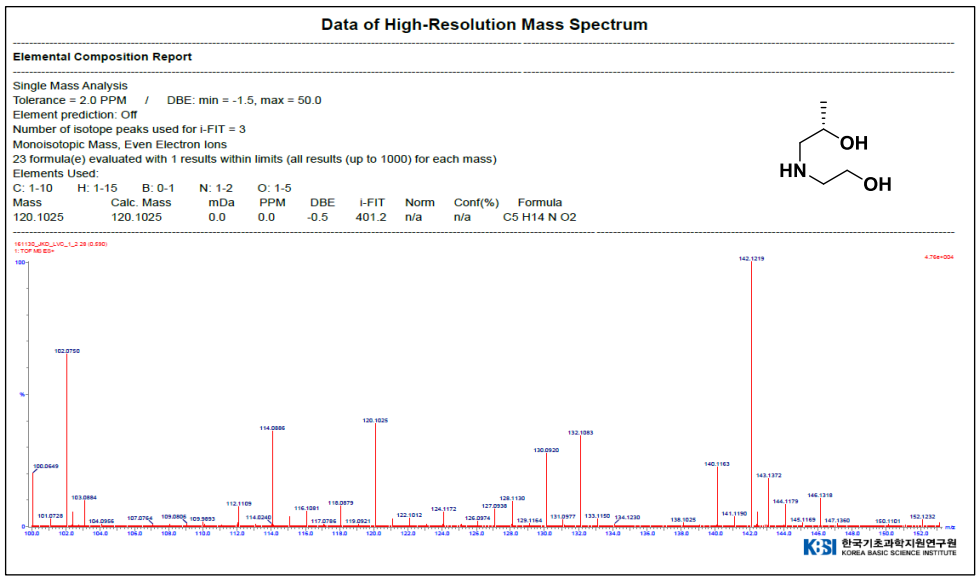

(*S*)-1-((4-methyl-*N*-(2-(tosyloxy)ethyl)phenyl)sulfonamido)propan-2-yl-4-methyl benzenesulfonate

▼^{1}H-NMR ($CDCl_3$, 400 MHz)

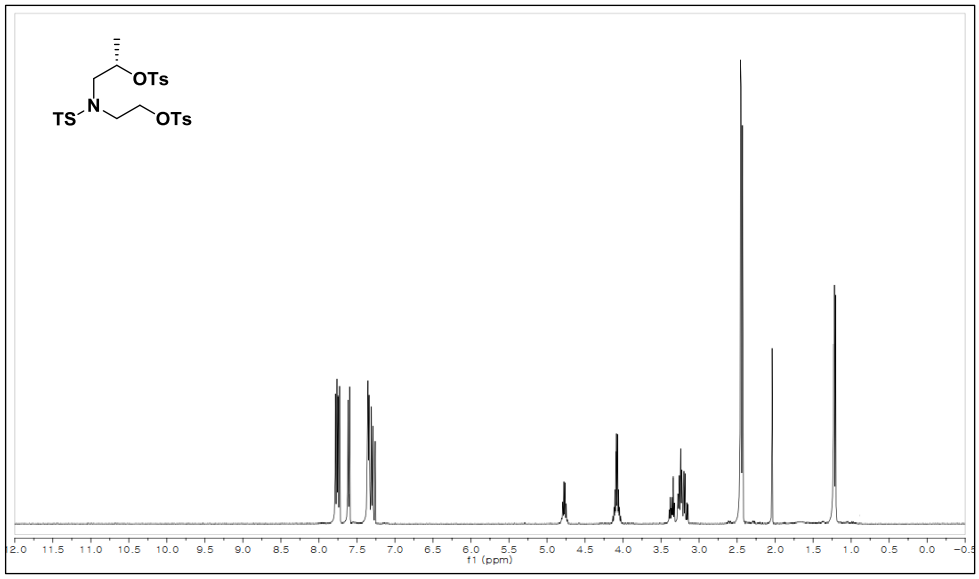

▼^{13}C-NMR ($CDCl_3$, 100 MHz)

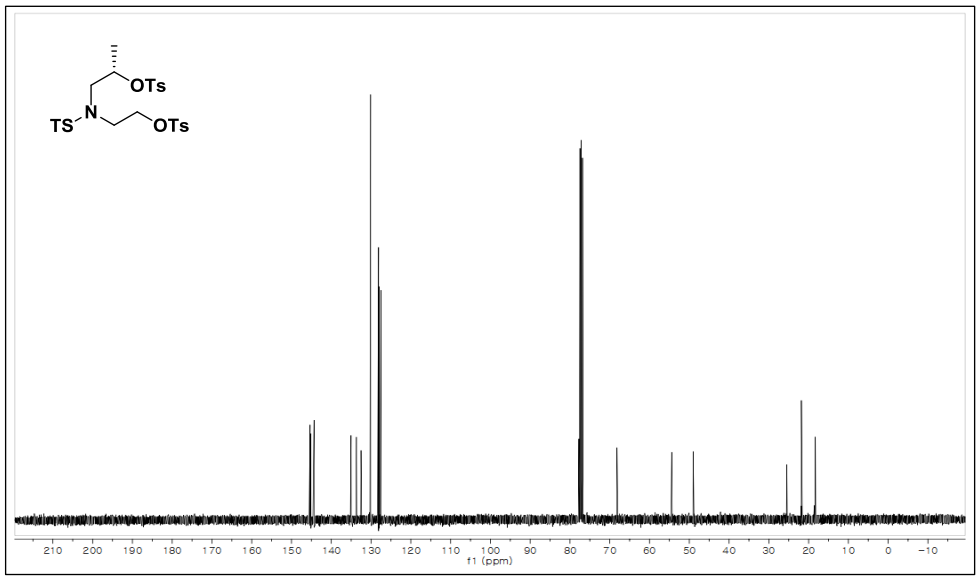

▼High-Resolution Mass

Data of High-Resolution Mass Spectrum

Elemental Composition Report

Single Mass Analysis
Tolerance = 2.0 PPM / DBE: min = -1.5, max = 50.0
Element prediction: Off
Number of isotope peaks used for i-FIT = 3
Monoisotopic Mass, Even Electron Ions
309 formula(e) evaluated with 1 results within limits (all results (up to 1000) for each mass)
Elements Used:
C: 1-30 H: 1-35 B: 0-1 N: 1-2 O: 1-10 Na: 0-1 S: 1-3

Mass	Calc. Mass	mDa	PPM	DBE	i-FIT	Norm	Conf(%)	Formula
604.1111	604.1110	0.1	0.2	11.5	129.6	n/a	n/a	C26 H31 N O8 Na S3

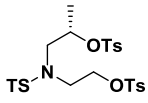

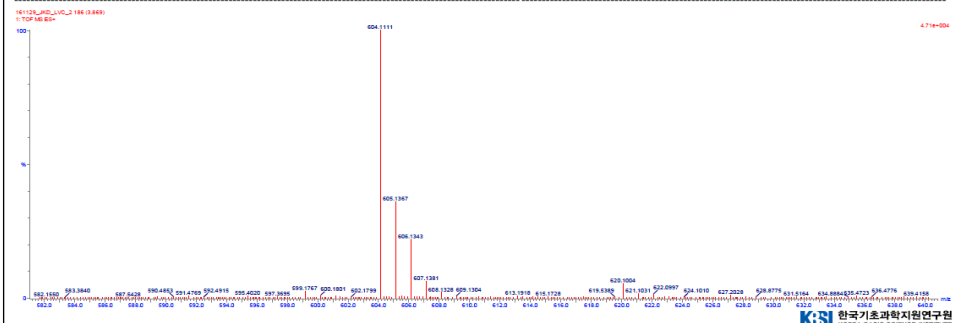

(3*S*)-3-methyl-4-phenyl-1-tosylpiperidine-4-carbonitrile

▼^{1}H-NMR ($CDCl_3$, 400 MHz)

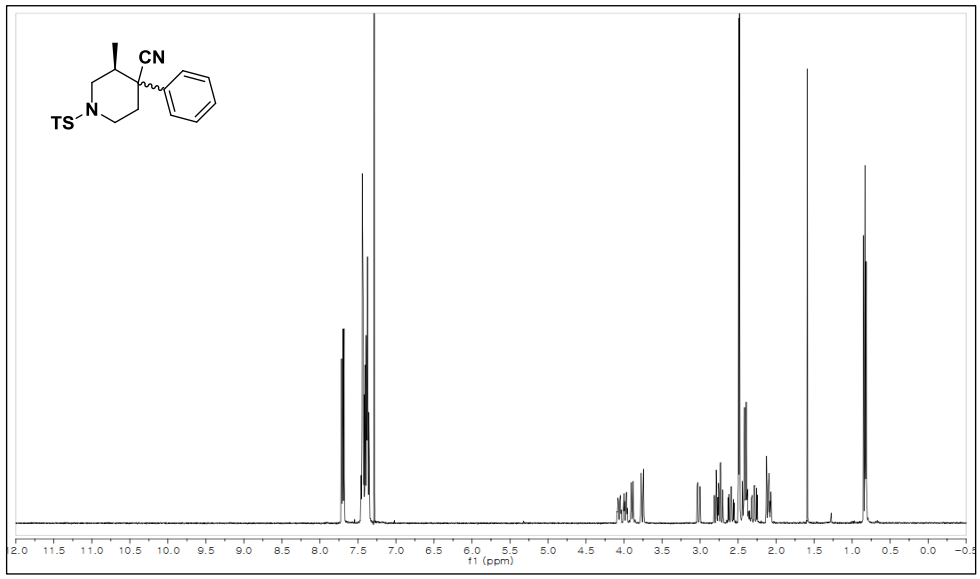

▼^{13}C-NMR ($CDCl_3$, 100 MHz)

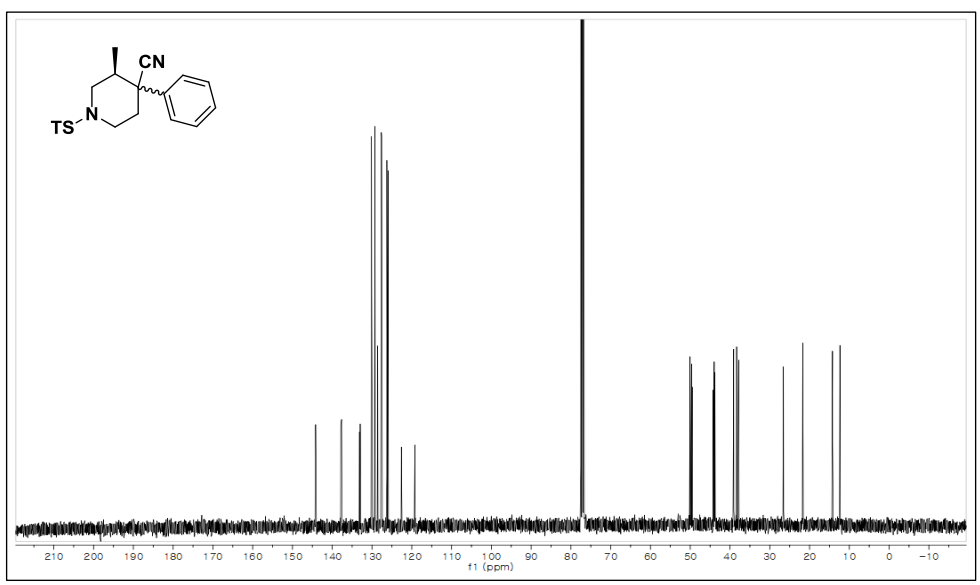

▼High-Resolution Mass

Data of High-Resolution Mass Spectrum

Elemental Composition Report

Single Mass Analysis
Tolerance = 2.0 PPM / DBE: min = -1.5, max = 50.0
Element prediction: Off
Number of isotope peaks used for i-FIT = 3
Monoisotopic Mass, Even Electron Ions
329 formula(e) evaluated with 1 results within limits (all results (up to 1000) for each mass)
Elements Used:
C: 1-30 H: 1-35 B: 0-1 N: 1-2 O: 1-10 S: 1-3

Mass	Calc. Mass	mDa	PPM	DBE	i-FIT	Norm	Conf(%)	Formula
355.1481	355.1480	0.1	0.3	10.5	187.4	n/a	n/a	C20 H23 N2 O2 S

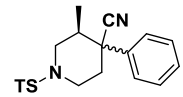

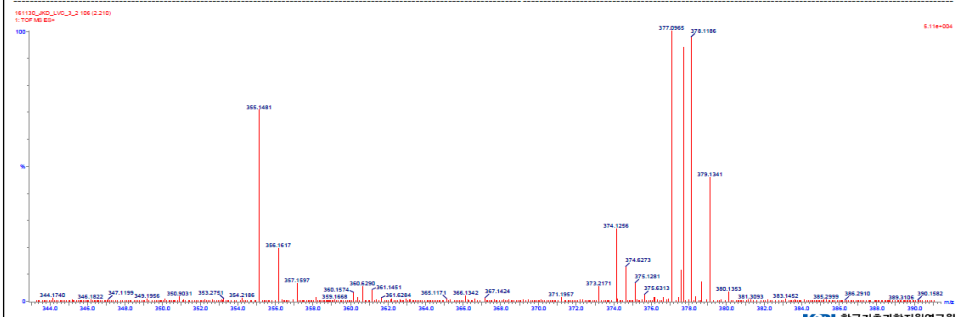

▼HPLC (dr = 53%)

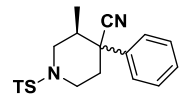


```
======================================================================
Acq. Operator   : LJM                          Seq. Line :  11
Acq. Instrument : HPLC1200                      Location : Vial 70
Injection Date  : 10/7/2015 1:46:18 PM              Inj :  1
                                               Inj Volume : 10.000 µl
Acq. Method     : C:\CHEM32\1\DATA\LVC-3\LVC-3 2015-10-07 19-14-56\LVC-4.M
Last changed    : 10/7/2015 2:53:43 AM by KSJ
Analysis Method : C:\CHEM32\1\METHODS\DIQUAFOSOL_ASSAY.M
Last changed    : 12/1/2016 10:56:53 AM by cgh
                  (modified after loading)
Sample Info     : 18.2 mg / 20 ml


Additional Info : Peak(s) manually integrated
```

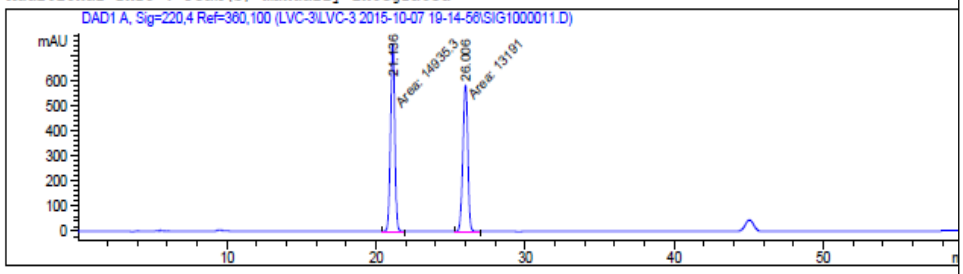


```
======================================================================
                        Area Percent Report
======================================================================

Sorted By             :      Signal
Multiplier:                   :      1.0000
Dilution:                     :      1.0000
Use Multiplier & Dilution Factor with ISTDs


Signal 1: DAD1 A, Sig=220,4 Ref=360,100

Peak RetTime Type  Width     Area      Height     Area
  #   [min]        [min]   [mAU*s]     [mAU]       %
----|-------|----|-------|----------|----------|--------|
   1  21.136 MM    0.3315 1.49353e4   750.86993  53.1007
   2  26.006 MM    0.3781 1.31910e4   581.53333  46.8993

Totals :                  2.81263e4  1332.40326


======================================================================
                        *** End of Report ***
```

(3*S*)-3-methyl-4-phenyl-1-tosylpiperidine-4-carboxylic acid

▼^{1}H-NMR ($CDCl_3$, 400 MHz)

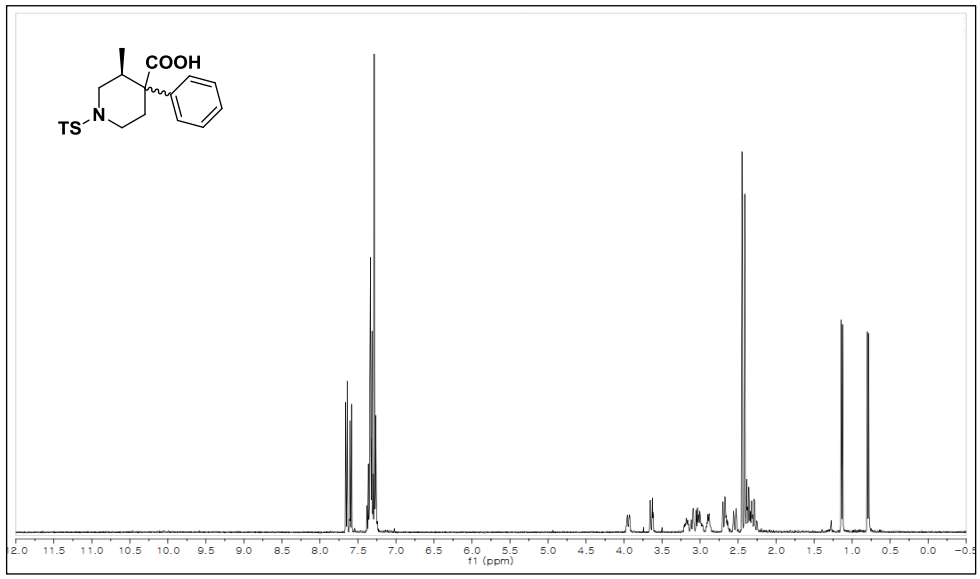

▼^{13}C-NMR ($CDCl_3$, 100 MHz)

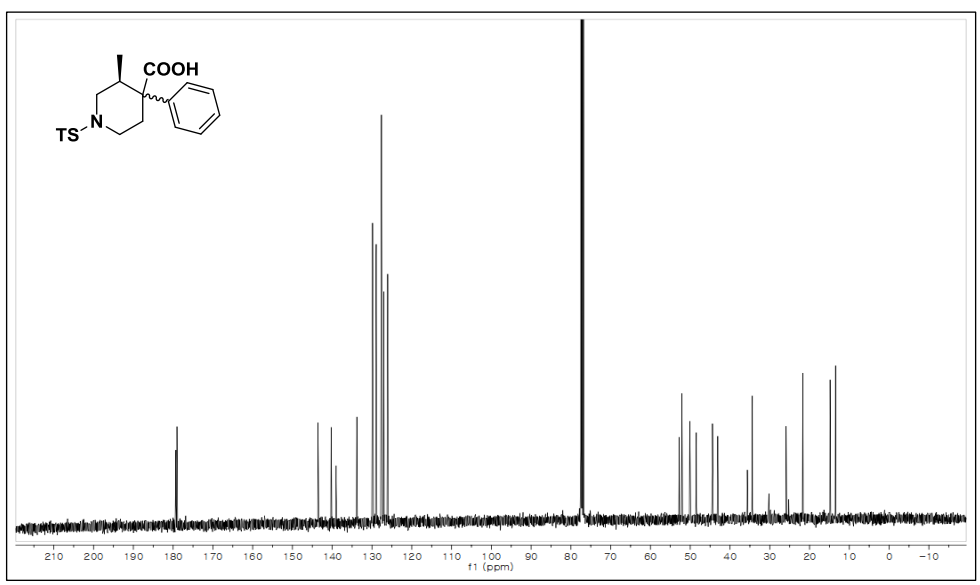

▼High-Resolution Mass

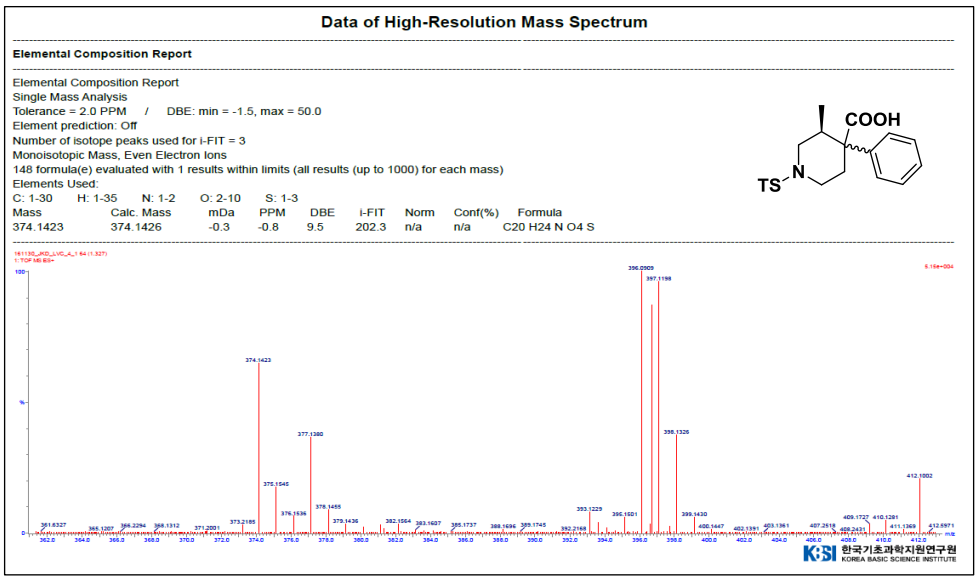

(3*S*,4*R*)-Benzyl-3-methyl-4-phenyl-1-tosylpiperidine-4-carboxylate

▼^{1}H-NMR ($CDCl_3$, 400 MHz)

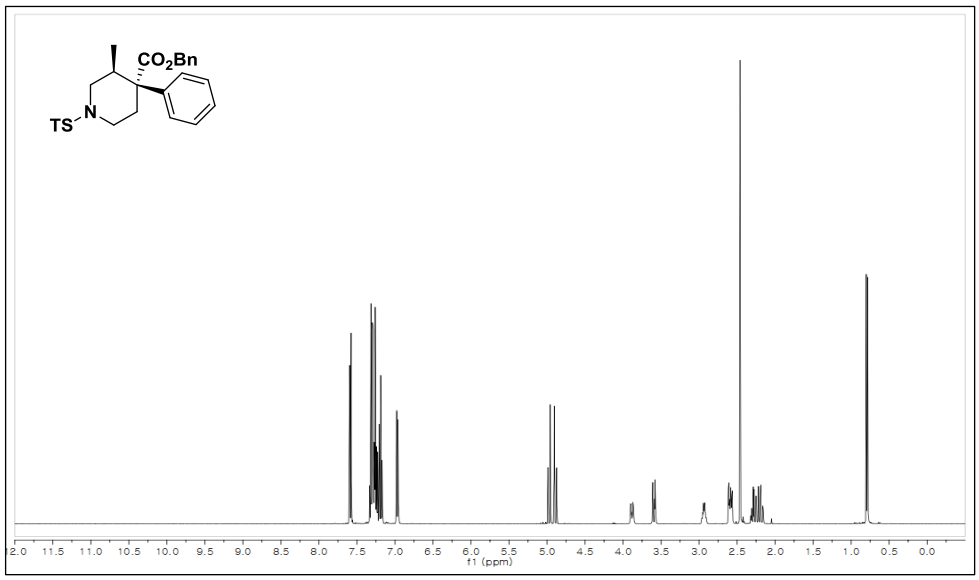

▼^{13}C-NMR ($CDCl_3$, 100 MHz)

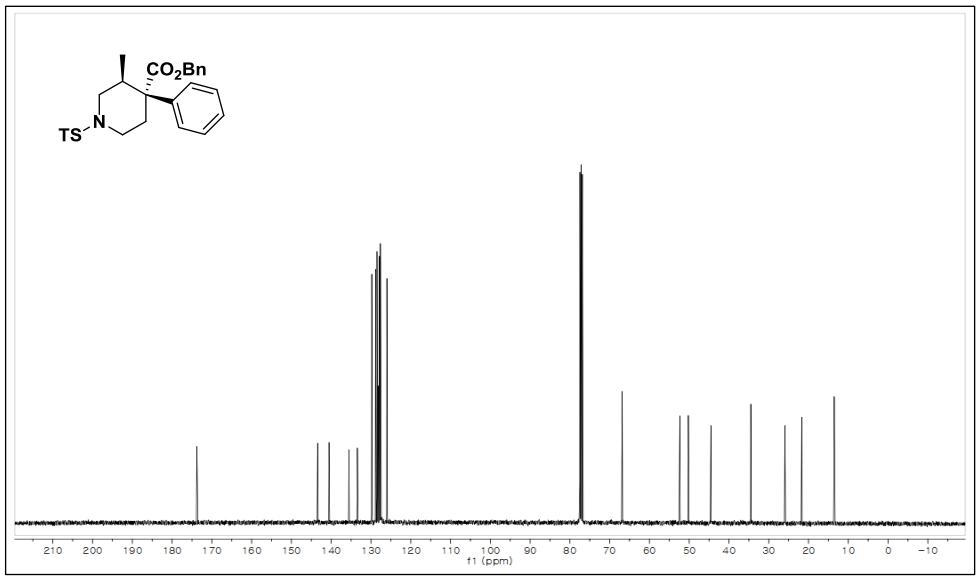

▼High-Resolution Mass

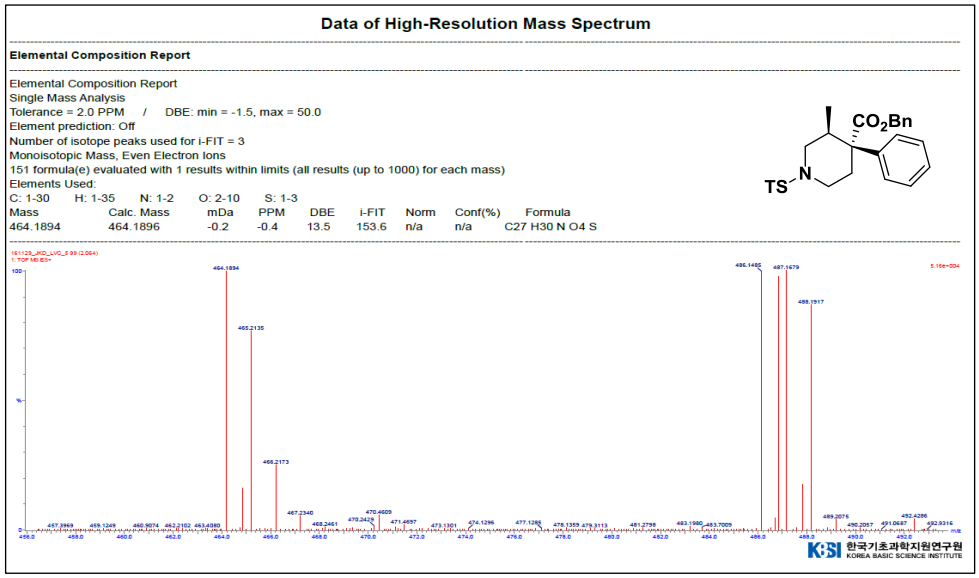

▼HPLC (dr = 99.4%)

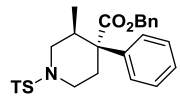


```
================================================================
Acq. Operator   :                          Seq. Line :   3
Acq. Instrument : HS-LC9                   Location :   62
Injection Date  : 3/9/2016 1:21:22 PM          Inj :   1
                                       Inj Volume : 10.000 µl
Acq. Method     : C:\Chem32\1\Data\Levovabastine\Levo_AJS 2016-03-09 12-04-51\Levocabastine(
                  Step4, Step5).M
Last changed    : 3/9/2016 12:04:51 PM
Analysis Method : C:\Chem32\1\Data\Everolimus-JJ\Everolimus 2016-11-16 12-16-24\Everolimus JJ
                  .M (Sequence Method)
Last changed    : 12/1/2016 1:08:32 PM
                  (modified after loading)
Additional Info : Peak(s) manually integrated
```

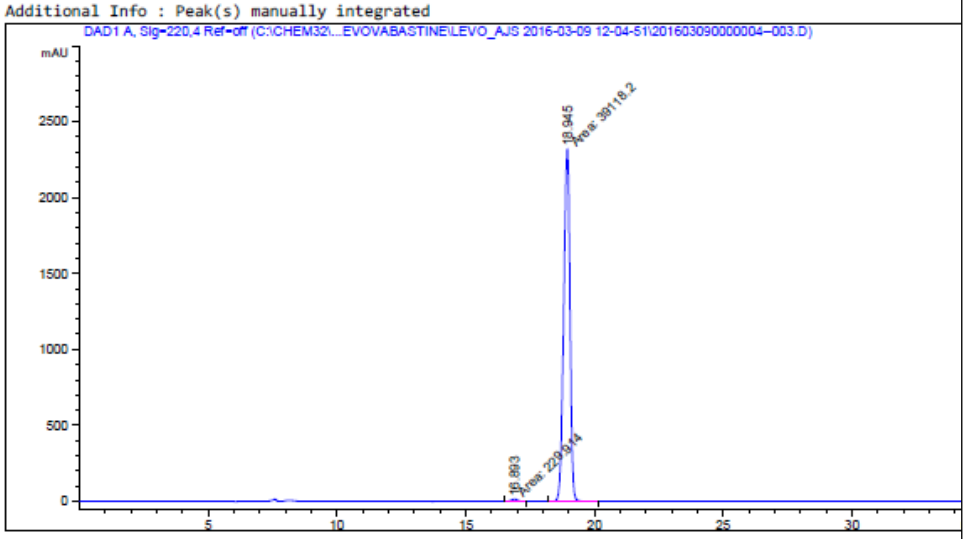


```
================================================================
                      Area Percent Report
================================================================

Sorted By             :      Signal
Calib. Data Modified  :      11/17/2016 9:39:53 AM
Multiplier            :      1.0000
Dilution              :      1.0000
Do not use Multiplier & Dilution Factor with ISTDs


Signal 1: DAD1 A, Sig=220,4 Ref=off

Peak RetTime  Type   Width     Area      Area    Name
  #   [min]          [min]   [mAU*s]      %
----|-------|------|-------|----------|--------|--------------------
   1  16.893 MM      0.2664  229.91402   0.5843 ?
   2  18.945 MM      0.2813 3.91182e4   99.4157 ?

Totals :                   3.93481e4
```

(3*S*,4*R*)-Benzyl-3-methyl-4-phenylpiperidine-4-carboxylate

▼^{1}H-NMR ($CDCl_3$, 400 MHz)

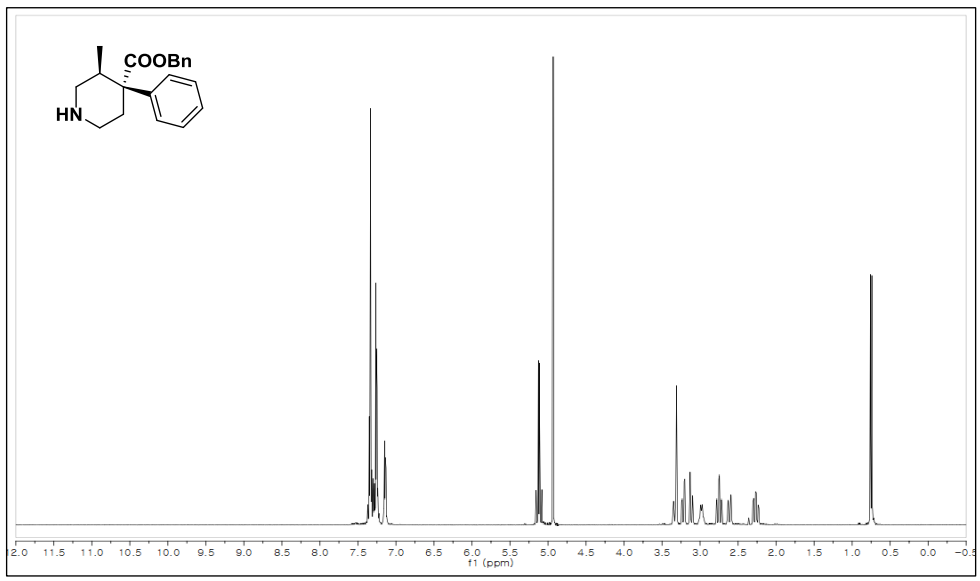

▼^{13}C-NMR (CD_3OD, 100 MHz)

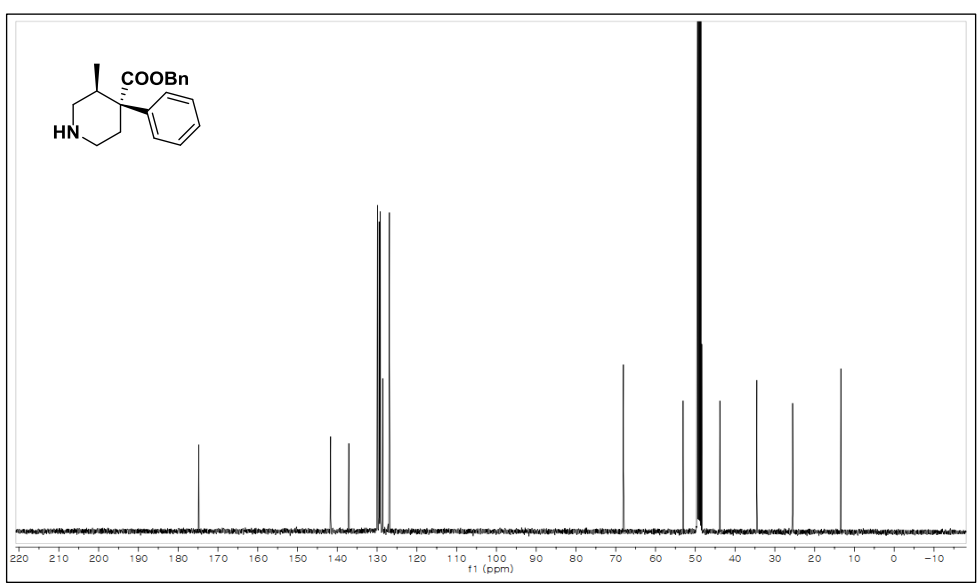

▼High-Resolution Mass

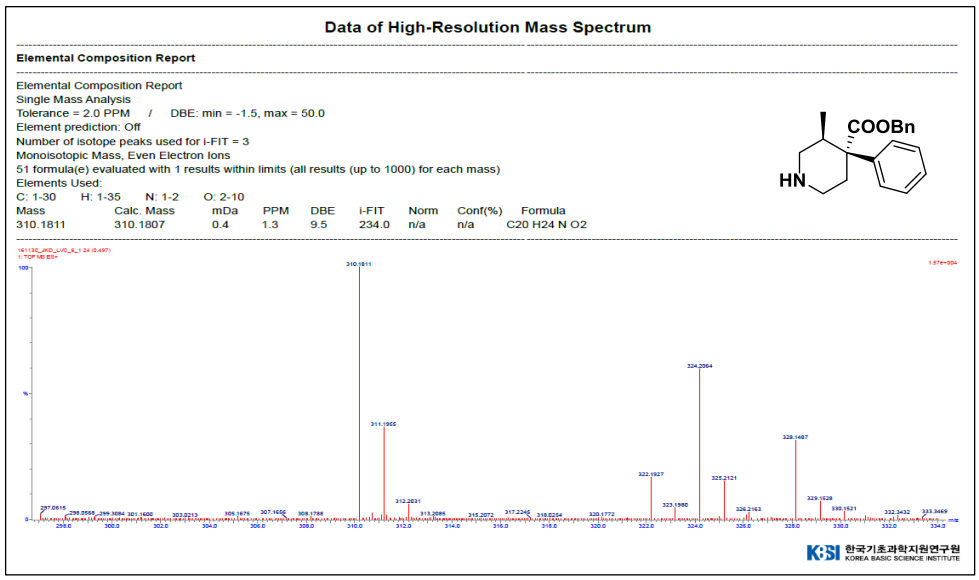

(3*S*,4*R*)-benzyl-1-((1*S*,4*R*)-4-cyano-4-(4-fluorophenyl)cyclohexyl)-3-methyl-4-henylpiperidine-4-carboxylate

▼^{1}H-NMR ($CDCl_3$, 400 MHz)

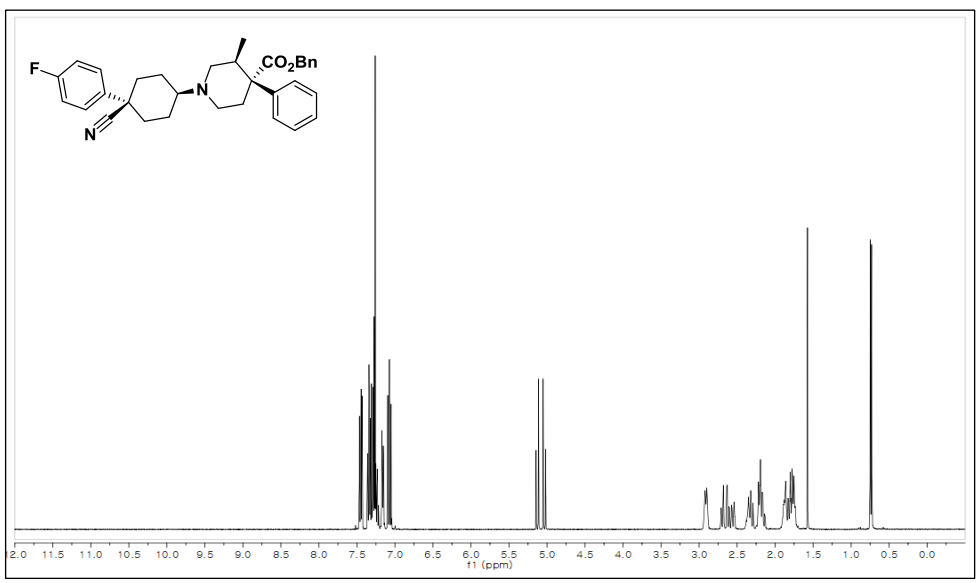

▼^{13}C-NMR ($CDCl_3$, 100 MHz)

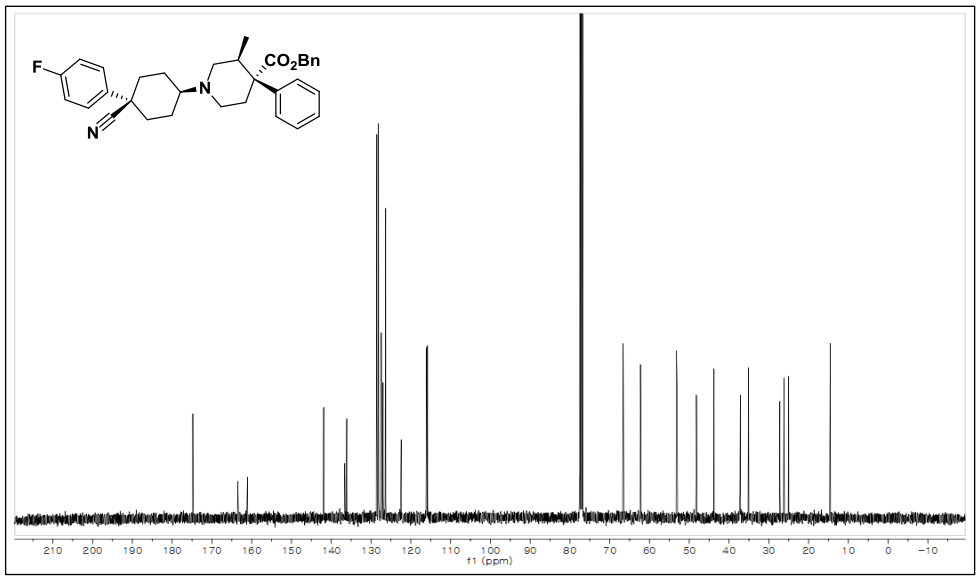

▼High-Resolution Mass

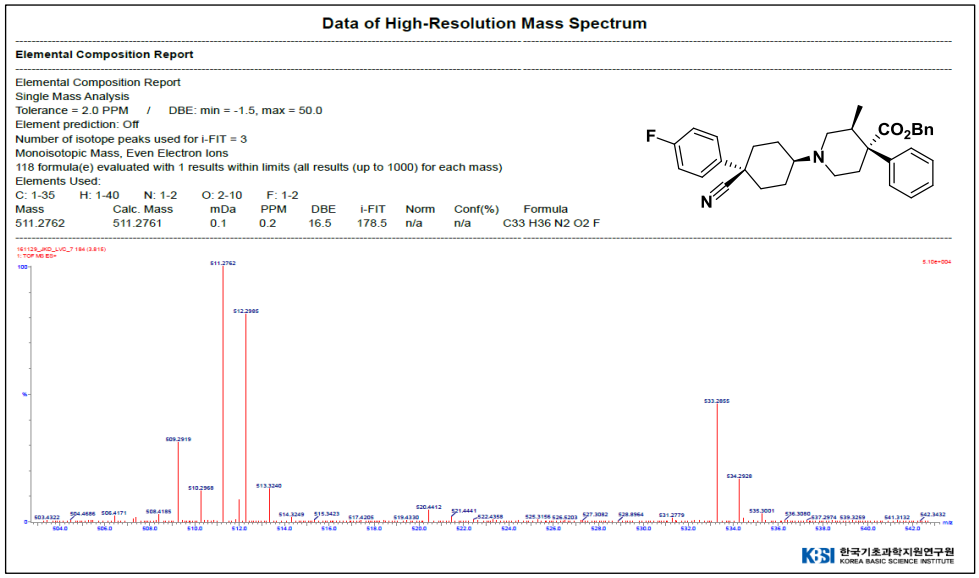

▼HPLC (Purity : 99.5%)

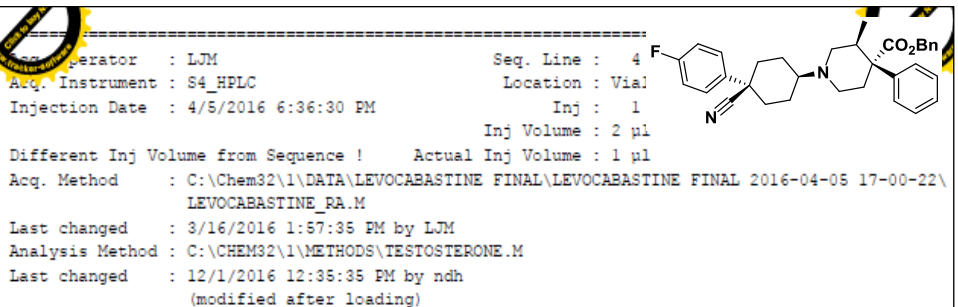


```
Operator    : LJM                                Seq. Line :   4
Acq. Instrument : S4_HPLC                        Location : Vial
Injection Date  : 4/5/2016 6:36:30 PM                Inj :   1
                                                 Inj Volume : 2 µl
Different Inj Volume from Sequence !     Actual Inj Volume : 1 µl
Acq. Method     : C:\Chem32\1\DATA\LEVOCABASTINE FINAL\LEVOCABASTINE FINAL 2016-04-05 17-00-22\
                  LEVOCABASTINE_RA.M
Last changed    : 3/16/2016 1:57:35 PM by LJM
Analysis Method : C:\CHEM32\1\METHODS\TESTOSTERONE.M
Last changed    : 12/1/2016 12:35:35 PM by ndh
                  (modified after loading)
```

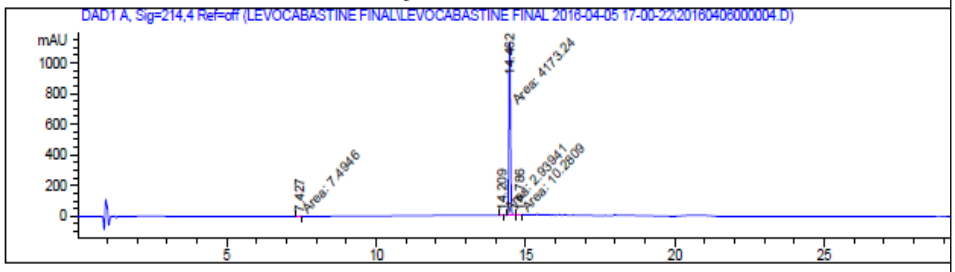


```
=====================================================================
                        Area Percent Report
=====================================================================

Sorted By             :      Signal
Multiplier            :      1.0000
Dilution              :      1.0000
Use Multiplier & Dilution Factor with ISTDs


Signal 1: DAD1 A, Sig=214,4 Ref=off

Peak RetTime Type  Width     Area      Height     Area
  #   [min]        [min]   [mAU*s]     [mAU]       %
----|-------|----|-------|----------|----------|--------|
   1   7.427 MM    0.1430    7.49460 8.73565e-1   0.1787
   2  14.209 MM    0.0685    2.93941 7.14928e-1   0.0701
   3  14.462 MF    0.0612 4173.23926 1137.14673  99.5061
   4  14.786 FM    0.1272   10.28088    1.34661   0.2451

Totals :                  4193.95415 1140.08183


=====================================================================
                        *** End of Report ***
```

▼HPLC (Geometric isomer of intermediate **10** < 0.1%)

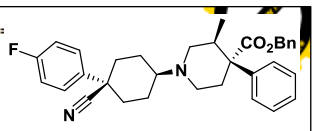


```
Operator    : LJM                                Seq. Line :   4
Acq. Instrument : S4_HPLC                         Location : Vial
Injection Date  : 4/5/2016 6:36:30 PM                Inj :   1
                                                  Inj Volume : 2 µl
Different Inj Volume from Sequence !     Actual Inj Volume : 1 µl
Acq. Method     : C:\Chem32\1\DATA\LEVOCABASTINE FINAL\LEVOCABASTINE FINAL 2016-04-05 17-00-22\
                  LEVOCABASTINE_RA.M
Last changed    : 3/16/2016 1:57:35 PM by LJM
Analysis Method : C:\CHEM32\1\METHODS\TESTOSTERONE.M
Last changed    : 12/1/2016 12:35:35 PM by ndh
                  (modified after loading)
```

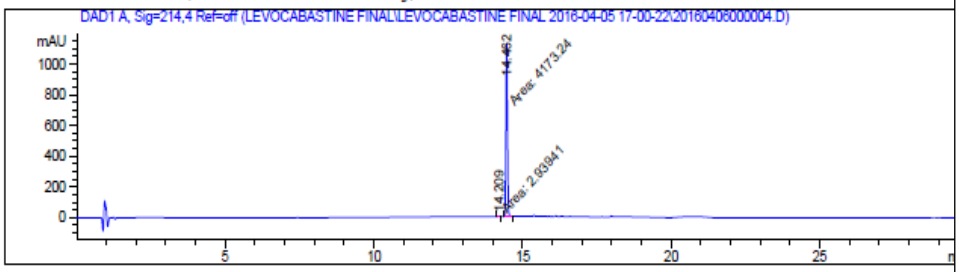


```
=====================================================================
                        Area Percent Report
=====================================================================

Sorted By             :      Signal
Multiplier            :      1.0000
Dilution              :      1.0000
Use Multiplier & Dilution Factor with ISTDs


Signal 1: DAD1 A, Sig=214,4 Ref=off

Peak RetTime Type  Width     Area      Height     Area
  #   [min]        [min]   [mAU*s]     [mAU]       %
----|-------|----|-------|----------|----------|--------|
   1  14.209 MM    0.0685    2.93941 7.14928e-1   0.0704
   2  14.462 MF    0.0612 4173.23926 1137.14673  99.9296

Totals :                  4176.17867 1137.86166


=====================================================================
                        *** End of Report ***
```

(3*S*,4*R*)-1-(*cis*-4-cyano-4-(4-fluorophenyl)cyclohexyl)-3-methyl-4-phenyl-4-piperidinecarboxylic acid, hydrochloride (levocabastine hydrochloride)

▼^{1}H-NMR ($CDCl_3$, 400 MHz)

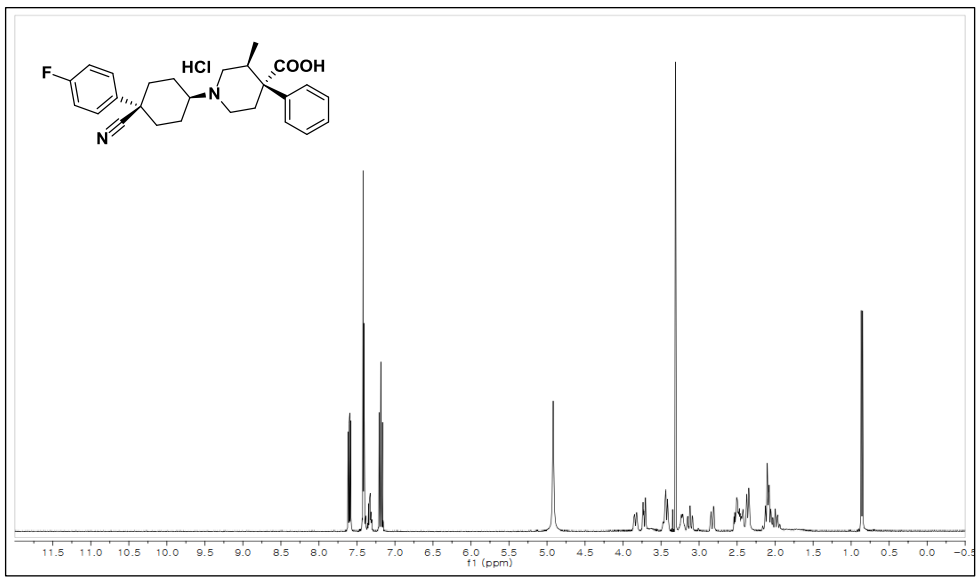

▼^{13}C-NMR (CD_3OD, 100 MHz)

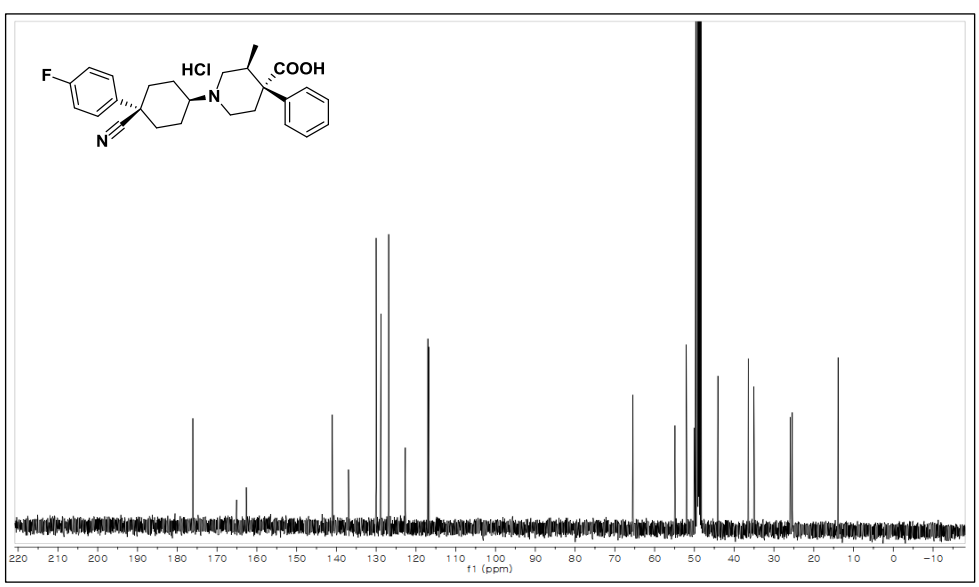

▼High-Resolution Mass

Data of High-Resolution Mass Spectrum

Elemental Composition Report

Elemental Composition Report
Single Mass Analysis
Tolerance = 2.0 PPM / DBE: min = -1.5, max = 50.0
Element prediction: Off
Number of isotope peaks used for i-FIT = 3
Monoisotopic Mass, Even Electron Ions
119 formula(e) evaluated with 1 results within limits (all results (up to 1000) for each mass)
Elements Used:
C: 1-35 H: 1-40 N: 1-2 O: 2-10 F: 1-2

Mass	Calc. Mass	mDa	PPM	DBE	i-FIT	Norm	Conf(%)	Formula
421.2292	421.2291	0.1	0.2	12.5	207.5	n/a	n/a	C26 H30 N2 O2 F

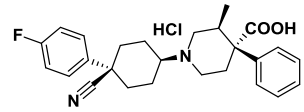

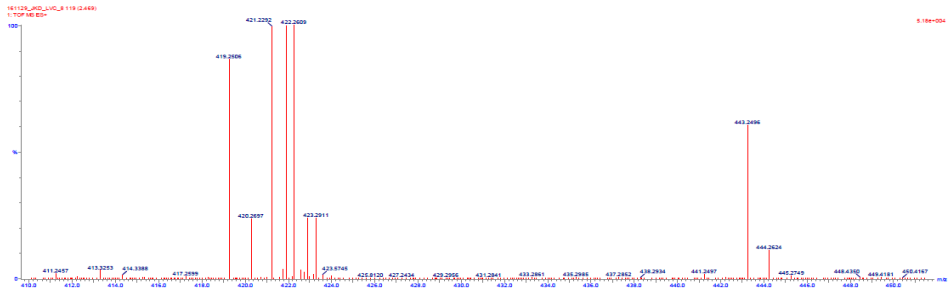

KBSI 한국기초과학지원연구원 KOREA BASIC SCIENCE INSTITUTE

▼HPLC (Purity = 99.7%)

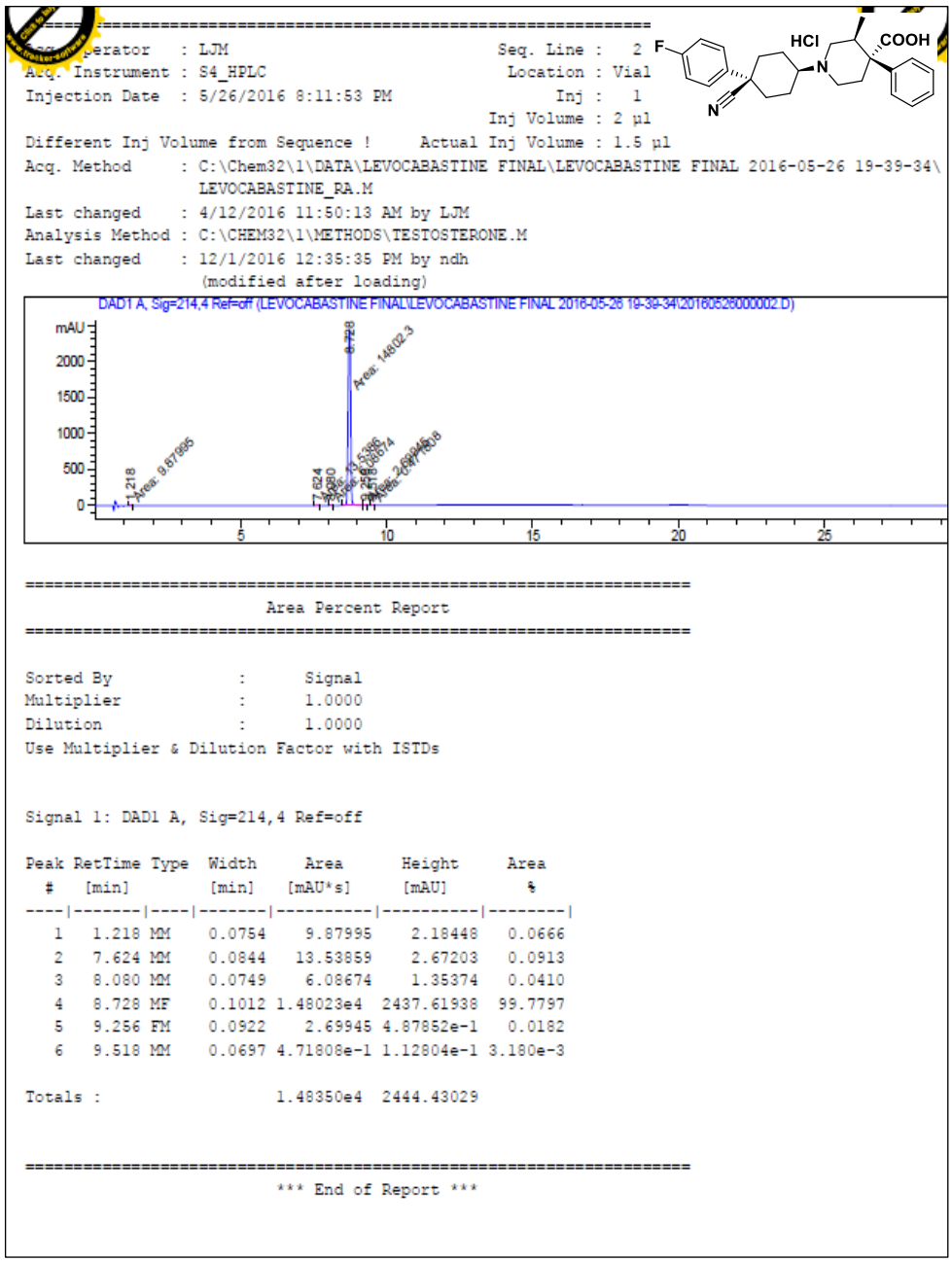

Area Percent Report

Sorted By : Signal
Multiplier : 1.0000
Dilution : 1.0000
Use Multiplier & Dilution Factor with ISTDs

Signal 1: DAD1 A, Sig=214,4 Ref=off

Peak #	RetTime [min]	Type	Width [min]	Area [mAU*s]	Height [mAU]	Area %
1	1.218	MM	0.0754	9.87995	2.18448	0.0666
2	7.624	MM	0.0844	13.53859	2.67203	0.0913
3	8.080	MM	0.0749	6.08674	1.35374	0.0410
4	8.728	MF	0.1012	1.48023e4	2437.61938	99.7797
5	9.256	FM	0.0922	2.69945	4.87852e-1	0.0182
6	9.518	MM	0.0697	4.71808e-1	1.12804e-1	3.180e-3

Totals : 1.48350e4 2444.43029

*** End of Report ***

▼HPLC (Geometric isomer of levocabastine hydrochloride < 0.1%)

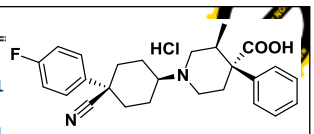


```
Acq. Operator   : LJM                          Seq. Line :   2
Acq. Instrument : S4_HPLC                      Location : Vial
Injection Date  : 5/26/2016 8:11:53 PM             Inj :   1
                                               Inj Volume : 2 µl
Different Inj Volume from Sequence !     Actual Inj Volume : 1.5 µl
Acq. Method     : C:\Chem32\1\DATA\LEVOCABASTINE FINAL\LEVOCABASTINE FINAL 2016-05-26 19-39-34\
                  LEVOCABASTINE_RA.M
Last changed    : 4/12/2016 11:50:13 AM by LJM
Analysis Method : C:\CHEM32\1\METHODS\TESTOSTERONE.M
Last changed    : 12/1/2016 12:35:35 PM by ndh
                  (modified after loading)
```

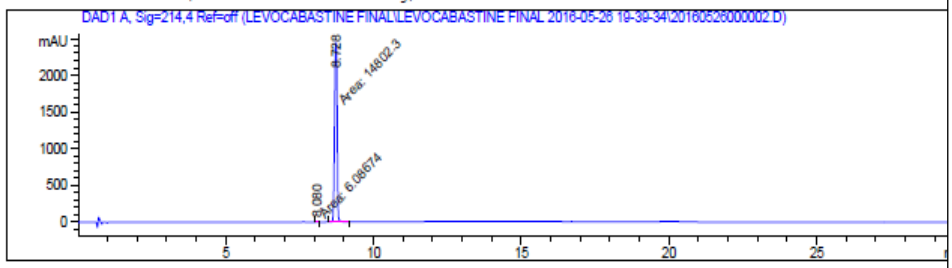


```
=====================================================================
                        Area Percent Report
=====================================================================

Sorted By             :      Signal
Multiplier            :      1.0000
Dilution              :      1.0000
Use Multiplier & Dilution Factor with ISTDs


Signal 1: DAD1 A, Sig=214,4 Ref=off

Peak RetTime Type  Width     Area      Height     Area
  #   [min]        [min]   [mAU*s]     [mAU]       %
----|-------|----|-------|----------|----------|--------|
   1   8.080 MM    0.0749    6.08674    1.35374   0.0411
   2   8.728 MF    0.1012 1.48023e4  2437.61938  99.9589

Totals :                  1.48084e4  2438.97313

=====================================================================
                        *** End of Report ***
```

VII. Abstract

Levocabastine (marketed by Janssen) is a selective second generation H_1 receptor antagonist and was discovered in 1979 for allergic conjunctivitis. As well as acting an antihistamine, levocabastine has also subsequently been found to act as a potent and selective antagonist for the neurotensin receptor NTS_2, and was the first drug used to characterise the different neurotensin subtypes. Levocabastine is composed of piperidine substituted with phenyl and cyclic hexane, and has three chiral centers. According to the procedure described in a previous report, piperidine intermediate **9** was synthesized using *N*,*N*-bis(2-chloroethyl)-4-methylbenzene-sulfonamide as a starting material in a sequence of piperidine ring formation, the chiral resolution of intermediate **5**, and detosylation with electrolysis. Subsequently, reductive amination with cyclic hexanone ring and hydrolysis afford to levocabastine. However, this procedure is considered not industrially suitable because it requires a chiral resolution, which lowered the yield and limited the utility of this synthesis in an economical process. Furthermore, the use of expensive platinum catalyst for reductive amination and electrolysis for detosylation remained as drawbacks for the commercial production.

Therefore, we studied an efficient and practical procedure for the preparation of levocabastine. The key part of our strategy involves an introduction of chiral starting material to afford an optically pure key intermediate **8**, replacement of electrolysis for detosylation, and removal of the use of platinum catalyst for reductive amination. By employing our process, we produced levocabastine hydrochloride with a 14.2% overall yield from a commercially available starting material, (*S*)-propylene oxide (**11**), on a multigram scale.

Keyword : Levocabastine, Chiral resolution, Electrolysis

Student Number : 2009-31060